CHARLES UNIVERSITY

Faculty of Pharmacy in Hradec Králové

Department of Pharmaceutical Technology

Doctoral Dissertation

Preparation of pharmaceutical formulations

based on polymeric and lipid carriers

Mgr. Jana Kubačková

2021

I hereby declare that this thesis is my original work which I solely composed by myself under the supervision of Assoc. Prof. Jarmila Zbytovská and co-supervision Dr. Ondřej Holas. All used literature and other sources are summarized in the list of references and properly cited. This work has not been submitted for any different or equal degree.

Prehlasujem, že táto práca je mojím pôvodným autorským dielom, ktoré som vypracovala samostatne pod vedením svojej školiteľky doc. Jarmily Zbytovskej a konzultanta Dr. Ondřeje Holasa. Všetky zdroje, z ktorých som pri spracovaní čerpala, sú uvedené v zozname použitej literatúry a v práci riadne citované. Práca nebola využitá k získaniu iného alebo rovnakého titulu.

Hradec Kralove   Jana Kubačková

ACKOWLEDGEMENTS

ABSTRACT

Charles University, Faculty of Pharmacy in Hradec Králové

Department of	Pharmaceutical Technology
Candidate	Mgr. Jana Kubačková
Supervisor	Assoc. Prof. Jarmila Zbytovská, Mgr., Dr. rer. nat.
Co-supervisor	PharmDr. Ondřej Holas, PhD.
Title of Doctoral Thesis	Preparation of pharmaceutical formulations based on polymeric and lipid carriers

Nanomedicine allows application of nanoscaled drug delivery carriers to achieve a therapy that can be tailored in terms of e.g. controlled release, site-specific delivery and protection of an active substance. From multiple nanoplatforms available for drug delivery, advantage was taken of biocompatible and biodegradable polymers and lipids to enable targeted intracellular delivery, delivery of a poorly water-soluble drug and delivery of a sensitive macromolecule.

In the study with biodegradable polymeric nanomaterial we worked with experimental poly(lactic-co-glycolic acid) (PLGA) polymers. The formulations were optimised for targeting to phagocytic macrophages – of size up to 300 nm and negative surface charge. For this purpose, two linear and one branched PLGA were screened in combination with one of four surfactants in low concentrations (0.1-1%). These PLGA polymers were formulated into nanoparticles and loaded with a hydrophilic fluorescent dye Rhodamine B using nanoprecipitation (NPM) or emulsification solvent evaporation method (ESE). Increased concentration of employed surfactant decreased particle size more efficiently in ESE than in NPM. The lowest tested concentration of a surfactant (0.1%) was sufficient to formulate negatively charged nanoparticles of 200 nm using NPM. ESE yielded smaller particles of 100 nm when 1% surfactant solution was employed and larger ones, >200 nm, at 0.1% of surfactant. A release study in three different media (isotonic saline solution and buffered saline solutions at pH 4.5 and 7.4) was performed with nanoparticles prepared from all three experimental polymers combined with 0.1% Pluronic F127 using NPM. Rapid release (90% of Rhodamine B in 12 hours) in isotonic pH 7.4 medium was observed in all polymers. In the other media, less than 50% was released by 12 hours. This trend could be related to spontaneous cyclic swelling reported in the experimental polymers at pH 7.4. The swelling seemed to enhance the release of the hydrophilic dye Rhodamine B.

The same preparation methods were implemented into preparation of lipid nanoparticles. Lipid nanoparticles have the ability to increase solubility of poorly water-soluble drugs, such as

indomethacin. This anti-inflammatory drug was loaded into nanostructured liquid carriers based solid lipids either stearic acid or glycerol monostearate. Addition of a liquid lipid, isopropyl myristate, supported formation of unstructured matrix of the carriers, as assessed using differential scanning calorimetry. Nanostructured lipid carriers based on stearic acid were formulated utilising NPM and resulted in nanoparticles of 175 nm with zeta potential of about -35 mV, enhancing solubility of indomethacin 5-times relative to its solubility in water. Glycerol monostearate-based lipid carriers formed nanoparticles of about 140 nm with zeta potential of about -45 mV prepared using ESE enabled 10-fold solubility enhancement of indomethacin.

Another investigated lipid-based nanodelivery system is well-established in oral delivery. Self-emulsification drug delivery system (SEDDS) based on tight junction opening, and thus permeation enhancing, excipients was utilised for local delivery of an oligonucleotide through the intestinal Caco-2 monolayer. The fluorescently labelled oligonucleotide was ion-paired with either dimethyldioctadecylammonium bromide (DDAB) or 1,2-dioleoyl-3-trimethylammonium-propane (DOTAP). The resulting hydrophobic complexes were loaded into one of two tested SEDDS formulation. Both SEDDS formulations readily dispersed forming nanostructures of about 200 nm in an aqueous environment. However, SEDDS can be distinguished by surface charge as neutral and negatively charged SEDDS. The neutral SEDDS offered a better protection of the sensitive nucleotide in the presence of nucleases, namely 58% remained intact in comparison to 16% of the protected oligonucleotide in the negatively charged SEDDS. Orlistat, a lipase inhibitor, slowed down lipolysis of this lipid-based drug delivery system. Both formulations enhanced permeability of the oligonucleotide through the Caco-2 monolayer into lamina propria. The permeability enhancement correlated with the decrease in transepithelial resistance that was more pronounced in the neutral SEEDS.

In summary, PLGA nanoparticles were optimised to act as promising intracellular macrophage-specific drug delivery systems. Nanostructured lipid carriers showed their ability to enhance solubility of a poorly water-soluble indomethacin. Lipid-based SEDDS can deliver an oligonucleotide across intestinal *in vitro* model. Drug delivery nanosystems offer multiple formulation approaches to maximise the potential of active substances.

ABSTRAKT

Univerzita Karlova, Farmaceutická fakulta v Hradci Králové

Katedra	Katedra farmaceutické technologie
Kandidát	Mgr. Jana Kubačková
Školiteľ	Assoc. Prof. Jarmila Zbytovská, Mgr., Dr. rer. nat.
Konzultant	PharmDr. Ondřej Holas, PhD.
Názov dizertačnej práce	Příprava farmaceutických formulací na bázi polymerních a lipidických nosičů

Nanomedicína umožňuje aplikáciu nanonosičov, ktorých úlohou je podávanie liečiv s cieľom dosiahnutia na mieru prispôsobenej terapie. Úlohou nanonosičou je medzi inými aj umožniť riadené uvoľňovanie liečiva, miestne špecifickú distribúciu a ochranu účinnej látky. Z viacerých nanoplatforiem dostupných na distribúciu liečiva sa táto práca zameriava na biokompatibilné a biologicky odbúrateľné polyméry a lipidy. Tieto materiály boli formulované tak, aby bolo umožnené cielené intracelulárne dodanie, dodanie liečiva málo rozpustného vo vode a dodanie senzitívnej makromolekuly.

V štúdii s biologicky odbúrateľným polymérnym nanomateriálom sme pracovali s experimentálnymi polymérmi kysliny poly(mliečnej-ko-glykolovej) (PLGA). Formulácie boli optimalizované na zacielenie do fagocytujúcich makrofágov, t.j. nanočastice s veľkosťou do 300 nm a negatívnym povrchovým nábojom. Na tento účel sa testovali dva lineárne a jeden rozvetvený PLGA polymér v kombinácii s jednou zo štyroch povrchovo aktívnych látok v nízkej koncentrácii (0,1 až 1%). Tieto PLGA polyméry boli formulované do nanočastíc pomocou nanoprecipitácie (NPM) alebo emulzne odparovacej metódy (ESE) s enkapsulovaným hydrofilným fluorescenčným farbivom Rhodamín B. Najnižšia testovaná koncentrácia povrchovo aktívnej látky (0.1%) bola dostatočná na vytvorenie negatívne nabitých nanočastíc s veľkosťou približne 200 nm pomocou NPM. ESE poskytla menšie častice vo veľkosti približne 100 nm, keď sa použil 1% roztok povrchovo aktívnej látky, a väčšie nanočastice, > 200 nm, pri 0.1% povrchovo aktívnej látky. Zvýšená koncentrácia použitej povrchovo aktívnej látky teda viedla k efektívnejšiemu zníženiu veľkosti častíc pri použití ESE, nie v prípade NPM. Uvoľňovanie Rodamínu B bolo testované v troch rôznych médiách (izotonický soľný roztok a pufrované soľné roztoky s pH 4.5 a 7.4). Experiment bol realizovaný s nanočasticami pripravenými pomocou NPM zo všetkých troch experimentálnych polymérov kombinovaných s 0.1% Pluronic F127. U všetkých polymérov bolo pozorované rýchle uvoľňovanie

(90% Rodamínu B za 12 hodín) v izotonickom prostredí s pH 7.4. V ostatných médiách bolo v priebehu 12 hodín uvoľnených menej ako 50% tohto fluorescenčného farbiva. Tento trend pravdepodobne súvisí so spontánnym cyklickým bobtnaním pozorovaným u experimentálnych polymérov pri pH 7.4. Je pravdepodobné, že bobtanie urýchlilo uvoľňovanie hydrofilného farbiva Rodamín B.

Obdobné metódy prípravy boli implementované pri príprave lipidických nanočastíc. Lipidické nanočastice majú schopnosť zvýšiť rozpustnosť liečiv málo rozpustných vo vode, ako je napríklad indometacín. Toto protizápalové liečivo bolo enkapsulované do nanoštrukturovaných lipidických nosičov založených na tuhých lipidoch, buď kyseline stearovej alebo glycerol monosteáráte. Prídavok tekutého lipidu, izopropyl myristátu, podporil vytvorenie neštrukturovaného matrix tohto nosiča, ako to bolo ohodnotené pomocou diferenciálnej skenovacej kalorimetrie. Nanoštrukturované lipidické nosiče založené na kyseline stearovej boli formulované pomocou NPM a výsledné nanočastice merali 175 nm s povrchovým zeta potenciálom okolo -35 mV. Rozpustnosť indometacínu v tejto formulácii bola 5-krát vyššia ako jeho rozpustnosť vo vode. Nanoštrukturované lipidické nosiče založené na glycerol monosteáráte mali veľkosť 140 nm a povrchový zeta potenciál približne -45 mV. Boli pripravené metódou ESE a zvýšili rozpustnosť indometacínu približne 10-krát.

Ďalší skúmaný nanosystém na distribúciu liečiv je taktiež založený na lipidoch a je všeobecne používaný pre orálne podanie. Skúmané samo-nanoemulgujúce systémy pre distribúciu liečiv (SEDDS) boli založené na excipientoch, ktoré otvárajú tesné spoje (tzv. tight junctions) medzi enterocytmi. Tieto excipienty zvyšujúce intestinálnu permeabilitu boli využité na lokálnu distribúciu oligonukleotidu cez intestinálny bunkový model Caco-2. Fluorescenčne značený oligonukleotid vytvoril iónové páry s jedným z testovaných kationických lipidov, bol použitý buď dimethyldioctadecylammonium bromid (DDAB) alebo 1,2-dioleoyl-3-trimethylammonium-propán (DOTAP). Výsledné hydrofóbne komplexy boli enakapsulované do jednej z dvoch testovaných SEDDS formulácií. Obe tieto SEDDS formulácie majú schopnosť sa dispergovať bezprostredne po kontakte s vodným prostredím na nanoútvary o veľkosti približne 200 nm, avšak líšia sa povrchovým nábojom na neutrálne a negatívne nabité SEDDS. Neutrálne SEDDS poskytujú lepšiu ochranu senzitívnemu oligonukleotidu v prostredí nukleáz, konkrétne 58% oligonukleotidu ostáva intaktných v porovnaní s 16% v prípade negatívne nabitého SEDDS. Aby sa predĺžil protektívny efekt toho systému na oligonukleotid, do formulácie bol pridaný orlistat, inhibítor lipáz, ktorý spomalil lipolýzu SEDDS. Obidve formulácie zvýšili permeabilitu oligonukleotidu cez Caco-2 monovrstvu do lamina propria. Zvýšenie permeability korelovalo so znížením transepiteliálnej rezistencie, ktorá bola výraznejšie u neutrálnych SEDDS.

V práci sme optimalizovali PLGA nanočastice k tomu, aby pôsobili ako sľubný systém na distribúciu liečiv intracelulárne do makrofágov. Nanoštrukturované lipidické nosiče potvrdili svoj potenciál v zvyšovaní rozpustnosti slabo vo vode rozpustného indometacínu. SEEDS založené na lipidoch umožnili permeáciu oligonukleotidu cez intestinálny *in vitro* model. Nanosystémy na distribúciu liečiv ponúkajú množstvo formulačných prístupov, ktoré umožnia naplno využiť potenciál podávaného liečiva.

x

TABLE OF CONTENTS

LIST OF ABBREVIATIONS

AFM	Atomic force microscopy
APIs	Active pharmaceutical ingredients
ATR-FTIR	Attenuated total reflectance-Fourier Transform Infrared spectroscopy
cryo-TEM	cryogenic transmission electron microscopy
DDAB	Dimethyldioctadecylammonium bromide
DOTAP	1,2-dioleoyl-3-trimethylammonium-propane
DI	Deionized
DSC	Differential scanning calorimetry
EE	Encapsulation efficiency
ESE	Emulsion solvent evaporation method
FDA	Food and Drug Administration
GI	Gastrointestinal
GMS	Glyceryl monostearate
GRAS	Generally recognised as safe
HLB	Hydrophilic-lipophilic balance
HPH	High pressure homogenisation
HPLC	High performance liquid chromatography
IND	Indomethacin
IPM	Isopropyl myristate
i.v.	intravenous
LDH	Lactate dehydrogenase
MAPC	Mono-acyl phosphatidyl choline
MCFA	Medium chain fatty acids
M_w	Molar weight
NLCs	Nanostructured lipid carriers
NPM	Nanoprecipitation method
NPs	Nanoparticles
PdI	Polydispersity index
PEI	Poly(ethylene imine)
PEG	Polyethylene glycol
PLA	Poly(lactic acid)
PLGA	Poly(lactic co-glycolic acid)
PLGA 5/5	Linear poly(lactic co-glycolic acid), lactic:glycolic acid ratio 50:50
PLGA 7/3	Linear poly(lactic co-glycolic acid), lactic:glycolic acid ratio 70:30

PLGA A2	Branched poly(lactic co-glycolic acid)
	lactic acid: glycolic acid: polyacrylic acid (M_w: 2000 g/mol; branching unit) – 49:49:2 (w/w)
PLGA T1	Branched poly(lactic co-glycolic acid)
	lactic acid: glycolic acid : tripentaerythritol (branching unit) – 49.5:49.5:1 (w/w)
PLGA T3	Branched poly(lactic co-glycolic acid)
	lactic acid: glycolic acid : tripentaerythritol (branching unit) – 48.5:48.5:3 (w/w)
PVA	Polyvinyl alcohol
SA	Stearic acid
SEDDS	Self-emulsifying drug delivery systems
SLNs	Solid lipid nanoparticles
TEER	Transepithelial electrical resistance
TJs	Tight junctions

1 INTRODUCTION

Already in 1900, a Nobel laureate Paul Ehrlich introduced new concept of "a magic bullet" that to this day still holds relevance. This concept describes a drug, the magic bullet, that directly targets the intended cells/pathogen without harming remaining tissue. Besides the need for site-specific targeting described by Paul Ehrlich, other limiting aspects of effective drug delivery were identified. There is a prevailing need for new approaches to increase bioavailability of administrated drugs, to maintain their concentration within the therapeutic window over desired time period, and to enable sustained or controlled release.

Nanotechnology is the engineering and manufacturing of materials at nanoscale. Nanotechnology has been applied to many fields where pharmaceutical sciences, and drug delivery in particular, are no exception. Multiple nanodelivery systems have been introduced over past 60 years and their number is continuously growing. A drug can be loaded into or conjugated onto a nanoparticulate carrier and released in a tailored pattern and/or in a targeted location, independently of the chemical structure of the drug. In other words, nanopharmaceutics have the ability to alter behaviour of the drug in the organism in a desired manner.

To put it simply, there are two fundamental ways to advance the current medical treatment: either by developing new substances or teaching the old drugs new tricks, such as application of advanced drug delivery systems. Nevertheless, to obtain the maximum benefit out of the available scientific advances, the cutting-edge technology should involve a combination of new biomacromolecules, such as proteins or nucleic acids, with nanotechnology platforms for drug delivery.

Out of multiple nanomaterials applied in biomedical settings and in drug delivery, polymers and lipids confirmed their dominant role in pharmaceutical sciences. Structural versatility, regulatory status, biocompatibility and often biodegradability make polymers and lipids suitable and versatile nanomaterials for drug delivery carriers.

Now, more than 100 years later, the therapy has progressed immensely. Even though we identified a potent approach to design "the magic bullets", there is still a long way to go. Reproducible up-scaling and manufacturing process as well as reliable and standardised analytical methods to ensure beneficial pharmacological and toxicological profile still remain a challenge. The field of nanomedicine is still at its early stage. Overcoming the aforementioned limitations could help to translate the extensive research from laboratories to safe and efficient therapy in clinical practice.

2 CURRENT STATE OF KNOWLEDGE

Currently available active pharmaceutical ingredients (APIs) show great potential. Many of them proved promising in *in vitro* tests if applied directly to its site of action. Nevertheless, once tested in more complex *in vivo* tests they often fail to confirm their efficiency. For instance, poorly water-soluble drugs do not reach the site of action in a sufficient amount or sensitive therapeutic peptides, proteins or nucleic acids that degrade before fulfilling their role. Another limitation related to potent pharmaceutical actives are their undesirable systemic side effects in off-targeted tissues.

These shortcomings can be overcome by nanoparticulate colloidal systems utilised as carriers in drug delivery. In order to provide benefits, several characteristics of nanocarriers need to be considered:

- Non-toxicity at administrated doses
- Biocompatibility and biodegradability
- Protection of the payload/minimization of drug degradation
- Site specific release
- Time- controlled release
- Regulatory status of nanomaterial
- Stability of formulation
- Additional value of a carrier to the formulation, such as improved solubility of the API, inhibition of degradation enzymes, permeation enhancement or overcoming multidrug resistance

It is generally accepted that nanotechnology represents systems with the length of at least one dimension of 1-100 nm. Whitesides argues that there are several reasons for expanding the term "nano" when dealing with biological systems. He points out relatively large size of biological structures, such as size of human cells in tenths of micrometres, and the existence of biological molecules in range of a few nanometres, such as nucleic acids or proteins [1]. Therefore, it is reasonable to work inside the range of 1-100 nm when developing systems that are supposed to closely interact with the biological environment. US Food and Drug Administration (FDA) and European Medicines Agency accepted that nanotechnology goes beyond its usual range of 1-100 nm in pharmaceutical sciences [2,3].

Colloids are systems consisting of particles varying from 1 to 1000 nm dispersed in a dispersion medium [4,5]. This size range is characteristic of colloids and relates them to several specific properties. Size reduction increases the surface area of dispersed particles opening up possibilities not only for surface modifications but also for more interactions with the surrounding medium or for more extensive repulsion from each other [5]. NPs do not sediment as they exhibit

only random thermal movement (Brownian motion) upon collisions with dispersing medium. However, sedimentation can occur over time as NPs aggregate into larger non-colloidal structures [5,6].

The application of nanotechnology in life sciences is known as nanomedicine. This interdisciplinary field can function as smart imaging, diagnostic tool or particle-based drug delivery for treatment [7]. One of the advantages of particulate delivery systems is the ability to deliver multiple substances in a single carrier. This fact resulted in a currently very attractive theranostic approach that combines delivery of an active substance and imaging agent [7,8]. Nanomedicine found application across various delivery routes and pathological conditions, such as, among many others, cancer diagnostics and therapy [9,10], therapy of infectious diseases [11], vaccination [12,13] or imaging of inflammatory sites [14].

2.1 Interactions of nanoparticles with biological systems

Nanoparticles (NPs) play a key role in nanomedicine. Physicochemical properties of NPs, such as size, surface charge, hydrophobicity, elasticity and shape of NPs guide the fate of NPs inside an organism. These properties can be deliberately tailored using various materials and technological procedures. Nevertheless, it is necessary to consider also significant changes of properties of NPs that occur upon biological exposure and varied responses of cells and tissues upon exposure to these subcellular structures and materials [15].

Due to their subcellular size, NPs can cross pathologically altered biological barriers easier than their larger counterparts. NPs following i.v. administration can be passively targeted to areas with so called enhanced permeation and retention (< 400 nm), such as leaky vasculature in tumours [16] or at inflammatory sites [17]. Size is an important parameter of colloidal carriers. In addition to size, also hydrophobicity impacts clearance and biodistribution of NPs (**Figure 1**). The surface hydrophobicity seems to be the factor crucial for opsonisation when NPs are covered by immunoglobulin, complement proteins and other plasma proteins such as albumin [18,19]. This modification facilitates phagocytosis of any exogenous material. Upon i.v. administration, the largest particles, above 6 μm, quickly accumulate in the narrow capillary beds in the lungs. Hydrophobic particles of size between 6 μm and 100 nm are quickly opsonised and phagocyted, finally accumulating in the liver and spleen. Reduction in hydrophobicity, such as via surface attachment of polyethylene glycol (PEG), prolongs circulation half-life of this size group. Particles smaller than 100 nm are less attractive for the mononuclear phagocyte system and thus persist longer in the systemic circulation. This applies particularly to PEGylated particles. Nevertheless, the size limit for long particle circulation is given by renal vascular fenestration. Particles smaller than 30 nm are readily excreted through kidneys [19,20].
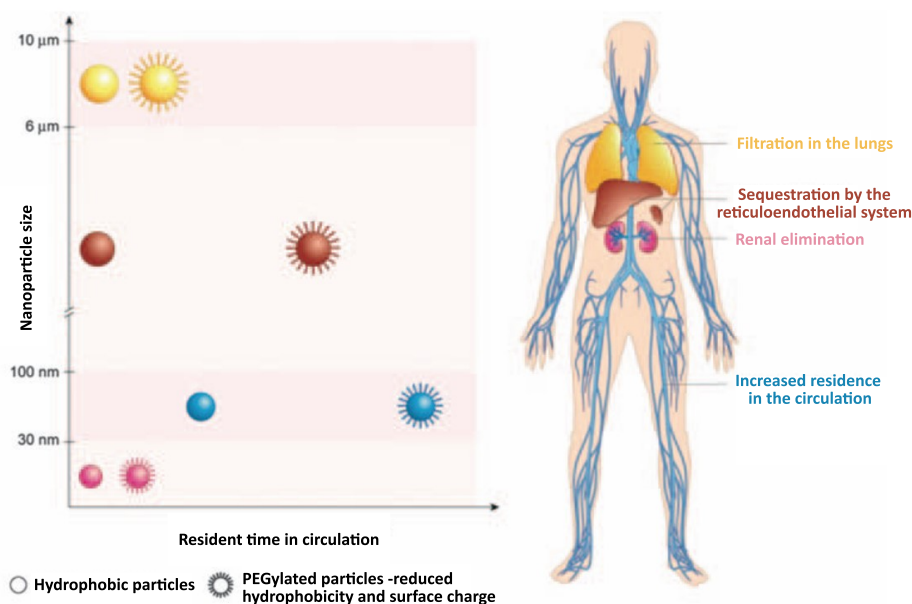
Figure 1: Passive targeting of NPs with size and PEGylation upon i.v. administration. Adopted from [19].

Another factor that influences the fate of NPs upon i.v. administration is the surface charge. This factor also impacts opsonisation as charged particles are readily opsonised, the level of opsonisation is proportional to the surface charge independently of its polarity [18,19]. Higher uptake of positively charged NPs was reported for nonphagocytic cells [21,22], such as osteoblasts [23] or HeLa and mesenchymal stem cells [24], in contrast to negatively charged NPs that are preferentially taken up by phagocytic cells [21,25]. In general, cell membrane carries negative charge resulting in attraction of positively charged NPs. However, phagocytes are designed to engulf bacteria whose surface also carries negative charge and this fact could explain their preferential uptake of negatively charges particles [21]. In contrast to the negative charge of cell membranes, overlying protective mucus is charged positively. Charge characteristics of a disease-altered tissue, such as overexpression of positively charged proteins in the inflamed intestinal tissue can be utilised to target a therapeutical formulation. In this case, negatively charged formulations are favoured [19,26].

As discussed above, the mononuclear phagocyte system recognises NPs upon i.v. administration and especially hydrophobic and charged particles are readily opsonised and phagocyted [27]. Hydrophilization of the nanoparticulate surface by forming a PEG corona prolongs the circulation half-life of such "stealth" NPs [20]. Surface PEGylation can be tailored in order to achieve the desired circulation time by adjusting PEG molecular weight or its surface density [27].

Not only surface chemistry, such as hydrophilicity/hydrophobicity, functionalization, and charge, but also inner characteristics like elasticity and shape of NPs have a significant impact on interactions with living cells. Influence of elasticity of nanoparticulate carriers was in detail

4

reviewed by Anselmo et. al. A collection of *in vitro* studies in the review demonstrated that soft particles are internalised less than their harder counterparts, even though mixed results were not uncommon. The decreased rate of internalization, in particular by immune cells, is a consequence of deformation of the soft particles during the internalization process [28]. A computer simulation study observed irregularities in distribution of ligands, which can bind specifically to receptors on the cell membrane, only in the soft NPs upon initiation of the internalization process. Depletion of ligands at later stages of the internalization process seemed to limit the process resulting in increased uptake of hard NPs [29].

Spherical shape of NPs is common for drug nanocarriers. However, geometry of NPs was shown to play an important role in interactions with the biological environment. Macrophages are known to recognise the local particle shape at the point of initial contact. Phagocytosis proceeds if a NP is approached along its major axis, however, the internalization process is hindered if the contact is initiated along the minor axis or from a flat side (**Figure 2**) [30]. Considering oral delivery route, Banerjee et al. compared performance of sphere-, rod- and disc-shaped NPs in terms of their uptake and transport in a complex intestinal cellular model. The research group demonstrated that both the uptake and transport of the rod- shaped polystyrene NPs were highest among the tested shapes [31]. New nanomanufacturing techniques open up possibilities for preparation of NPs of a particular shape optimized not only in terms of geometrical parameters, but also for disease-triggered drug release [32].
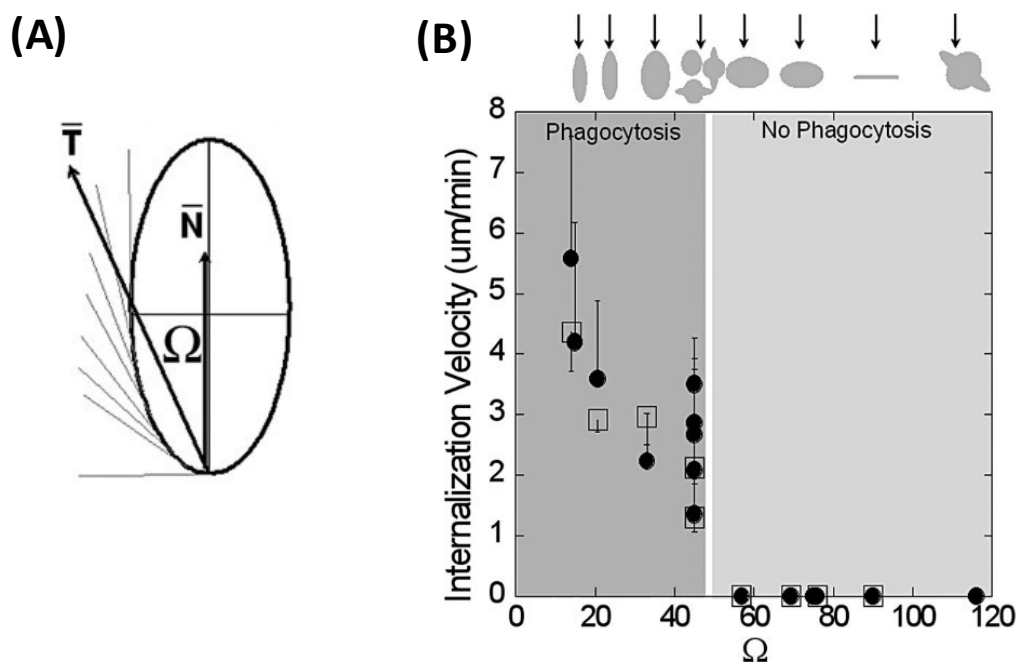
Figure 2: Impact of particulate shape on phagocytosis. (A) The angle Ω is defined as an angle between the membrane normal (N) at the point of initial contact and a vector T that represents the average of tangential angles. (B) Relationship between the particulate shape (described by Ω) and velocity of the internalization process. No phagocytosis was assigned if the internalization was not completed within 2 hrs. Full circles represent non-opsonised particles, open squares stand for IgG-opsonised particles. The velocity of phagocytosis in inversely proportional to Ω, the internalization process is severely impaired at Ω> 45° (Ω=45°for spheres). Adopted from [30].

Besides passive targeting that relies on physicochemical properties of NPs, such as size or surface characteristics, elasticity, and shape, active targeting can be employed to target NPs by surface modification. The surface of a NP is decorated by molecules that are ligands to molecules or receptors occurring predominantly in the targeted tissue. Once the NPs accumulated in their target, the payload is supposed to release. Thus, targeting minimises the impact on off-targeted tissues, as well as undesired side effects [19,20].

NPs are commonly employed in therapy of cancer and their surface is often decorated with ligands to receptors overexpressed on tumour cells, such as transferrin receptor, integrins, folate receptors, epidermal growth factor receptors, HER2 receptor, and CD44 receptor [22,33]. Another example is targeting to phagocytic immune cells with so called "eat me" signalling molecules attached to the surface of NPs, such as large phosphatidylserine [34] or small (<500 Da) primary amines, alcohols carboxylic acids or anhydrides [35].

2.1.1 Nanoformulations in clinical use and in clinical trials

Intensive research in nanoformulation was translated into practice by the FDA approval of the first nanoformulated drug Doxil® in 1995 (**Figure 3A**). From 1995, liposomal drugs were proceeded by polymer-based formulations and nanocrystals on the market (**Figure 3B**). Nevertheless, liposomes remain an attractive drug delivery carrier, as shown by data of nanoformulations in preclinical evaluation (**Figure 3C**). In years between 1995-2007, liposomes comprised more than 50% of all nanoformulations in clinical trials. **Figure 3A** provides just a brief overview of the most important polymeric and liposome-based nanoformulations. For a detailed list, the reader is referred to more comprehensive reviews [21,36–40].
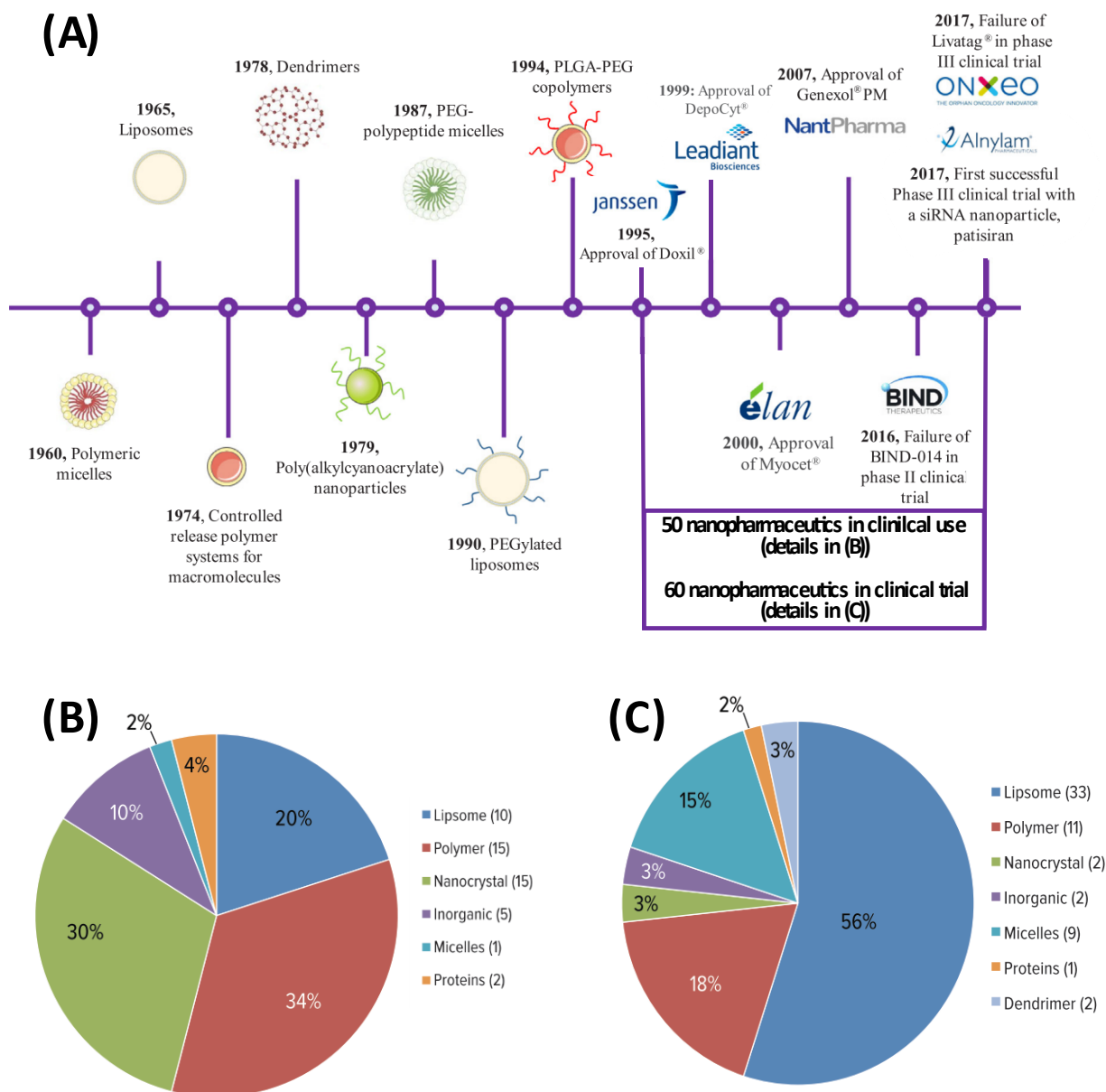
Figure 3: Nanoformulations in clinical practice and undergoing clinical trials between years 1995-2017. (A) Timeline of polymeric and lipid-based carriers from their early development up to approved drugs (adopted from [41]). (B) and (C) show the type of nanoformulation in clinical use and in clinical trials, respectively. Adopted from [40].

Design of nanoformulations needs to be carefully considered based on demands from the clinical practice. Ventola reminds of the ever-present challenges of development of nanoformulations in connection to their translation into clinical practice. The author calls for further characterisation of accumulated knowledge in the field and systematization of the collected data, not only in terms of design of nanocarriers, but also in interactions with biological systems and safety evaluation. In addition, regulatory guidelines more specific for nanoformulations would facilitate the approval process [40].

The current pandemics of a respiratory virus SARS-CoV-2 is an excellent example of a flexible reaction of nanomedicine to medical needs. The pandemics has led to the fast-track

development of multiple vaccines based on nanomedicine. Several vaccines made it into the clinical practice for less than a year. Among the first approved ones, there are mRNA-based vaccines in lipid NPs (Pfizer/BioNTech, Moderna) or vaccines based on viral vectors (Astra Zeneca/Oxford, CanSino). The ongoing demand for the vaccines has paved the way to the largest Phase 4 Trial of nanomedicine. [42–44].

2.2 Inorganic carriers

Inorganic carriers represent a heterogenous group of a wide range of nanomaterials used in drug delivery, such as metal, silica, or carbon. They have usually well contorlled shape as well as size up to 100 nm that make them smaller than their organic counterparts described below. Another difference lies in the common way of attachment of API. In inorganic NPs, API is usually attached to the surface unlike being encapsulated by the organic ones. The inorganic carriers are biocompatible [45]. However, evaluation of their fate in the organism after fulfilment of their role, especially in the case of chronic administration, needs to be carefully assessed for each particular design [46]. In this section, the most commonly used inorganic nanocarriers for drug delivery are briefly introduced (**Figure 4**).
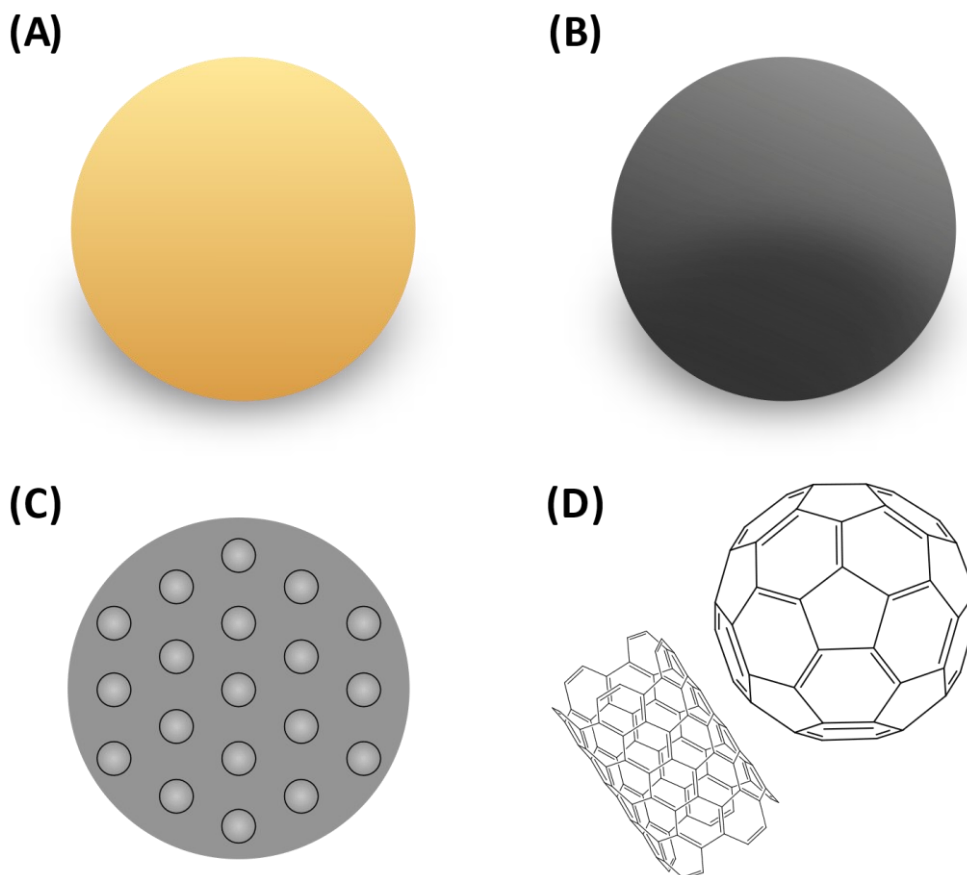
Figure 4: Schemes of inorganic NPs. (A) gold NP, (B) iron oxide NP, (C) mesoporous silica NP, and (D) carbon-based tubular and spherical fullerenes

Gold NPs are composed of bioinert gold with functionalized surface. They can be manufactured in various shapes and their size ranges usually from 10-100 nm. Due to their direct interactions with light upon accumulation in a tumour, they became well-established in photoimaging as well as photothermal and photodynamic therapy of cancer [47]. In drug delivery, surface conjugation of API is a common approach performed either via covalent bonding or physical (non-covalent) absorption. Gold NPs are also utilised for drug delivery of small molecules in cancer treatment as well as in gene and protein delivery [48]

Iron oxide (i.e., Fe_2O_3, Fe_3O_4) NPs, characteristic with their intrinsic magnetic capabilities, have been extensively used in imaging techniques. Multiple preparation methods have been reported, enabling preparation of NPs of various shape and size, usually ranging from 10 to 100 nm. Preparation of the NPs is accompanied or followed by biocompatible coating, e.g. with dextran or PEG. The coating improves biocompatibility and stability of iron oxide NPs in the biological environment, and it enables surface functionalization. In drug delivery, APIs can be conjugated onto the surface of NPs non-covalently or covalently. Both strategies have been extensively employed in cancer therapy. Iron oxide NPs have a great potential to develop further as magnetic guided carriers for cancer theranostic [49–51].

Mesoporous silica NPs are characterised by highly ordered porous structure. Large pore volume increases the surface area and creates two functional surfaces: cylindrical pore surface available for drug loading and exterior particle surface tailorable for interactions with the biological environment. The size of mesoporous silica NPs as well as pore size is adjustable, usually ranges from 50-300 nm and 2-50 nm, respectively. The porous structure results in large surface that enables high drug load. Mesoporous silica NPs are utilised in delivery of a wide range of APIs, such as poorly-water soluble drugs or macromolecular nucleic acids. In cancer therapy, mesoporous silica NPs can be optimised into stimuli-responsive systems. [52–54].

Carbon-based carriers or fullerenes are hollow structures of spherical, ellipsoidal or tubular shape. Fullerenes are hydrophobic in nature, but the surface can be functionalized with hydrophilic moieties. In drug delivery, APIs are usually covalently attached to the surface. An advantage of these carriers is their small size about 1 nm that facilitates crossing through barriers, such as the tight blood-brain barrier. Another unique feature is the ability to produce reactive oxygen species under certain conditions and this has been employed in photodynamic therapy. Fullerenes enable delivery of anticancer agents as well as delivery of nucleic acids [55,56].

2.3 Polymeric carriers

Polymers are defined as large molecules built up from a large number (>100) of small repeating units, monomers. Polymers found multiple applications in pharmaceutical sciences and drug delivery is no exception [57]. From the vast array of polymeric drug delivery carriers, this chapter discusses the most commonly utilised systems.

2.3.1 Dendrimers

Dendrimers are highly branched molecules that constitutes from repeated structural entities (**Figure 5**). These macromolecules have a well-defined three-dimensional chemical structure of a spherical shape as well as controlled monodisperse size (1-15 nm). Surface chemical groups are available for tunable functionalization and inner cavities can host molecules for drug delivery [36,58]. Multiple types of dendrimers have been synthetised and used as drug carriers. Poly(amidoamine) dendrimers belong to the most commonly used ones [36,59]. There are two main approaches to poly(amidoamine) dendrimers as drug delivery system, namely non-covalent entrapment of a drug inside inner cavities or covalent conjugation on dendrimers [59].

★ surface groups
● branching units
▲ core moiety
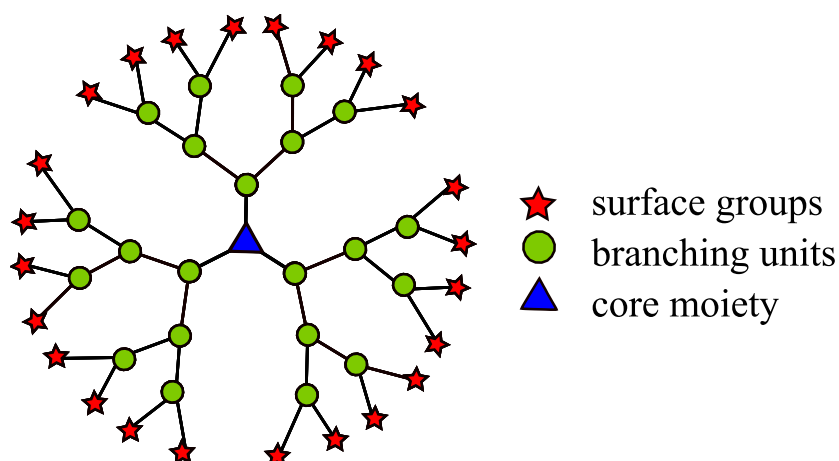
Figure 5: Structure of a dendrimer. Adopted from [60].

2.3.2 Polymeric micelles

Polymeric micelles are core-shell self-assembles of block co-polymers (**Figure 6**). Above their critical micellar concentration, the amphiphilic co-polymers associate into the hydrophobic micellar core and hydrophilic shell. The formed spherical micelles can solubilise poorly water-soluble entities and ensure their sustained release. The most commonly used co-polymers are poloxamers, PEG-poly(L-aminoacid)s and PEG-poly(ester)s [61]. In addition to these well-established materials, novel stimuli-responsive block co-polymers are paving the way to site-specific triggered release. The novel co-polymers can be pH-, thermo-, light- sensitive, enzyme- or ultrasound-responsive and the release is triggered by external stimuli or due to specificities of the pathological microenvironment [62]. Micelles formed using more than a single kind of a co-

polymer are more beneficial in terms of increased micelle payload, prolonged circulation half-life as well as enhanced thermodynamic stability of such mixed micelles [63].
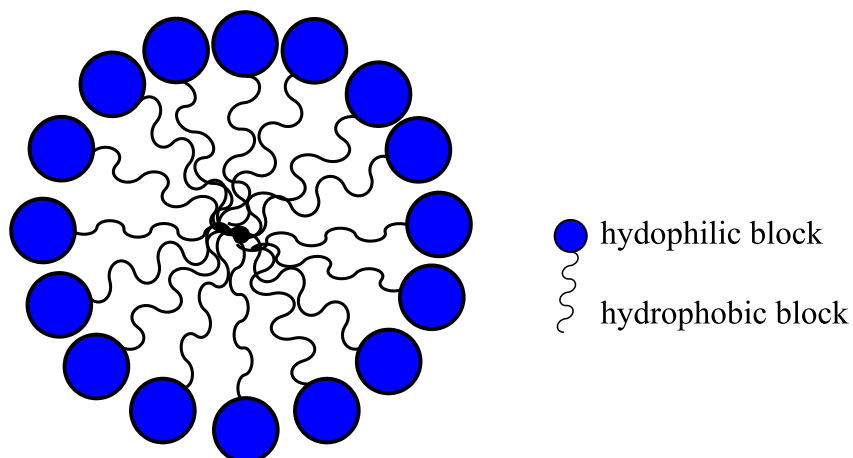
Figure 6: Structure of a polymeric micelle.

2.3.3   Polymeric nanoparticles

Multiple biodegradable polymers have been widely investigated as nanoparticulate carriers (**Figure 7**) in drug delivery [19].
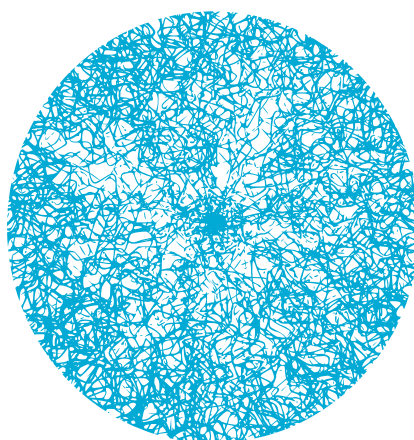
Figure 7:Scheme of a polymeric NP. Adopted from [60].

- hydrophobic polyesters: Poly(Lactic Acid) (PLA), Poly(Lactic Co-Glycolic Acid) (PLGA), Poly(ε-Caprolactone), Poly(Alkylcyanoacrylates)

  PLA is a well-described polymer that has a wide range of applications ranging from degradable sutures, scaffolds to delivery nanosystems across medical disciplines PLA exists in two optical isomers L- and D-lactic acid (**Figure 8AB)** and properties and biodegradability of polymeric PLA (**Figure 8C**) is influenced by optical form of the monomers. Poly(L-lactic acid) is a semi-crystalline hard polymer, in contrast to amorphous racemic poly(DL-lactic acid) polymer. Crystallinity impacts the rate of PLA

degradation. The crystallinity level, and thus the degradation rate, can be tailored by the selection of monomers [64].

This polymer was further developed into a more hydrophilic co-polymer with glycolic acid – PLGA that is thoroughly discussed in section 2.3.3.1.
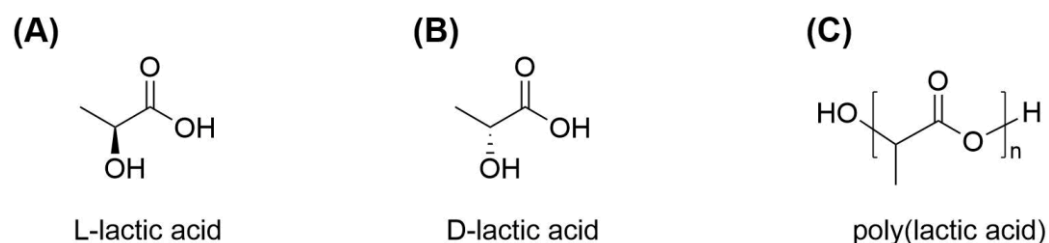
Figure 8: Lactic acid exists in optical forms: (A) L-lactic acid, (B) D-lactic acids. The form of monomers impacts propertis of (C) poly(lactic acid).

Poly (ε-caprolactone) found its application in tissue engineering (**Figure 9A**). Its nanocomposites can be utilised as supportive scaffolds with tailorable degradation rate and mechanical properties [65]. In drug delivery, poly (ε-caprolactone) is commonly used as a co-polymer with PEG to enhance drug accumulation at the site of action [66]. Moreover, other chemical and physical modifications have been applied to alter formulation design in terms of degradation, reactivity, hydrophilicity and other properties of the polymer [67].

Poly(alkylcyanoacrylates) are polymers manufactured by a rapid and controllable polymerization of cyanoacrylic monomers (**Figure 9B**). Adapting method of synthesis, several types of NPs can be prepared, such as nanospheres and oil- or water-containing nanocapsules [68,69].
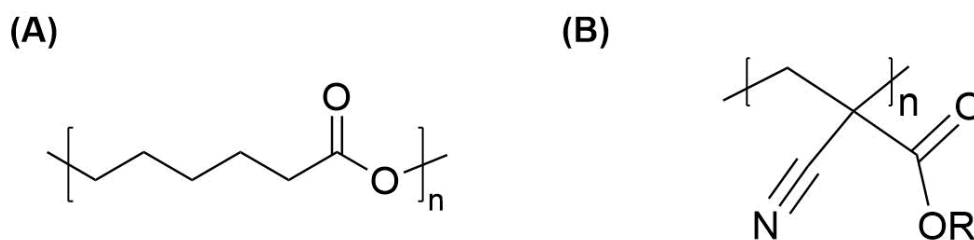
Figure 9: Chemical structure of (A) poly (ε-caprolactone), (B) poly(alkylcyanoacrylates), R=alkyl.

- hydrophilic polysaccharides: Chitosan, Alginates

Chitosan, whose chemical structure is shown in **Figure 10A**, is a natural cationic polysaccharide obtained by deacetylation of chitin. It demonstrates antibacterial and antifungal activity that establish chitosan as a wound healing agent [70]. In addition, mucoadhesivity and permeation enhancement make nanoparticulate chitosan a perspective mucosal drug delivery system [71].

Alginates are anionic biopolymers extracted from brown algae (**Figure 10B**). Besides their traditional role in wound healing and *in vitro* cell culture, alginates can be also employed as NPs in drug delivery [19,72].

(A)   **(B)**
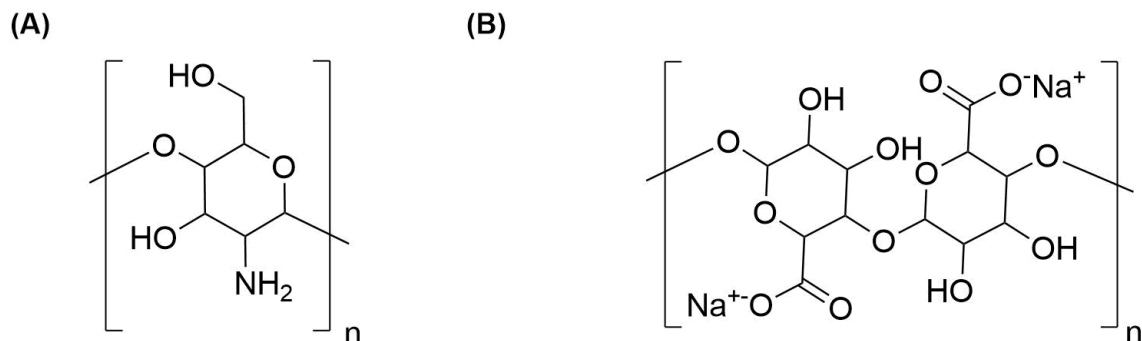
Figure 10: Chemical structure of (A) chitosan, (B) alginates.

Moreover, the relative ease of synthesis of polymers further increases the number of novel nanomaterials [73]. In addition to conventional, non-responsive nanomaterials, stimuli-responsive polymers can release their payload upon internal or external stimuli. This characteristic is supposed to enhance site-specific release [74]. The further progress into clinic of any novel nanomaterial may be hampered by their regulatory status.

2.3.3.1   PLGA nanoparticles

PLGA is a co-polymer consisting of lactic and glycolic acid connected with ester bond at a various molar ratio of the monomers. Chemical structure of PLGA is depicted in **Figure 11**.
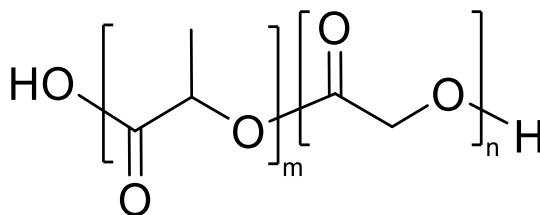
Figure 11: Chemical structure of poly(lactic-co-glycolic acid) (PLGA)

PLGA is one of the most utilised nanomaterials in drug delivery due to its specific properties that lead to beneficial characteristics and vast use in drug delivery.

- biodegradation + easy designing → controlled drug release

Ester bonds in PLGA polymeric chain are hydrolysed into lactic and glycolic acid. These monomers enter citric acid cycle (Krebs cycle) and finally are eliminated as carbon dioxide and water (Figure 12). This degradation process makes PLGA fully biodegradable and biocompatible [19,75].

Moreover, hydrolytic degradation of PLGA formulations is influenced by factors that can be designed during synthesis of the polymer. Slower degradation of PLGA chains is related to their higher molar weight, higher ratio of lactic acid and ester-terminated (CH_3 capped) polymers [75]. Controlled release from PLGA carriers is described further.

lactic acid

glycolic acid

Poly (lactide-co-glycolic acid) PLGA

Hydrolysis

citric acid cycle

CO_2 + H_2O
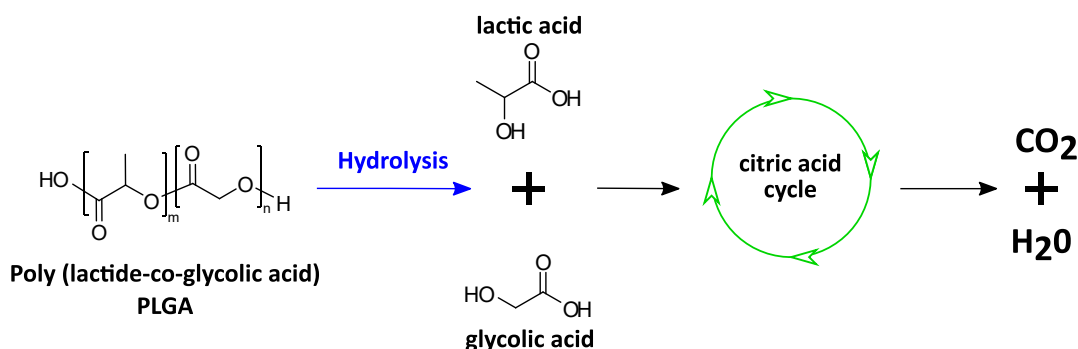
Figure 12: PLGA degradation

- surface functionalisation → active targeting, prolonged circulation half-life

In acid terminated PLGA, carboxyl end groups of the polymer are utilised for functionalisation by various agents. The reaction can be based on hydrophobic or ionic interaction or the functional group can be covalently conjugated [76]. Martins et al. reviewed PLGA surface modification for active targeting of NPs, including ligand-receptor interaction and antigen-antibody interactions [76]. In addition to active targeting, surface functionalisation using cell penetrating agents, stimuli responsive agents or imaging agents were reported [77].

Hydrophilization of surface of PLGA NPs prolongs the circulation half-life by reducing opsonisation [20]. The most commonly used agent is PEG, followed by much less utilised polysaccharides and poloxamers [19,76,78,79].

- endosomal escape → delivery of macromolecules into the cytosol

PLGA NPs possess negative surface charge at alkaline and neutral pH. After cellular internalisation by non-specific endocytosis, NPs are transported into acidic endosomes and lysosomes. At low pH between 4 and 5 the surface charge of NPs turns positive. Positively charged NPs interact with negatively charged endosomal membrane leading to its local destabilisation upon contact with the NP. This was not observed in polystyrene NPs without charge reversal after endosomal entrapment [80]. In order to enhance cytosolic delivery of protein aggregates, poly(ethylene imine) (PEI) was entrapped into PLGA NPs together with protein aggregates. PEI is a positively charged polymer known for its "proton sponge effect"

that can lead to rupture of endosomes. In addition, it was found that positively charged PEI PLGA NPs enter cells also via direct translocation [81].

- US FDA approval for clinical use [19,75,82]

The abovementioned versatility has been translated in multiple applications of PLGA as a drug delivery system, as summarized in **Figure 13** [77].
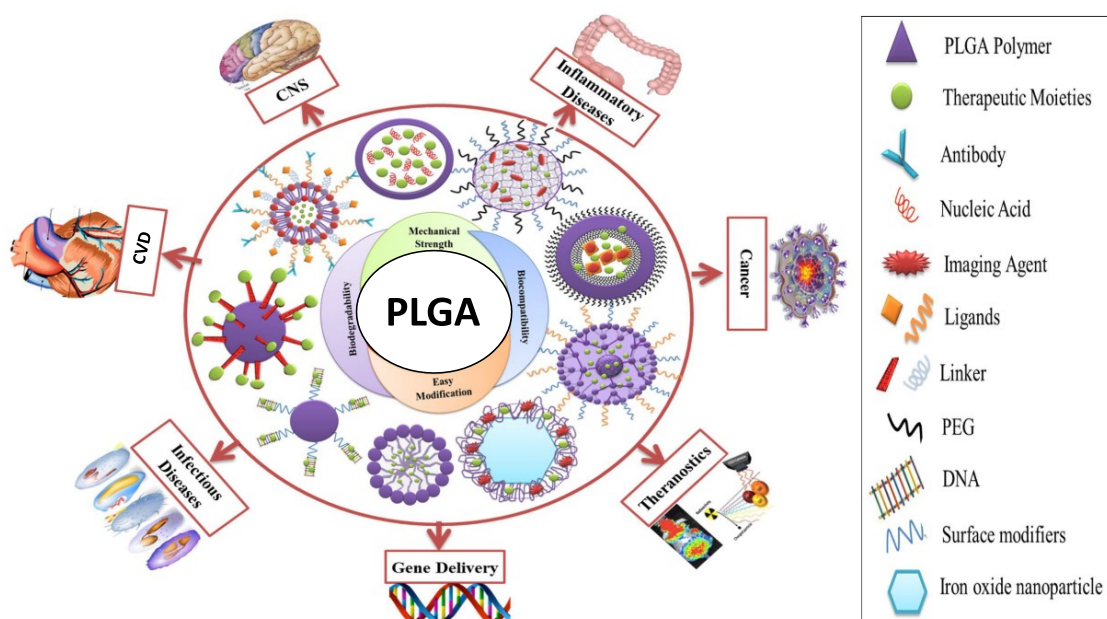
Figure 13: Versatility of applications of PLGA in drug delivery. CNS central nervous system, CVD cardiovascular diseases. Adapted from [77].

Controlled release

PLGA formulated into particles undergoes bulk (homogenous) erosion. Polymer degradation, cleavage of polymeric chains by hydrolysis of ester bond, is slower than water penetration into the delivery system. Therefore, particles do not erode primarily on the surface and the erosion occurs homogenously throughout the system. Dimensions of the system do not change; however, the length of polymer chains decreases together with molar weight. This leads to increased molecular mobility, pore formation and finally diffusion of an encapsulated drug [83].

The degradation process is well described in microparticles. Inside microparticles, short acid-terminated chains of polymers are generated as the system undergoes bulk erosion. These acid-terminated chains diffuse out of the particle and are neutralised by surrounding bulk fluid. In addition, basic compounds from the surrounding bulk liquid diffuse into the particle and neutralise the acid-terminated polymeric chains. However, this diffusion mass transport is relatively slow leading to acidification within the microparticle. Decreased pH autocatalyzes polymer degradation inside the particles. Therefore, there are 2 considerable parameters of particles – size, determining the length of diffusion pathway and porosity, influencing the mobility of diffusing molecules [83,84].

Factors that have an impact on drug release were summarised by Xu et al. [85], as shown in **Figure 14**. The authors divided the factors into 3 main categories, such as material (physicochemical properties of both polymer and drug), processing (system design factors controllable and adjustable during the synthesis) and physiological factors (related to the release medium). The factors are shortly described with reference to several excellent comprehensive reviews [75,77,85].
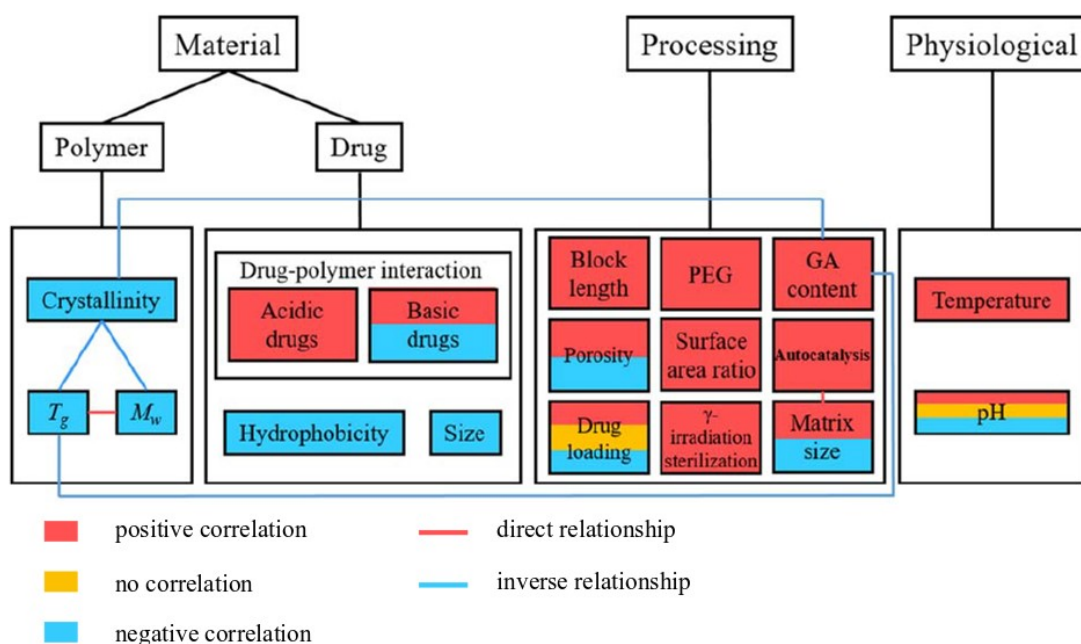
Figure 14: Factors influencing drug release from PLGA-based drug delivery systems. Adopted from [34]. T_g – glass transition temperature, M_w – molar weight

In terms of material of PLGA polymer, the increase in crystallinity, molar weight (M_w) and glass transition temperature (T_g) slow down drug release rate. The higher the level of these factors, the slower degradation of polymer chains. Drug-polymer interactions play also an important role. Acidic drugs are known to accelerate autocatalysis and thus drug release. Drugs that have basic properties show a varying behaviour ranging from acceleration of the release by nucleophilic drugs to neutralization and thus suppression of the autocatalytic effect. In addition, smaller or/and hydrophilic drugs can diffuse faster from the polymer matrix [75,77,85].

One of the most important processing factors is the lactic/glycolic acid ratio. Higher content of glycolic acid makes PLGA more hydrophilic and amorphous, both these characteristics increase the release rate. In addition, longer blocks of lactic and glycolic acid and surface PEGylation accelerate drug release. Porosity is reported to accelerate diffusion-based drug release in the initial phase, however, in a later stage, porous systems might result in faster neutralisation of autocatalysis and slower degradation and release rate. A review of influence of size of PLGA-system reports an opposing effect on drug release. On one hand, in larger systems drug concentration gradient decreases and the diffusion pathway shortens leading to slower release

rate. On the other hand, increasing autocatalysis promotes pore formation that facilitate drug release. Shape of polymeric matrix also affects the release. Larger surface area available accelerates drug release. Sterilisation for i.v. administration by γ-irradiation at higher irradiation dose may cause random cleavage of polymeric chains and thus accelerate polymer degradation. The role of drug loading is a drug-specific feature influenced mainly by its type and chemical functionalities. Nevertheless, higher drug loading results in higher initial burst release [75,77,85].

A significant impact on drug release has the composition of release medium, e.g. pH, or osmotic properties [86]. Phosphate buffer saline pH 7.4 is a commonly tested release medium, however, it does not reflect *in vivo* situation properly. Degradation of PLGA systems is faster in serum and plasma due to the effect of serum/plasma proteins. PLGA degradation is also faster in alkaline or strong acidic environment, however, the autocatalysis rate shows no difference between slightly acidic and neutral media. Increased temperature enhances polymer mobility and thus facilitates drug release. Setting temperature above physiological 37 °C is utilised in accelerated dissolution tests [86].

Preparation methods

Preparation methods of PLGA nano- and microparticles can be divided into 3 main groups [75,87]

- chemical methods: polymerization of monomers
- mechanical methods: polymer in dispersion, methods such as spray drying, supercritical fluid technology, microfluidics
- physicochemical methods: polymer in dispersion, methods such as solvent evaporation methods, solvent displacement method, phase separation method

The following section introduces physicochemical methods. The methods are of increasing attention as they are easy to perform without any expensive instrumentation from already preformed polymer.

- o Solvent evaporation method is a high-energy emulsification method based on emulsification of two immiscible solvents - an organic volatile solvent such as chloroform, dichloromethane, ethyl acetate or 2-butanone and an aqueous solution of a surfactant (e.g. polysorbates, poloxamers, polyvinyl alcohol (PVA) etc.). A preformed polymer and a drug are dissolved in the organic solvent and emulsified using high-speed homogenizer or ultrasonication. Formed particles are allowed to solidify by evaporation of the organic volatile solvent under stirring at room temperature or reduced pressure [88–91].
- o Solvent displacement method, also known as nanoprecipitation, is a low-energy approach that utilises two miscible solvents. A preformed polymer and a drug are soluble only in

one of them, a semipolar solvent, such as acetone, ethanol, or dimethyl sulfoxide. This lipophilic solution is added under stirring into another solvent, an aqueous solution of surfactant, in which the polymer is not soluble. This leads to rapid desolvation of the polymer and displacement of the semipolar solvent. As the solvent of the polymer diffuses into the polymer-non-solvent, the polymer precipitates and entraps the drug. This method overcomes use of chlorinated solvents, formed particles are characterised by narrow size distribution and low surfactant concentrations [78,89–91]. Reproducibility of this method is dependent on the geometry of mixing of the two solvents. The need of easy and reproducible upscaling in controlled conditions has led to expansion of advanced microfluidic approaches [92].

o Phase separation method is mostly represented as a salting out method. This method employs a water-miscible solvent of a polymer and a drug, such as acetone or tetrahydrofuran. This lipophilic solution is emulsified into an aqueous phase containing surfactant and high concentration of electrolytes, such as magnesium chloride hexahydrate. Due to the high ionic strength, the miscibility properties of water change and there is no solvent diffusion at this point. Subsequent addition of water decreases ionic strength and induces migration of the organic solvent under stirring [78,89]. This method is often utilised for protein encapsulation [93].

Molecular architecture of PLGA polymers

PLGA polymers of high molar weight (tens of thousands of Daltons) and with long degradation time over several weeks (e.g. about 10 weeks) are utilised as implants [76]. For particulate drug delivery systems degradation time within hours or days is more favourable. The degradation time shortens by increase of polymer hydrophilicity. One of the approaches to achieve faster degradation time by polymer hydrophilization is polymer branching. Branched polymers contain more end groups that are available for contact with water and finally are more hydrophilic [94].

Branched PLGA polymers were mainly investigated in delivery of hydrophilic drugs, such as proteins or FITC-dextran. Davaran et al. investigated star-like polymers for encapsulation of insulin using glucose or β-cyclodextrin as a branching unit [95]. A different architecture of branching was applied by Pistel et al. The research group grafted hydrophilic PVA with PLGA screening various molar weights of these polymers successfully encapsulating various hydrophilic macromolecules into microparticles [96]. Brush-like polymers were prepared also by Li et al. Copolymer metoxyPEG-b-PLGA was grafted on oligomeric collagen. Due to the amphiphilicity of the resulting polymer, assembled into micelles that were shown to be pH sensitive. Doxorubicin was loaded into the micelles that were stable at neutral pH releasing the payload in the acid microenvironment of tumour [97]. A wide range of branched PLGA polymers was synthetized

by melt polycondensation by assoc. prof. Dittrich, Faculty of Pharmacy in Hradec Kralove. The synthesis was thoroughly described preparing several star-like polymers branched on mannitol, penta-, dipenta- and tripentaerytritol with and a brush-like polymer using acrylic acid as the

(A)   **(B)**
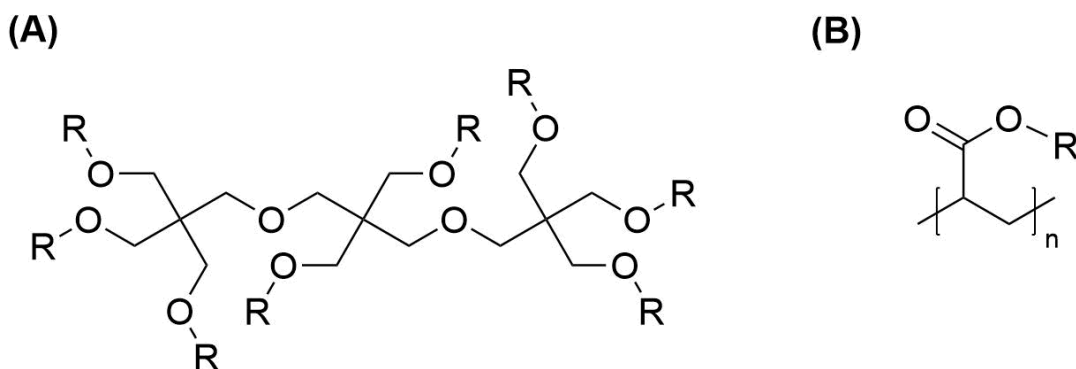
branching unit (**Figure 15**) [94].

Figure 15: Chemical structure of branched PLGA polymers. (A) star-like PLGA polymer with tripentaerythritol as the branching unit. (B) brush-like PLGA polymer with acrylic acid as the branching unit. R = PLGA

2.4   Lipid carriers

A broad definition of lipids covers biological compounds insoluble in water but well soluble in organic solvents [98]. The definition can be narrowed down to lipids as fatty acids and their derivates, and substances that are biosynthetically or functionally related to these substances [99]. The Lipid Metabolites and Pathways Strategy consortium has recently created a more precise classification considering chemical functional backbone of lipids as well as their biosynthetic perspectives. Therefore, lipids can be divided into eight categories: fatty acids, glycerolipids, glycerophospholipids, sphingolipids, sterol lipids, prenol lipids, saccharolipids and polyketides [98,100]. Such a wide range of structures can be even widen using variable chain length and possible presence of multiple functional groups. This pool of compounds offers a wide variety of physicochemical properties and has enabled development of multiple lipid-based nanocarriers. These carriers take advantage of lipid biocompatibility, versatility and regulatory status [37,101].

2.4.1   Lipid nanoparticles

Lipid NPs consist of solid lipids, alternatively these are combined with liquid oils, remaining solid at both room and body temperature and are stabilised by surfactants [102,103]. Lipid biocompatibility and versatility together with the possibility to regulate drug release, encouraged the development of several types of lipid NPs [102].

- Solid-lipid nanoparticles (SLNs) consist of biocompatible and biodegradable solid lipids. SLNs were formed in the early 90s as nanospheres of solid lipids without any use of organic solvents.

- However, the unsatisfactory low drug load and drug expulsion during storage propelled modifications that resulted into nanostructured lipid carriers (NLCs). Unlike SLNs, the core of NLCs is based on a mixture of solid and liquid lipids (**Figure 16**).

- To enable delivery of hydrophilic drugs and take the advantage of kinetic stability and rigid morphology of lipid NPs, the hydrophilic drug can be conjugated with a lipid to create a hydrophobic drug-lipid conjugate. This water-insoluble conjugate can be subsequently loaded into the lipid, SLNs or NLCs based, matrix [103].
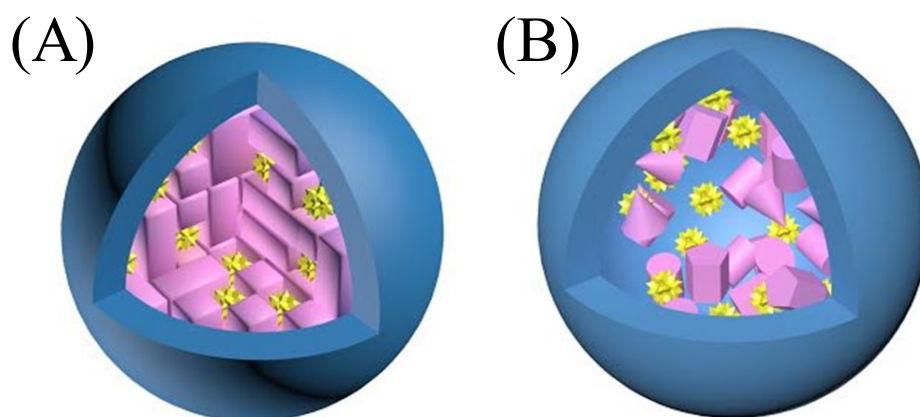
Figure 16: Structural differences between (A) SLNs with "brick wall" structure and (B) NLCs with an unstructured matrix. Adopted from [60]

2.4.1.1 Impact of the structure on long-term stability

Molecules of solid lipids form different crystalline structures. Thus, they exist in different polymorphic forms of various stability. There are 3 pre-dominant forms arranged by increasing stability: unstable α modification < metastable β′modification < the most stable β modification. With the increasing stability, the density of molecular packaging increases and the most stable β modification forms a perfect crystalline lattice, so called "brick-wall" structure [104,105].

Bulk lipids are usually in β modification, however, the manufacturing process of SLNs triggers changes in polymorphic forms with a fraction of unstable α and metastable β′modifications present in nanoparticulate lipids. These changes in the crystalline lattice arrangement reduce not only the melting temperature, but also impact the long- term stability of SLNs. The newly formed less-stable polymorphic modifications tend to undergo transformation to the most stable β modification. The transformation is time- and temperature- dependent. It leads

to the rearrangement of the lipid molecules that become more structured what results in expulsion of the incorporated active [105–107]. Nevertheless, when this burst release happens relatively fast (e.g. within one to three days) it can be utilised as a targeting strategy [105].

The undesired repulsion led to development of a new generation of lipid NPs – NLCs (Figure 16). In order to form imperfections in the crystalline lattice, a fraction of a solid lipid is replaced by liquid oils. The unstructured matrix allows to increase drug load and improve long-term stability [106].

The literature describes 3 basic types of SLNs (**Table 1**) and NLCs (**Table 2**). The type of the carrier depends on utilised lipids, properties and solubility of the active in the lipids and manufacturing method [103,105,108]:

Table 1: Types of SLNs. Stars denote presence of a drug.

SLNs Type	Model	Characterisation	Visualisation
Type I	homogenous matrix	• a solid solution of a drug in lipids as solvents, a mixture of lipids with a molecularly dispersed drug • produced by cold homogenisation	
Type II	drug-enriched shell	• a hot mixture of lipids without a drug precipitates first forming the active-free core • concentration of the drug increases up to its saturation solubility and both the drug and remaining lipid precipitate into the drug-enriched shell	
Type III	drug-enriched core	• produced by hot homogenisation using high concentration of the drug • during the cooling process the drug quickly precipitates as its concentration is close to the saturation solubility resulting in the drug-rich core surrounded by precipitated drug-free lipid	

Table 2: Types of NLCs

NLCs Type	Model	Characteristics of utilised lipids
Type I	imperfect crystal model	spatially varied lipids in terms of chain length and saturation increase imperfections
Type II	amorphous model	lipids, such as hydroxyoctacosnyl hydroxystearate and isopropyl myristate, form amorphous solid structures that hinder crystallization upon cooling
Type III	multiple model	the amount of oil exceeds its solubility in solid lipids and leads to phase separation. A drug is dissolved in the oily droplets in a multiple oil-in-fat-in-water dispersion

2.4.1.2 Production methods

Manufacturing methods have been evolving together with development of lipid NPs and are well reviewed throughout the literature [103,105,108,109]. Hereby, the most common methods are briefly described, referring to the aforementioned authors for a detailed reference.

- High energy approaches

High pressure homogenisation (HPH) is a well-established technique due to its easy upscaling and cost-effectivity. In hot HPH, a drug is dissolved in a lipid melt and it is emulsified in hot solution of a surfactant using high-sheer homogeniser or ultrasonication. This micro pre-emulsion is passed 3 to 5 times through a micron-sized gap under high pressure causing sheer stress and cavitation forces generate NPs. Thermolabile drugs can be processed by cold HPH. The drug-lipid melt is rapidly cooled down and milled. Resulting microparticles are dispersed in a cold solution of surfactant and subjected to HPH.

- Low energy approaches

A microemulsion technique is based on addition of drug-lipid melt into a preheated solution of highly concentrated surfactants. The hot microemulsion is rapidly cooled by addition of cold water. This results in recrystallization of highly diluted lipid NPs.

A phase inversion method employs several heating-cooling cycles (85-60-85°C) of a mixture of lipids, a drug and surfactants. Hydrophilic-lipophilic balance (HLB) of polyoxyethylated surfactants increases with increasing temperature, so the thermal treatment increases their affinity to the lipophilic phase and inverses o/w emulsion to w/o emulsion. This emulsion is cooled rapidly by dilution of cold water leading to recrystallization of NPs. However, presence of additional molecules may influence the inversion process.

- Approaches with organic solvents

Solvent displacement method/Solvent injection method/Nanoprecipitation uses water-miscible organic solvents, such as acetone, ethanol or isopropanol. Lipids and a drug dissolve in

the organic solvent and this solution is rapidly injected into an aqueous solution of a surfactant. Lipid NPs are formed upon rapid diffusion of the organic solvent across the solvent-lipid interface with the aqueous phase [110].

Unlike the previous method, emulsification solvent evaporation method utilises organic solvent immiscible with water, such as chloroform or ethyl acetate. Organic solution of lipids and a drug is dispersed in the aqueous solution of a surfactant using a high-speed homogenizer or an ultrasonic probe sonicator. Formed lipid NPs are allowed to harden and the organic solvents evaporates under continuous stirring.

2.4.1.3   The role of (nanoparticulate) lipid material in various delivery routes

Lipid NPs have a potential to interact with physiological barriers, such as the skin barrier, blood brain barrier and gastrointestinal (GI) barrier. However, their application is not limited to these barriers, lipid NPs were formulated also for pulmonary or ocular delivery. Increased loading of poorly-water soluble drugs in lipid NPs, together with longer retention of nanoparticulate formulations apply to all the delivery routes [106,108,111,112]. Lipid NPs can offer sustained release of poorly water-soluble drugs in a physiological and biocompatible lipid matrix [107]. In addition, specific points to topical and oral delivery are discussed below.

Topical application of lipid nanoparticulate formulations impacts the skin barrier. Adhesive properties of lipid NPs (~200 nm) enable formation of a tight film with small pores that hinders water molecules from evaporation leading to improved skin hydration. Particles of micro dimensions do not adhere to the skin surface sufficiently tight with interspaces between particles [105,113]. Occlusive properties of lipid NPs not only improve skin water loss that is frequently present in skin pathologies, but also facilitates skin permeation of the encapsulated substance. SLNs and NLCs show no difference in occlusivity, however, permeability differs as a matter of composition [114]. Permeation enhancement is a complex multifactorial process influenced by properties of both the carrier and active [106,115].

Lipid NPs also enhance oral absorption of poorly water-soluble drugs. Talegoankar et al. summarises several mechanisms that are involved in this enhancement. Besides adhesiveness of NPs to the GI mucosa, lipid NPs are digested by lipases present in the GI tract. Products of lipolysis solubilise poorly water-soluble drugs enhance their absorption. Another mechanisms involves enhancement of lymphatic transport and use of excipients acting as inhibitors of P- glycoprotein [106,111,116]. Besides application of lipid NPs for systemic delivery, they found their use also in treatment of local GI disorders. Physiological role of lipids supports their use as carriers acting alongside with the encapsulated active. For instance, phosphatidylcholine was shown to have anti-inflammatory effects with possible application in patients suffering from ulcerative colitis [117]. Moreover, Beloqui et al. demonstrated decreased *in vitro* production of

TNF-α, a cytokine playing the central role in inflammatory bowel disease [118], also in the presence of blank nanostructured lipid carriers. The nature of the carrier contributed to reduction of the pro-inflammatory cytokine [119,120].

2.4.2 Liposomes

Liposomes are defined as closed globular bilayer phospholipid vesicles of size 50-1000 nm [38,121]. The vesicular structure forms a core-shell structure, as show in **Figure 17**. Liposomes consist of the hydrophilic core and lipophilic shell enabling loading of a hydrophilic or/and lipophilic drug, respectively. This characteristic has led to a wide-spread use of liposomes in delivery of both small molecules and macromolecular genes [122]. An inherent disadvantage of use of liposomes as delivery systems is the risk of leakage through the fluid bilayer. Nevertheless, the leakage can be reduced by increasing the bilayer rigidity by the addition of cholesterol or sphingomyelins into the bilayer [38]. Multiple kinds of liposomes have been formulated and they can be classified in several categories, the most commonly based on their lamellarity (uni- and multilamellar liposomes) or circulation time (conventional and long-circulating liposomes) [121,123]. Besides the large number of applications in i.v. delivery [38,121,122], liposomes are considered attractive also as a topical delivery system [124].
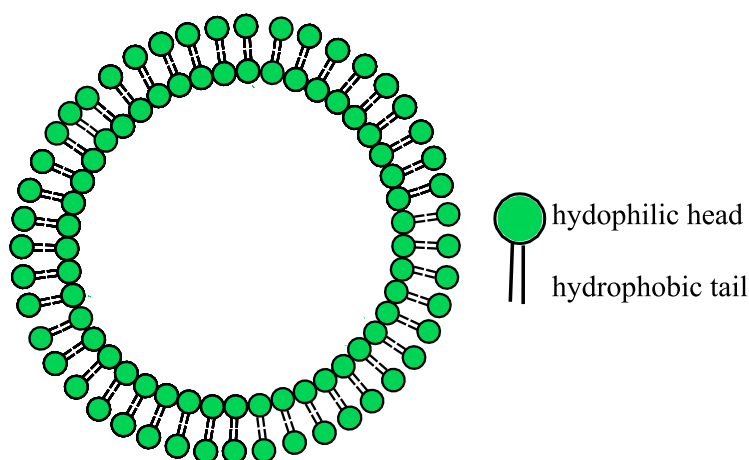
Figure 17: Structure of a liposome. Adopted from [60].

2.4.3 Nanoemulsions

Nanoemulsions are known as dispersions consisting of 2 immiscible liquids stabilized by an amphiphilic surfactant with size of the dispersed phase < 500 nm (**Figure 18**). Based on the distribution of the dispersed and the continuous phase, simple biphasic (oil-in-water O/W or water-in-oil W/O) or multiple (W/O/W) nanoemulsions are distinguished. Nanoemulsions are formed from macroemulsion and the process can be accomplished either by high energy or low energy approaches. High energy methods use HPH or ultrasonication to reduce the size of droplets of a preformed O/W macroemulsion into an O/W nanoemulsion. On the contrary, in low energy

approaches. size reduction of droplets of a W/O macroemulsion is completed by phase inversion into an O/W nanoemulsion and is induced by changes in composition or temperature of the system. This drug delivery platform is utilised in delivery of hydrophobic drugs via multiple administration routes. Besides parenteral and oral application, it found application in topical, nasal and ocular delivery [125–128].
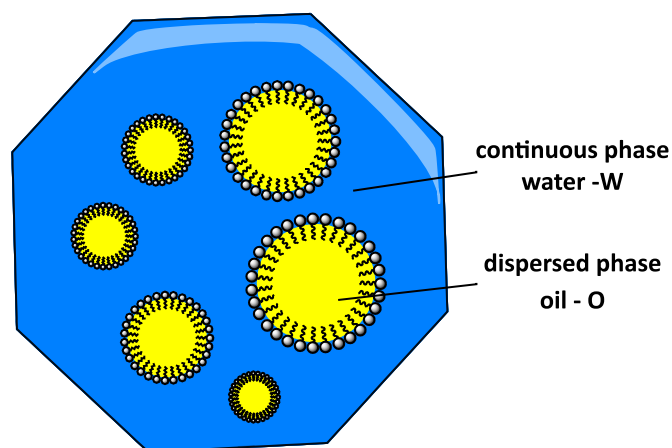
Figure 18: Structure of O/W (oi-in-water) nanoemulsion. Adopted from [60].

2.4.4 Pro-colloidal lipid systems: Self-emulsifying drug delivery systems

Self-emulsifying drug delivery systems (SEDDS) are isotropic mixtures of oils, surfactants, co-surfactants, and co-solvents forming fine oil-in-water nanoemulsions upon dispersion in an aqueous environment upon gentle agitation. These lipid-based systems are intended for oral delivery, traditionally for improvement of bioavailability of poorly water-soluble drugs [129,130]. SEDDS are administrated in soft gelatine capsules (**Figure 19**). From the industrial point of view, self-emulsifying drug delivery present an easily scalable and cost-effective drug delivery system. In addition, as the nanoemulsion is spontaneously formed at the site of action, e.g. in the GI tract, the long-term stability associated with the aggregation of nanodroplets is not of production concern [130,131].
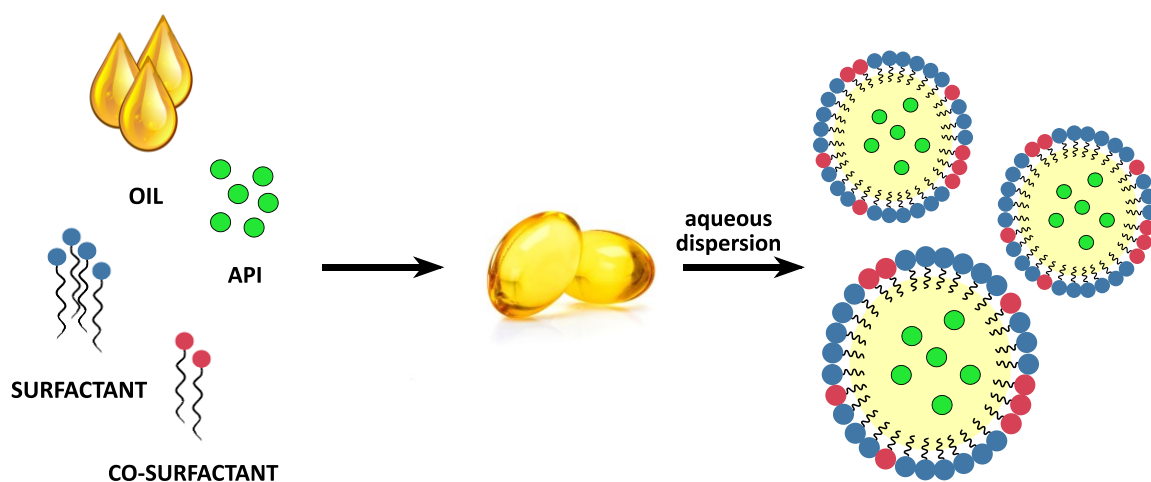
Figure 19: A scheme of self-nanoemulsifying drug delivery system (API – active pharmaceutical ingredient)

The mechanism of self-emulsification is yet to be fully understood. It is accepted that at a given temperature, self-emulsification occurs when the change in entropy of dispersion is greater than the energy required to increase the surface area of the dispersion [132]. In contrast, spontaneous dispersion does not occur as the interfacial energy of the newly formed interface is too high what makes the process thermodynamically unfavourable. The emulsification energy needs to be added to overcome this barrier. Self-emulsification occurs as less emulsification energy is required. Surfactants and co-surfactants reduce the interfacial energy by creating a monolayer on the surface of emulsion preventing them from coalescence (**Figure 19**) [133].

2.4.4.1   The role of lipid material

The role of lipids in increasing bioavailability of poorly water-soluble drugs paved the way for designing these delivery systems. Poorly water-soluble molecules are usually well-soluble in lipids and SEDDS deliver these molecules to the site of absorption in a dissolved state. However, this process is much more complex, as the environment of the GI tract comes to interplay, such as lipid digestion, present solubilising bile acids and endogenous phospholipids [134]. This leads to formation of various colloidal phases, the drug can partition between them and finally gets absorbed [135]. These processes circumvent the limiting dissolution of the drug in the GI tract and thus increases bioavailability [130].

However, lipid excipients used to form SEDDS act not only as a carrier, but also can impact drug absorption via multiple mechanisms [136,137]. Lipids slow gastric emptying [138] and some lipids and surfactants reduce P-glycoprotein efflux transporter [139,140] or drug metabolism via cytochromes [139,141]. In addition, for highly lipophilic drugs with logP > 5 and with solubility in triacylglycerols > 50mg/g, unsaturated long chain fatty acids promote lymphatic transport reducing first-pass metabolism by the liver [142,143].

Recently, the interest has expanded from improving bioavailability of poorly water-soluble drugs also to hydrophilic macromolecules, such as peptides, proteins or nucleic acid-based drugs. In the first step, a hydrophilic macromolecule is made more hydrophobic. For this purpose, it is complexed with a surfactant by hydrophobic ion pairing [144]. The complex can be formed through either electrostatic bonding or dipole-dipole interaction [145].

Subsequently, the hydrophobic complex is dissolved in a SEDDS preconcentrate (undispersed, water-free SEDDS). The SEDDS can be designed to enhance permeation enabling delivery of macromolecular payload. They are based on excipients that act as permeation enhancers, such as medium chain fatty acids (MCFA). SEDDS containing MCFA act as physiological permeation enhancers [146] and promote paracellular absorption unlike SEDDS composed of long chain fatty acids [147].

A detailed mechanism beyond promotion of paracellular transport and opening of TJs between enterocytes was examined by Hayashi et al. MCFA increase intracellular calcium level that induces contraction of actin filaments leading to TJs opening [148]. More recent studies show that MCFA and excipients derived from them act also as transcellular permeation enhancers via mild mucosal aberration. This effect seems to be concentration dependant involving also paracellular transport at lower concentrations of MCFA [145].

Various macromolecules, such as proteins, polysaccharides or nucleic acids, were successfully formulated into SEDDS, as reviewed by Mahmood et al. [131]. However, deeper understanding of processes after emulsification and interactions between hydrophobic complexes and the complex GI environment is necessary.

2.4.4.2 Excipients utilised in SEDDS formulation

- Captex 300

Captex 300 is a MCFA triglyceride, containing around 70% of caprylic fatty acid (C8) and around 27% of capric fatty acid (C10) (**Figure 20A**), traces of caproic (C6) and lauric fatty acid (C12) can occur. Captex 300 originates from food-grade vegetable materials and is generally recognised as safe (GRAS) [149]. Captex 300 is a polar insoluble non-swelling lipid, an oil creating the oily phase of emulsion [130,150] and is soluble in most organic solvents. MCFA, in particular C10, were found to act as potent physiologically acting intestinal permeation enhancers [146]. Their triglycerides, however, do not enhance permeation. GI lipases have to digest these lipids to liberate MCFA [151].

- Labrasol

Labrasol is a liquid non-ionic surfactant known under a chemical name caprylocaproyl macrogol-8 glyceride (**Figure 20B**). It composed of C8/C10 fatty acids of mono-and diesters of

PEG 400 and mono-, di- and triacylglycerides with mainly C8 and C10 and some free PEG 400 [130]. Labrasol has HLB value of 14 that classifies it as a water-soluble amphiphile according to Small´s classification of lipids [150]. It is listed in both European Pharmacopeia and FDA Inactive Ingredients Guide [149]. Labrasol enhances oral bioavailability. At lower concentrations (0.1 -1 %) Labrasol was shown to open TJs of enterocytes and thus act as a paracellular permeation enhancer [152]. As the concentration increases over 1%, it tends to act transcellularly causing mild mucosal aberration [145,153]. Labrasol can be employed to enhance intestinal permeability of hydrophilic drugs, such as gentamicin [154] or insulin [153].

- Mono-acyl phosphatidyl choline (MAPC)

MAPC, also known as lysophosphatidyl choline, is a digestion product of phosphatidyl choline that is absorbed by passive diffusion in the small intestine.. [155]. Its chemical structure is displayed in **Figure 20C**. As a soluble amphiphilic lipid (IIIA), it proved its ability to act as a natural emulsifier for o/w emulsions [150,155]. In addition, MAPC enhanced permeability of 1-deamino-8-D-arginine-vasopressin (~ 1 000 Da) across Caco-2 monolayer [156] and also permeability of dextrans (3 000 and 10 000 Da) in a rat experimental model [157]. Besides reduction of synthetic surfactants in formulations, MAPC also inhibits lipolysis of glycerides and Labrasol [158].

- Citrem

Citrem is a complex mixture of various citric acid esters of mono- and diglycerides and mono- and diacylglycerides. Oleic and linoleic fatty acid together represent over 85% (w/w) of total fatty acids in Citrem (**Figure 20D**). Citrem is a common emulsifier in the food industry [159]. This food additive described as GRAS has found its application also in pharmaceutical technology, e.g. stabilizing infant formula [159]. Azmi et al. investigated Citrem-phospholipid nano-assemblies. Increasing Citrem content resulted in increasing negative surface charge and thus provided better electrostatic stabilization of nano-assemblies [160]. In addition, local decrease of pH related to the negative surface charge forms an unfavourable environment for protease. This could be beneficial in oral peptide/protein delivery [161].

- Maisine CC

Maisine CC is a trade name glyceryl monolinoleate (**Figure 20E**). It conforms with the description of the monograph in European and US Pharmacopeia and is considered GRAS [149]. It is a liquid excipient derived from corn oil glyceride. Its HLB value of 1 makes it a suitable oily vehicle. Upon oral administration, Maisine is digested by lipases, promotes lymphatic absorption and enhances oral bioavailability [162]. Therefore, it is one of typical excipients used of SEDDS [130].

- Peceol

Peceol is composed mainly of glyceryl monooleate (**Figure 20F**). Its properties are similar to Maisine CC, being a liquid excipient of HLB value 1 it could be used as an oily vehicle for bioavailability enhancement [162]. Peceol is considered GRAS and is used for oral bioavailability enhancement [130,149].
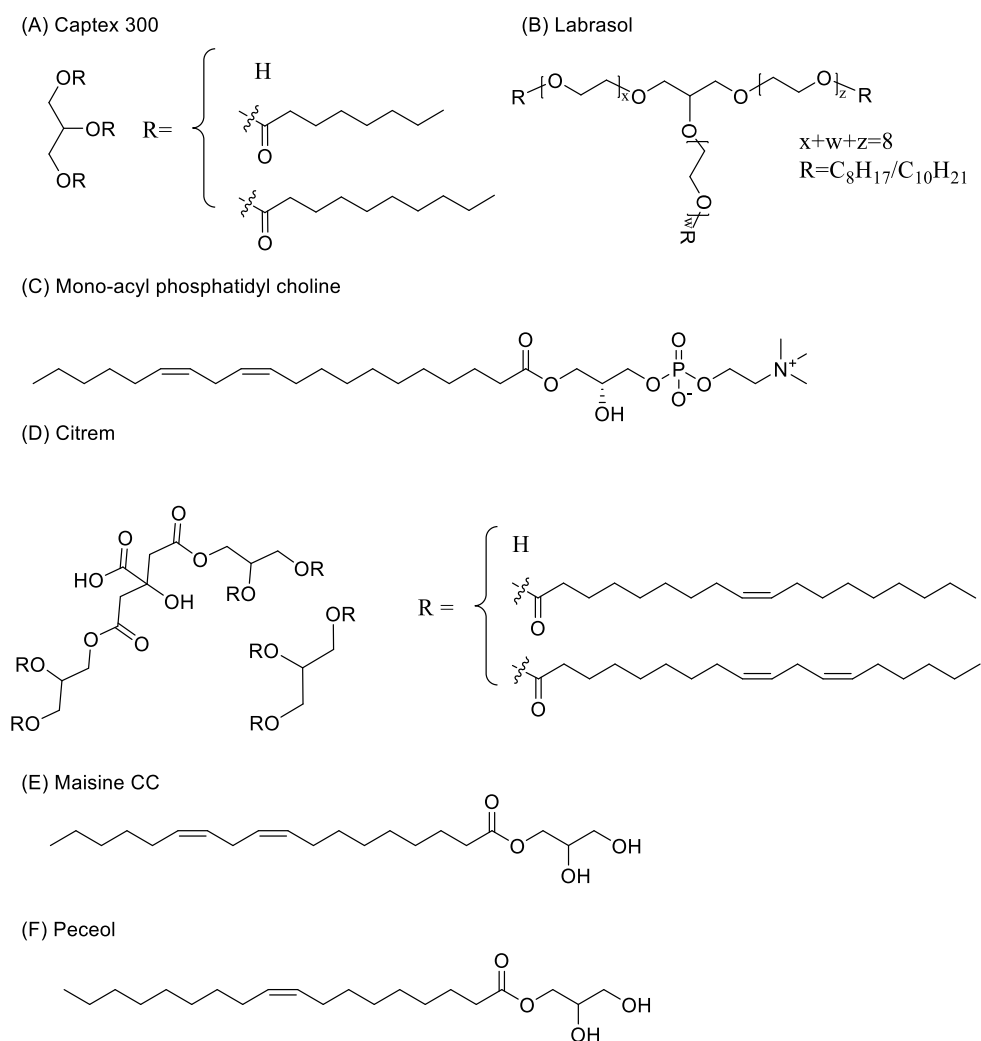
Figure 20: Chemical formulas of SEDDS excipients. (the structure of Labrasol adapted from [163], the structure of Citrem adapted from [159]).

2.5 Nanomaterials for immunomodulation

The immune system is a powerful and complex defence system of an organism. In a diseased state this system loses the right balance. Its dysfunction can be characterised by its reduced activity known as immunosuppression or, on the other extreme, by hyperactivity against own antigens. Immunomodulation is a process of restoring the function of the immune system to the physiological range and nanomaterials can play an important role in this process. The use of nanomaterials is an emerging approach to immunomodulation.

Direct immunomodulation is provided by the nanomaterial itself, in contrast, indirect immunomodulation centres around a substance loaded in a nanoparticulate carrier and the loaded substance is in charge of the action. There have been many nanomaterials utilised, however, biocompatible and biodegradable biologically relevant materials are gaining more attention.

Among the most utilised nanomaterials for immunomodulation are directly acting fullerenes as well as versatile liposomes and micelles that can be made of a wide range of lipids. Lipid NPs can successfully combine the action of a carrier and loaded substance on the immune system. In addition, easily adjustable polymer-based NPs open up the way towards stimuli responsiveness in immunomodulation. Well-defined structure of dendrimers with multiple possibilities of surface functionalisation found their application mainly in immunostimulation. Self-assembling nanogels are known to act as chaperons of biomolecules also in field of immunology, and nanoemulsions became well-established as vaccine adjuvants.

Delivery of immunomodulators by conventional drug delivery systems is often accompanied by adverse effects outside the targeted tissue or cell population. Nanomaterials have showed a tremendous potential for site specific delivery and sustained release. Moreover, a nanomaterial itself could provide benefits to restoration of the right balance of the immune system.

This topic was summarised and reviewed in detail by Kubackova, J., et al. as Nanomaterials for direct and indirect immunomodulation [60]. The published review can be found as *Appendix I*.

2.6 Challenging formulations

2.6.1 A hydrophilic tracer as a model for intracellular delivery

In many chronic inflammatory disorders, inflammation exceeds its originally protective function and overproduction of pro-inflammatory mediators harms the organism itself. This leads to extensive production of numerous components of the immune system that participate in inflammatory response. One of the key players that increases inflammation and stimulates the immune system are macrophages. These cells are a part of the mononuclear phagocytic system and exhibit phagocytic activity in order to scavenge foreign particles, blood debris or pathologically altered body cells. The largest population of tissue macrophages, Kupffer cells, reside in the liver and are considerably involved in the innate immune response. Their activation leads to production of proinflammatory mediators [164] and the inflammation develops further.

The idea of regulating the inflammation at the very beginning of the inflammatory process is particularly attractive. Thus, the level of gene expression via intracellular receptors is often targeted. Current anti-inflammatory treatment downregulates this level of inflammation
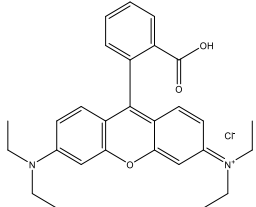
employing intracellular receptors, namely agonists for corticosteroid receptors are widely utilized in the ant-inflammatory therapy. However, due to unspecific targeting of systematically applied drug, adverse effects (e.g. increased risk of infections or changes in metabolism) are common. All the serious adverse effects stress the demand for new approaches.

Intracellular receptors, such as Pregnane X Receptor, have been found to play an important role in inflammatory responses [165,166]. The attention has been turned to alternative intracellular receptors influencing inflammation process, e.g. Liver X receptor [167]. Agonists of these receptors inhibit inflammatory reactions more effectively than commercially available drugs, e.g. dexamethasone [168].

Drug delivery systems can optimize delivery of the potent agonists to the aforementioned intracellular receptors. In search of suitable carriers, polymeric NPs have shown their potential [77,79]. Subcellular size ranging between 100 nm and 300 nm and negative surface charge NPs enhance passive targeting to phagocytic macrophages in the liver and spleen [19]. In the bloodstream, the negatively-charged PLGA nanoparticles are rapidly opsonised and thus recognised and cleared by macrophages, mainly by Kupffer cells in the liver sinuses [169]. In addition, inflamed tissue is characterised by increased vascular permeability that enables passive targeting of the nanosized carriers [17]. The advantage can be taken of many other properties of this dosage form, such as biocompatibility and sustained drug release profile [85]. Sustained drug release profile can be of interest for action on intracellular receptors.

In this study, we aimed to create a non-toxic carrier enabling intracellular delivery and sustained release over a period of several days. Due to further potential use of the NPs for delivery to phagocytic cells, we employed biodegradable low-molar weight PLGA to formulate NPs attractive to phagocytic cells (size up to 300 nm, negative surface charge). In order to better understand interactions between the formulated NPs and phagocytic cells, we loaded the NPs with a fluorescent tracer Rhodamine B (RhB). We worked towards optimisation of two preparation methods, namely nanoprecipitation and evaporation solvent emulsification method. In addition, we evaluated impact of several variables (type and concentration of surfactant, type of PLGA polymer) on the key properties of formulations, such particle size, zeta potential and encapsulation efficiency.

Table 3: Physicochemical properties of Rhodamine B. n.a.=not applicable
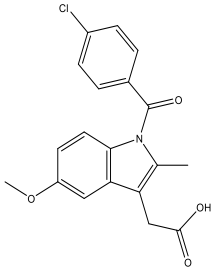
	Chemical structure	Molecular weight	pKa	Log P	Water solubility	Reference
Rhodamine B		479 g/mol	n.a.	1.95	very soluble	PubChem

2.6.2 Poorly water-soluble indomethacin

Non-steroidal anti-inflammatory drugs are frequently utilised in the management of inflammation. These drugs inhibit cyclooxygenase enzymes. Cyclooxygenase-2 is an enzyme inducible at inflammatory sites and in governs production of inflammatory mediators – prostaglandins. On the other hand, cyclooxygenase-1 regulates physiological processes and its inhibition during the anti-inflammatory treatment causes adverse effects such as GI problems. In addition to the adverse effects related to non-specific targeting, poor water-solubility hampers their delivery. These facts made non-steroidal anti-inflammatory drugs suitable candidates that benefit from encapsulation in polymeric or lipid carriers [170]. Kumar et al. investigated preparation of SLNs made of Capmul (glycerol stearate) and Gelucire (stearoyl-macrogol-32 glycerides). Encapsulation and controlled release of ibuprofen, ketoprofen and nabumetone from the lipid NPs were tested [171]. Diclofenac sodium was formulated into SLNs (glycerol monostearate, phospholipids) and the formulation was thoroughly characterised [172].

Indomethacin (IND) is one of the widely utilised nonsteroidal anti-inflammatory drugs. It is an indoleacetic acid derivative practically insoluble in water. Its physicochemical properties are summarised in **Table 4**. Castelli et al. formulated IND NLCs using high-speed stirring homogenisation followed by ultrasonication of hot pre-emulsion from Compritol (glycerol behenate) and Miglyol 812 (caprylic and capric triglycerides) [173]. Hippalgaonkar et al. prepared SLNs also based on Compritol aimed for ocular administration. Hot pre-emulsion was homogenised by a high speed-stirrer and subsequently subjected to high pressure homogenisation. Obtained 140 nm SLNs showed increased corneal permeation relative to IND solution and IND cyclodextrin-based formulation [174].

Table 4: Physicochemical properties of IND

Drug	Chemical structure	Molecular weight	pKa	Log P	Water solubility	Reference
Indomethacin		357.8 g/mol	4.5 (weak acid)	4.27	0.937 mg/L at 25 °C (practically insoluble)	PubChem

In this study, we have chosen formulation approaches with organic solvents instead of high energy approaches previously utilised in formulation of IND lipid NPs. GMS and SA are commonly used in formulation of lipid NPs [170,171,175] and due to its availability they were utilized also in this study. Lecithin is poorly soluble in water-miscible organic solvents, such as ethanol or acetone, thus is not suitable for nanoprecipitation method. In this method we replaced it with a surfactant that has a similar HBL value. Span 20 (sorbitan monolaureate) is a non-ionic surfactant with HLB of 8.6 miscible with alcohols and thus it could be used to prepare lipid NPs using nanoprecipitation. The properties of utilised excipients are summarized in **Table 5**.

Table 5: HLB values and solubility of NLCs excipients.

		Solubility [177]	
	HLB [176]	Water-miscible solvents	Water-immiscible solvents
Glycerol monostearate	3.8	hot ethanol, hot acetone	✔
Isopropyl myristate	-	✔ ethanol, acetone	✔
Lecithin	~ 8	✗	✔
Stearic acid 50	-	✔ ethanol	✔
Span 20	8.6	✔	✔
Kolliphor P188		✔ water, ethanol	
	29	✗ isopropanol, propylene glycol	✗ xylene

2.6.3 Sensitive oligonucleotide for oral delivery

Gene therapy is based on introduction of protein-coding or non-coding DNA or RNA into an organism in order to reverse pathological processes. The introduced nucleic acid is designed to supress pathological overexpression of proteins, to correct malfunctioning proteins, or to enhance expression of missing proteins [178]. Naturally occurring nucleic acids are water soluble polyanionic molecules sensitive to degradation by abundantly present nucleases. Moreover, their polyanionic and macromolecular nature leads to poor permeability across the cell membrane of targeted cells [179,180].

In order to take advantage of highly potential gene therapy, the limiting properties of nucleic acids have to be circumvented. The most common approaches include chemical modifications of these macromolecules or protective drug delivery systems of viral or non-viral origin [180]. Non-viral carriers have gained more attention due to their increasing safety profile, even though their efficiency is lower compared to their viral counterparts [178,180].

A widely utilised non-viral strategy to deliver anionic DNA is to complex them with cationic lipids (mainly preformed liposomes) or cationic polymers, forming lipoplexes or polyplexes, respectively [181]. Large DNA molecules collapse upon interaction with polycationic lipids or polymers forming relatively stable complexes. In contrast, shorter oligonucleotides, e.g. siRNA, are more prone to destabilisation upon contact with the complex environment of an organism. Nevertheless, it is accepted that in the case of lipid complexes, the basic mechanism of encapsulation of a nucleic acid in a lipid shell is independent of the kind and length of the nucleic acid [182].

Besides commonly utilised approach using preformed liposomes consisting of cationic and neutral lipids [181], hydrophobic ion pairing represents a more straightforward technique, in which cationic lipids are added as monomers or in micellar form. The technique is based on replacement of counterions of a nucleic acid by cationic lipid-based surfactants that form a lipid shell around the core consisting of the nucleic acid [144]. Hydrophilicity of the complexed nucleic acid decreases and the formed ion-paired complex results into a lipophilic reverse micelle [183,184]. The critical physicochemical properties of oligonucleotides (OND), such as hydrophilicity and polyanionic nature, are influenced by their phosphodiester backbone [179]. The properties conserved across any nucleotide sequence would enable application of this delivery strategy to any desired functional OND with only minor modifications of the delivery strategy. In this study, hydrophobic ion pairing was employed to reduce hydrophilicity of a non-specific 20-mer fluorescently labelled OND to enable loading of this macromolecule into SEDDS.

By utilising SEEDS as a well-established oral drug delivery system, we intended to deliver the complexed OND locally into the lamina propria of the small intestine affected by inflammation. Pathophysiological changes characteristic for the inflammatory lesions can be utilised to enhance targeting to this area. The changes include leaky epithelium, alteration in the protective mucus layer and overexpression of positively charged proteins. In addition, highly active phagocytic cells invade the inflamed intestinal tissue [26,185]. An anti-inflammatory acting oligonucleotide, such as anti-TNFα RNA, delivered locally into pro-inflammatory macrophages could attenuate the intestinal inflammation.

The aim of this project was to investigate the possibility of delivery of OND into the intestinal lamina propria employing TJs opening SEDDS. The utilised excipients are described in detail in section 2.4.4.2. The objective was to formulate a drug delivery system that could protect

OND upon oral administration and deliver it locally across the intestinal Caco-2 cell monolayer. The formulation scheme is shown in **Figure 21**.
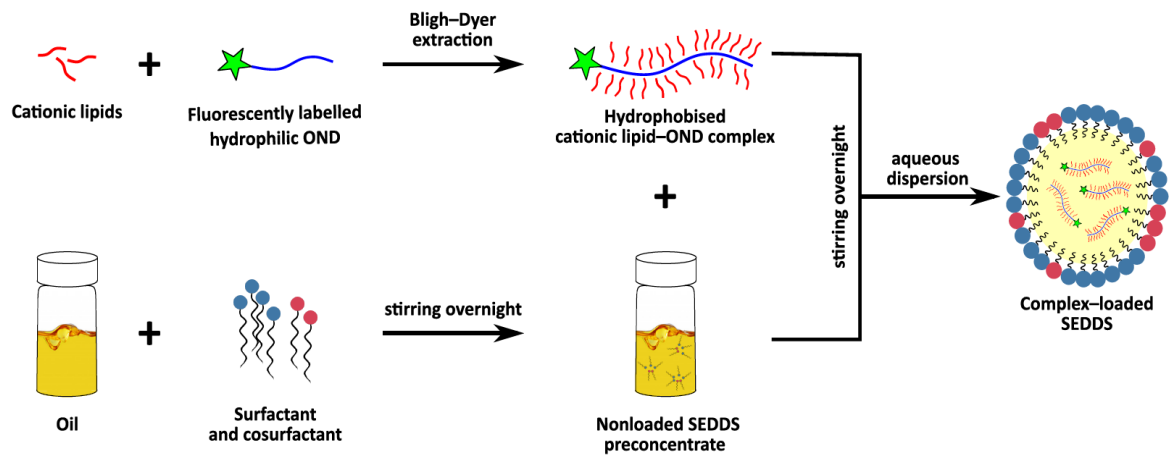
Figure 21: Formulation scheme of an oligonucleotide (OND) into self-emulsifying der delivery system (SEDDS) for oral administration.

3   AIM OF THE WORK

The aims of this work were as follows:

- Formulation of polymeric nanocarriers with sustained release
    - Optimization of nanoprecipitation and emulsification solvent evaporation method for formulation of monodisperse stable nanoparticles of size up to 300 nm and negative surface charge
    - Evaluation of the role of various kinds of surfactants, their concentration in the preparation method and on properties of yielding nanoparticles
    - Performance of a release study and evaluation of impact of pH on the release profile

- Formulation of lipid-based nanocarriers for delivery of a poorly water-soluble drug
    - Optimization of nanoprecipitation and emulsification solvent evaporation method for formulation of monodisperse stable nanoparticles of size up to 300 nm and negative surface charge
    - Characterization of phase behaviour of lipid nanoparticles
    - Assessment of solubility of indomethacin in lipid nanoparticles

- Formulation of lipid-based self-emulsifying drug delivery system for oral administration of an oligonucleotide
    - Hydrophobization of an oligonucleotide by formation of ion-paired complexes between an oligonucleotide and a cation lipid
    - Loading of the formed hydrophobic complexes into a tight- junction opening self-nanoemulsifying drug delivery, characterisation of the dispersed systems in terms of size, surface charge, protective effect against nucleases and behaviour in the presence of lipases
    - Evaluation of the loaded systems *in vitro* in intestinal Caco-2 monolayer to assess permeability and cytotoxicity of these systems

4 POLYMERIC NANOCARRIERS WITH SUSTAINED RELEASE TARGETING INTRACELLULAR RECEPTORS OF MACROPHAGES

The aim of this chapter was to optimise preparation methods of polymeric NPs. The overall objective was to prepare NPs enabling intracellular delivery of a model fluorescent substance RhB. We aimed to identify appropriate combinations of a polymer and a surfactant for the formulation. The NPs were intended for the liver resident macrophages, Kupffer cells. Moreover, the most promising formulations were subjected to release studies in various model media relevant to their fate upon i.v. administration.

The tailored composition of PLGA NPs and optimised preparation methods were utilised to formulate RhB into NPs for delivery to macrophages. Results of this study were published by Boltnarova et al. in PLGA Based Nanospheres as a Potent Macrophage - Specific Drug Delivery System [25]. The publication can be found as *Appendix II*.

4.1 Materials and methods

4.1.1 Materials

Tested polymers, linear PLGA 5/5 (Lactic: Glycolic acid ratio 50:50, M_w: 2 400 g/mol) and PLGA 7/3 (Lactic: Glycolic acid ratio 70:30, M_w: 3 200 g/mol), branched PLGA, star-like PLGA using a branching unit tripentaerythritol in concentration 1 (PLGA T1) and 3% (PLGA T3) (equimolar ratio of lactic and glycolic acid, M_w 12 300 g/mol, 17 400 g/mol and 10 900 g/mol, respectively), and comb-like PLGA branched on a backbone of polyacrylic acid (M_w 2 000 g/mol) in concentration 2% (PLGA A2) (equimolar ratio of lactic and glycolic acid, M_w 14 400 g/mol) [94] were kindly provided by assoc. prof. Dittrich, Faculty of Pharmacy in Hradec Kralove, Charles University. Rhodamine B, Pluronic® F127. Kolliphor® P188, Tween® 20 and PVA (M_w 31 000 – 50 000 g/mol, 87 – 89% hydrolysed) were purchased from Sigma-Aldrich (Merck Group, Darmstadt, Germany). Deionised (DI) water was purified by Elix Essential Water Purification System (Merck, Darmstadt, Germany). All other chemicals were of analytical grade and commercially available.

4.1.2 Preparation of polymeric NPs

4.1.2.1 Nanoprecipitation method (NPM)

30 mg of a tested polymer and 250 µg of RhB were dissolved in 1 mL of acetone. This organic solution was added into 10 mL of 0.1% or 1% (w/v) aqueous solution of a tested surfactant under stirring at constant speed (300 rpm).

4.1.2.2 Emulsification solvent evaporation method (ESE)

30 mg of a tested polymer and 250 µg of RhB were dissolved in 1 mL of ethyl acetate. The organic phase was added into 5 mL of 0.1%, 0.5% or 1% (w/v) aqueous solution of surfactant and sonicated for 1 min at the power output 70 W using the sonication probe Mikrospitze (Bandelin sonoplus, Berlin, Germany). while being cooled in the ice bath. Subsequently, the formed emulsion was poured into 5 mL of 0.1% (w/v) aqueous solution of surfactant.

4.1.2.3 Purification of NPs prepared using NPM and ESE

Formed NPs were allowed to harden by evaporation of the organic solvent for 2 hours under atmospheric pressure and constant stirring (300 rpm). The DI water was added to final volume of the 10 mL, if necessary. Subsequently, the dispersion was centrifuged with the MPW 260R, MPW Medical Instruments centrifuge (MPW, Warsaw, Poland). Upon centrifugation, the supernatant was discarded, and pelleted NPs were resuspended in DI water. The procedure was repeated three times.

4.1.3 Characterisation of polymeric NPs

4.1.3.1 Particle size and zeta potential

100 µL of raw nanosuspension was added to 3900 µL of DI water. The diluted nanosuspension was evaluated in terms of size, polydispersity index (PdI) and zeta potential with Zetasizer Nano ZS (Malvern Panalytical, Malvern, United Kingdom). Size and PdI were evaluated using dynamic light scattering. The intensity of scattered light was measured at a backscattering detection angle of 173° and the intensity size distribution was reported. Zeta potential was measured using electrophoretic light scattering in DTS1070 folded capillary cuvettes. Both for size and zeta potential measurement, the samples were allowed to equilibrate at 25 °C for 120 seconds and the measurement was performed for three times.

4.1.3.2 Determination of encapsulation efficiency

Encapsulation efficiency (EE) was calculated using Equation (1). NPs collected upon centrifugation were dissolved in acetonitrile. Absorbance at wavelength of 556 nm of the solution was measured using Specord 205 (Analytik Jena, Jena, Germany). Applying this method, we determined encapsulated amount of RhB. Collected mass of NPs was evaluated gravimetrically upon evaporation of acetonitrile.

$$EE = \frac{encapsulated\ amount\ of\ RhB}{initial\ amount\ of\ RhB} \times 100\ \% \qquad (1)$$

4.1.4 Stability study

Stability of NPs was evaluated in particles prepared by NPM from PLGA A2 in combination with 0.1% F127, as described in section 4.1.2. NPs were stored in the fridge (4-8°C) in water, phosphate buffer saline (PBS), pH7.4 and in acetate buffer, pH 4.0 for 30 days. Each workday a sample was withdrawn, and the size and PdI were measured using Zetasizer Nano ZS (Malvern Panalytical, Malvern, United Kingdom).

4.1.5 Drug release

Drug release from PLGA NPs prepared by NPM was tested using membrane diffusion method [186]. The tested media involved saline solution (154 mM sodium chloride), 0.01 M acetate buffer in saline solution of pH 4.5 (4.5 mM sodium acetate, 5.5 mM acetic acid, 154 mM sodium chloride) and 0.01 M HEPES buffer in saline solution of pH 7.4 (10 mM HEPES, 154 mM sodium chloride).

Upon purification of NPs, the supernatant was discarded, and the pelleted NPs were redispersed in the sufficient amount of the tested medium. The dialysis membrane (cellulose, MWCO 6 000-8 000) was cut into 10 cm-long pieces. A membrane piece is bent into a U-shaped loop was filled with 1 mL of nanosuspension. The ends of the membrane were folded and glued together with superglue.

The filled dialysis membrane was placed into a 20 mL vial. 10 mL of medium is pipetted in carefully. Vials were placed into a shaking water bath tempered at 37°C. Samples were withdrawn at 30 min, 1, 2, 4, 6, 12, 24, 32 and 48 hours. At every time point, the entire volume of the medium was collected into a beaker and replaced by 10 mL of fresh medium. After the experiment, 200 µL of the samples were pipetted into a transparent 96-well plate and fluorescence was evaluated using the plate reader at excitation/emission 485 nm/620 nm (Synergy 2 Biotek plate reader (BioTek, Winooski, VT, USA).

4.1.6 Statistical analysis

Statistical analysis was performed with the Graph Prism 8 (GraphPad Software, San Diego, California, USA). Data was assessed by two-way ANOVA followed by a suitable post hoc test. Data is presented as mean ± standard deviation (SD). Significant difference was considered at $p < 0.05$.

4.2 Results and discussion

4.2.1 Preliminary experiments

The concentration of 30 mg PLGA/10 mL aqueous phase was chosen as this was the highest amount of the polymer that did not lead to significant aggregation upon preparation of NPs. Regarding the choice of surfactant concentration, we aimed to use as low concentrations as possible due to their reported toxic effect in *in vitro* experiments. The study by Grabowski et al. showed a toxic effect of surfactant concentrations above 1 mg/mL (0.1%) in nanoparticulate formulations [187]. It is noteworthy that the final concentration of surfactant is expected to lower after purification of prepared NPs.

In NPM, we initially worked with two linear polymers (PLGA 5/5 and PLGA 7/3) and three branched polymers (PLGA T1, PLGA T3 and PLGA A2) in combination with one of two poloxamers (poloxamer 407: Pluronic® F127 and poloxamer 188: Koliphor® P188), PVA and Tween® 20. After initial screening experiments, both T branched polymers showed low EE (< 20%) of RhB and poor stability. This might be influenced by absence of anionic terminal carboxyl groups and relatively higher hydrophilicity of these star-branched polymers. Finally, we excluded the PLGA T1 and PLGA T3 from all further experiments.

In ESE optimisation we tested high sheer homogenizer and ultrasonication probe as energy sources to emulsify two immiscible phases, ethyl acetate and the aqueous solution of surfactant. When working with the homogenizer, the resulting nanosuspension was heterogeneous (PdI>0.5) and the size of formed NPs was unsatisfactory (>500 nm). The results obtained from emulsification with the ultrasonication probe were more favourable and are presented in the following sections. This emulsification method of choice was further optimised in terms of ratio of organic and aqueous phase used in sonication. We tested ratios 1:10, 1:5 and 1:1 (organic: aqueous phase) while cooling the sonicated system in the ice bath. Sonication of a system at ratio 1:10 resulted into foam formation and NPs of undesirable size (>500 nm). In the case of ratio 1:1, the emulsion tended to disintegrate upon pouring into the remaining aqueous phase and further sonication was required. Based on these observations, we sonicated two immiscible phases at ratio 1:5 (organic: aqueous phase) in the experiments presented further.

4.2.2 Formulation process

4.2.2.1 Nanoprecipitation method (NPM)

In order to better understand the formulation process of PLGA NPs, we screened through three kinds of polymers, PLGA 5/5, PLGA 7/3 and PLGA A2, and four kinds of surfactants, namely Pluronic F127, Kolliphor P188, PVA and Tween 20 (**Figure 22**).

The formulated NPs were evaluated in terms of size and PdI, as shown in **Figure 22AB**. No significant effect of either the kind of polymer or surfactant was observed. The size of NPs was influenced neither by higher molar weight nor by branched molecular architecture of PLGA A2 and particulate size was comparable to its linear polymeric counterparts. All formulations could be considered monodisperse as PdI value was lower than 0.2 [188].

Figure 22C shows zeta potential of PLGA NPs prepared by NPM. The tested surfactants are non-ionic, and the negative surface charge of NPs is due to acid-terminated PLGA. No significant difference was observed among various kinds of PLGA polymers formulated with the same surfactant. A difference was observed as NPs formulated with PVA showed significantly higher zeta potential ($p<0.05$) relative to other surfactants. Deposition of PVA on the surface of NPs prepared by NPM was previously reported as increased amount of surfactant correlated with bigger NPs. In the study, zeta potential was not assessed [189]. Therefore, it could be hypothesised that the deposition of this surfactant resulted in masking of the surface charge. We observed that an increase in PVA concentration from 0.1 % to 1% changed the surface charge from - 17.1 ± 1.7 mV to -9.5 ± 0.9 mV, respectively (data reported as the average of zeta potential from all PLGA polymers tested). However, the size did not increase significantly when using higher concentration of PVA, as it could be expected due to the potentially deposited layer of PVA.

Finally, the effect of the utilised polymer and surfactant on EE of RhB was investigated (**Figure 22Error! Reference source not found.D**). Significantly higher EE was observed in combination of surfactant Pluronic F127 with polymers PLGA 7/3 and PLGA A2 relative to combination of Kolliphor P188, PVA and Tween 20 with these polymers (*p<0.05). In addition, branched PLGA A2 NPs were capable of loading the highest quantitates of RhB (#p<0.05, relative to other polymers when formulated with 0.1% Pluronic F127). This confirmed our hypothesis, that RhB loading is achieved mainly via ion-pairing mechanism between PLGA carboxyl groups and RhB quaternary nitrogen. Amongst all tested materials, PLGA A2 is the one that is characterized with the highest number of carboxyl groups per mol owing to use of polyacrylic acid as branching entity.
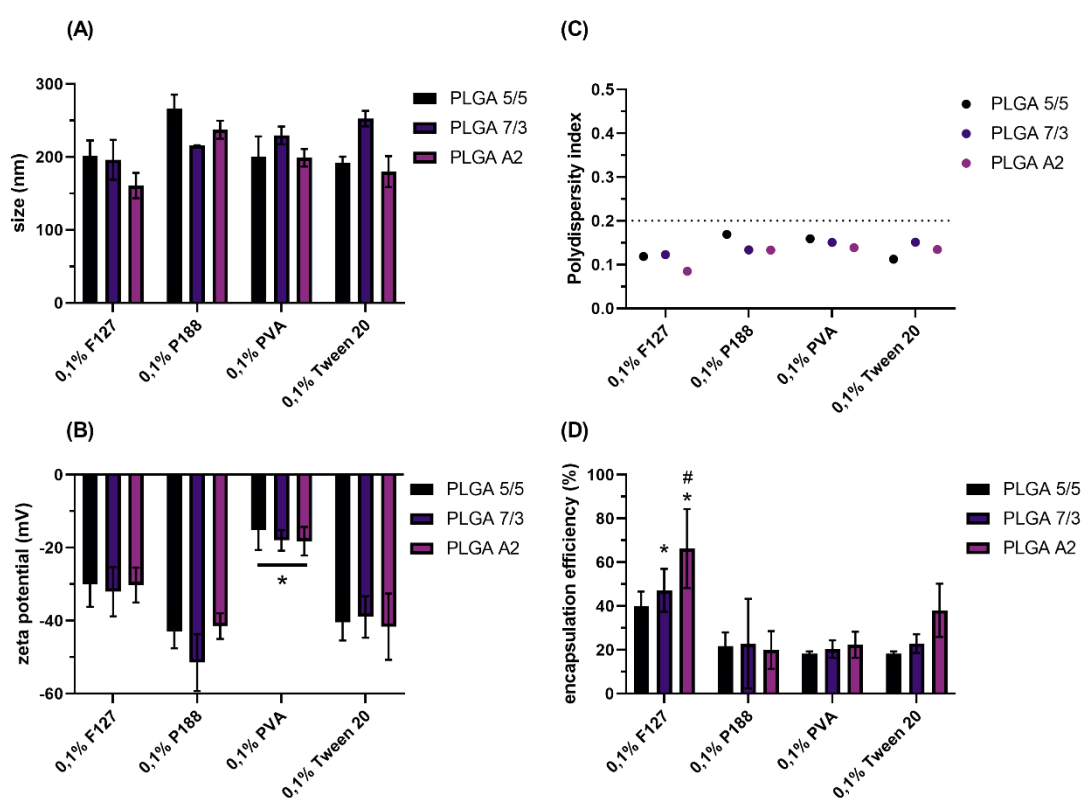
Figure 22: Characterisation of PLGA NPs prepared using NPM. NPs were characterised in terms of (A) size, (B) polydispersity index, (C) zeta potential, and (D) encapsulation efficiency. The dotted line in (B) depicts the limit up to which NPs are considered monodisperse. In (C), *p< 0.05 statistically significant difference in zeta potential relative to formulations prepared with other surfactants. In (D), *p< 0.05 statistically significant difference in EE relative to other surfactants in combination with the same polymer. #p< 0.05 statistically significant difference in EE relative to other polymers in combination with the same surfactant. Data is presented as mean ± SD, n=2-5. F127 – Pluronic F127, P188- Kolliphor P188

4.2.2.2   Emulsification solvent evaporation method (ESE)

For the experimental setup of ESE, two polymers were evaluated, the linear PLGA 5/5 and the branched comb-like PLGA A2, in combination with three surfactants at three concentrations (**Figure 23**). The main characteristics, such as size, PdI, zeta potential and EE, were assessed.

Figure 23AB depicts the size dependence of size of NPs on the concentration and the type of used surfactant, the type of utilised polymer did not play a role (except from 0.1%PVA). In both polymers (except from PLGA A2 in combination with 0,1% solution of surfactants), the analysis showed a significant impact of the type of surfactant, however, the concentration of a surfactant had a more pronounced influence. Increased surfactant concentration decreases surface tensions more efficiently so smaller NPs can be formed with increasing surfactant concertation. This phenomena has already been described with increasing concentration of PVA, however, we extended the range of tested surfactants [189–191]. Out of the three tested surfactants, poloxamer 407 (Pluronic® F127) enabled formation of the smallest particles at the given concentration (except from PLGA A2 in combination with 0.1% solution of surfactants where no significant size difference was shown among the different surfactants). The HLB of F127 is 22 and is higher than the values of the other surfactants, namely 16.7 and 18 for Tween 20 and PVA, respectively (HLB values were obtained from the manufacturers). However, HLB itself is not an ultimate predictor of surfactant efficacy in particle size decrease. Viscosity of the organic phase was also shown to play a role: bigger particles being formed with increasing viscosity of the organic phase [190].

PdI values are shown in **Figure 23CD**. As mentioned above, the value 0.2 is considered an indicator of sample monodispersity [188] and thus lower tendency to instabilities and more predictable behaviour in terms of usability as drug-delivery system. The formulated NPs were mainly of values below this threshold, even though in the case of polysorbate Tween® 20, the polydispersity was slightly higher. The explanation could be found in polysorbates structures that is characterized by three PEG chains on the sorbitan moiety. This could lead to less effective accumulation on water-organic interface and lower protection against collisions of particles.

The effect of the tested compositions on zeta potential is summarized in **Figure 23EF**. As previously described in NPM, all prepared formulations carried negative surface charge. In both polymers in F127 and PVA, the formulations with the lowest concentration of surfactants (0.1%) showed significantly lower zeta potential compared to the higher surfactant concentrations. This could suggest that at concentrations of over 0.5% of F127 and PVA molecules of the stabilizer form a hydrophilic corona on particles` surface and thus shield PLGA surface charge by covering PLGA nanoparticle surface more effectively. This trend was not observed in Tween 20, in which all the tested concentrations reached the same zeta potential. A possible explanation presents itself when the structure of stabilizers is compared. (**Figure 24**). Tween 20 bears relatively short PEG chains in its molecule. Whereas F127 (poloxamer 407) is characterized as a large linear molecule with two PEG chains consisting each of 101 monomers. PVA is also a long linear molecule with extensive hydrophilic and hydrophobic domains. Both, PVA and F127, are able to form a corona much more effectively than Tween 20. Finally, the

overall tendency to decrease zeta potential could be summarised as PVA< Pluronic F127< Tween 20.

Due to technical limitations of purification method, EE could not be analysed in the formulation prepared by ESE. Using centrifugation, it was difficult to quantitatively collect the small NPs and in the case of the smallest NPs, the recovery of polymeric material was less than 5%. Ultracentrifugation or centrifuge fillers could be employed for a more effective collection of NPs (>75 nm) in further experiments.
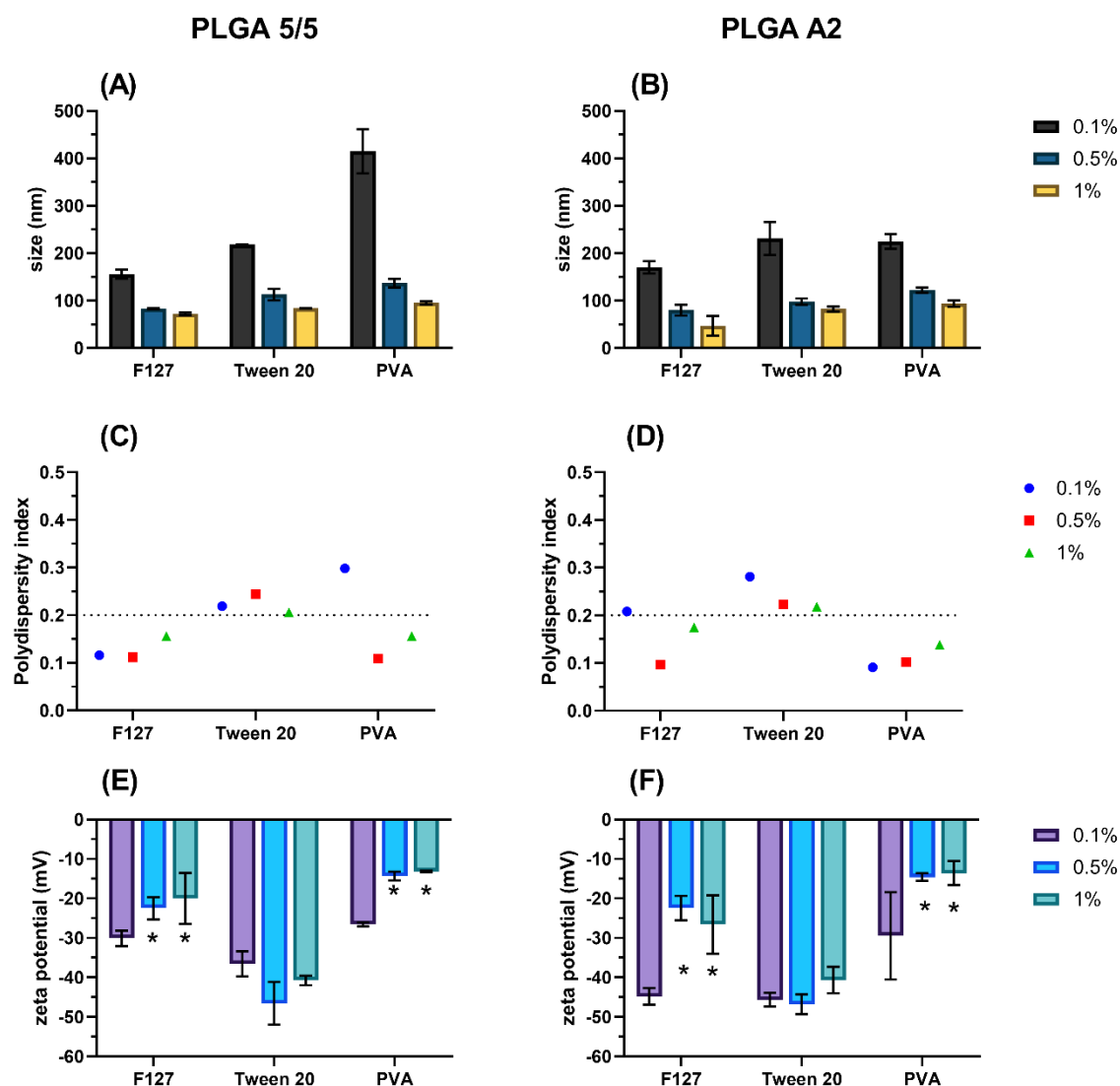
Figure 23: Characterization of PLGA NPs prepared by ESE. NPs were characterised respectively in PLGA 5/5 and branched PLGA A2 in terms of (A)(B) size, ((C) (D) PdI, (E) (F) zeta potential. In (A) and (B) significant difference (p<0.05) between the types of surfactants and concentrations, except from PLGA A2 in combination with 0.1% of all surfactants. In (E) and (F) *< 0.05 statistically significant difference in comparison to respective 0.1% surfactant solution. Data is presented as mean ± SD, n=2-5. F127 – Pluronic F127
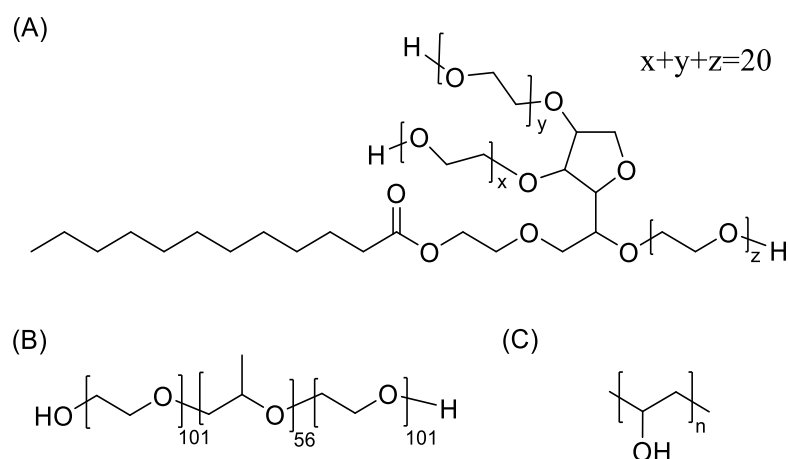
Figure 24: Chemical structure of surfactants utilised in ESE. (A) Tween® 20 [192], (B) Pluronic® F127 (poloxamer 407) [193], (C) PVA.

The role of surfactants and their concentration was shown to be of higher importance in ESE relative to NPM. Surfactants play a crucial role in prevention of coalescence as the emulsion is formed, both in decrease of surface tension and increase of viscosity of the aqueous phase [189–191]. From our results, NPM resulted into production of NPs of narrow size distribution, which is in accordance of previously reported results [89].

Comparing the effect of PVA on increase of zeta potential relative to other surfactants, the rise of this value was much more pronounced in NPM. Using this preparation method, increase in the amount of PVA correlated with increase in zeta potential. A similar phenomenon was observed in ESE not only for PVA, but also in Pluronic F127.

EE is known to be influenced by interactions with the polymer. In our study, we worked with acid-terminated polymers carrying a negative surface charge. Electrostatic interactions with the positively charged RhB were likely to be the driving force to load the substance. In further experiments, we showed a significantly lower EE in a commercially available ester-terminated PLGA [25].

4.2.3   Stability study

The behaviour of PLGA A2 NPs was evaluated over a period of 30 days at the fridge temperature. in water, PBS and acetate buffer. **Figure 25A** shows normalized size values of NPs in different environment. The size was considerably stable over the time of the experiment in acetate buffer and in water. On the contrary, cyclic size changes of size reduction and increase were observed in PBS buffer. Corresponding results were observed in normalized PdI values (**Figure 25B**). The normalized values observed in water and acetate buffer fluctuated approximately around the value 1. In PBS buffer, repeated peak correlating to size reduction were observed.

The phenomenon of cyclic size fluctuations was already described in the linear experimental polymers utilised in this study was described by Dittrich et al. as spontaneous cyclic swelling. Spontaneous cyclic swelling is initiated by formation of new end groups upon PLGA chain cleavage inside the system as aqueous solvent penetrates a PLGA system. Accumulation of the end groups increases osmotic pressure that leads to swelling of the system. During the swelling process, molecules with osmotically active end-groups diffuse out of the system. Subsequently, the osmotic pressure decreases, and the system becomes more hydrophobic and hydrophobic domains aggregate. The aggregation causes deswelling of the system [194]. Dittrich et al. demonstrated a phenomenon of cyclic swelling in macroscopic systems made of >50mg polymer and in our study we observed this phenomenon also in a nanoparticulate system.
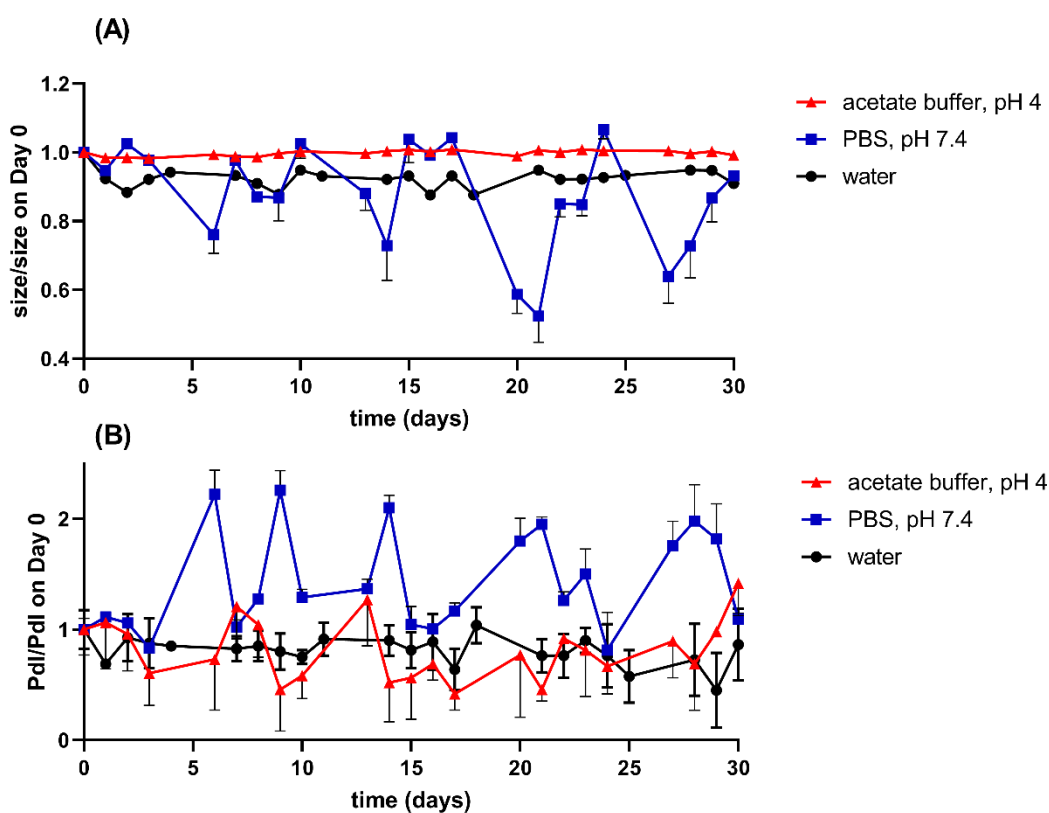
Figure 25:Stability of PLGA A2 NPs over 30 days at the temperature 4-8°C in water, PBS buffer and acetate buffer. (A) normalized size values, (B) normalized PdI values. Data is presented as mean ± SD, n=3.

4.2.4 Drug release

Initially, release of RhB was tested in 3 media, namely isotonic saline solution, acetate buffer in saline solution of acidic lysosomal pH 4.5 and HEPES buffer in saline solution of physiological pH 7.4 in order to compare release profiles in pH 4.5 and 7.4 in isotonic conditions. The presented set of experiments in HEPES buffer confirmed our previous results in PBS buffer that is more commonly used to mimic physiological environment. Isotonic conditions of saline

solution were maintained to mimic osmotic properties of an organism. As it was shown by Tomic et al. that osmotic pressure impacts release from PLGA microspheres [86].

Results of this experiment are depicted in **Figure 26A**. The tested polymers showed no significant difference among each other in the saline solution and HEPES buffer saline, the release was influences by the used polymer in the acetate buffer saline (**Figure 26B**). The release was governed by the medium and release of RhB from NPs was significantly faster in the HEPES buffer saline. The initial burst was the most pronounced in the HEPES buffer at pH 7.4 and basically the entire amount of RhB released during the initial 24 hours. Surprisingly, we did not observe any difference in the saline solution and HEPES buffer saline among the structurally different polymers, such as linear PLGA and branched PLGA A2 with molar weight more than 3-time higher than the linear ones. It could be partially ascribed to good water solubility of RhB that allowed for fast RhB diffusion. The profiles in the tested media corresponded to the biphasic release characterised by the initial burst and followed by the saturation phase. The initial burst can be cause by formation of cracks in NPs or hydration of drug molecules on the surface. A hydrophilic drug, such as RhB can be readily hydrated and thus the initial burst is high [85].

(A)

(B)
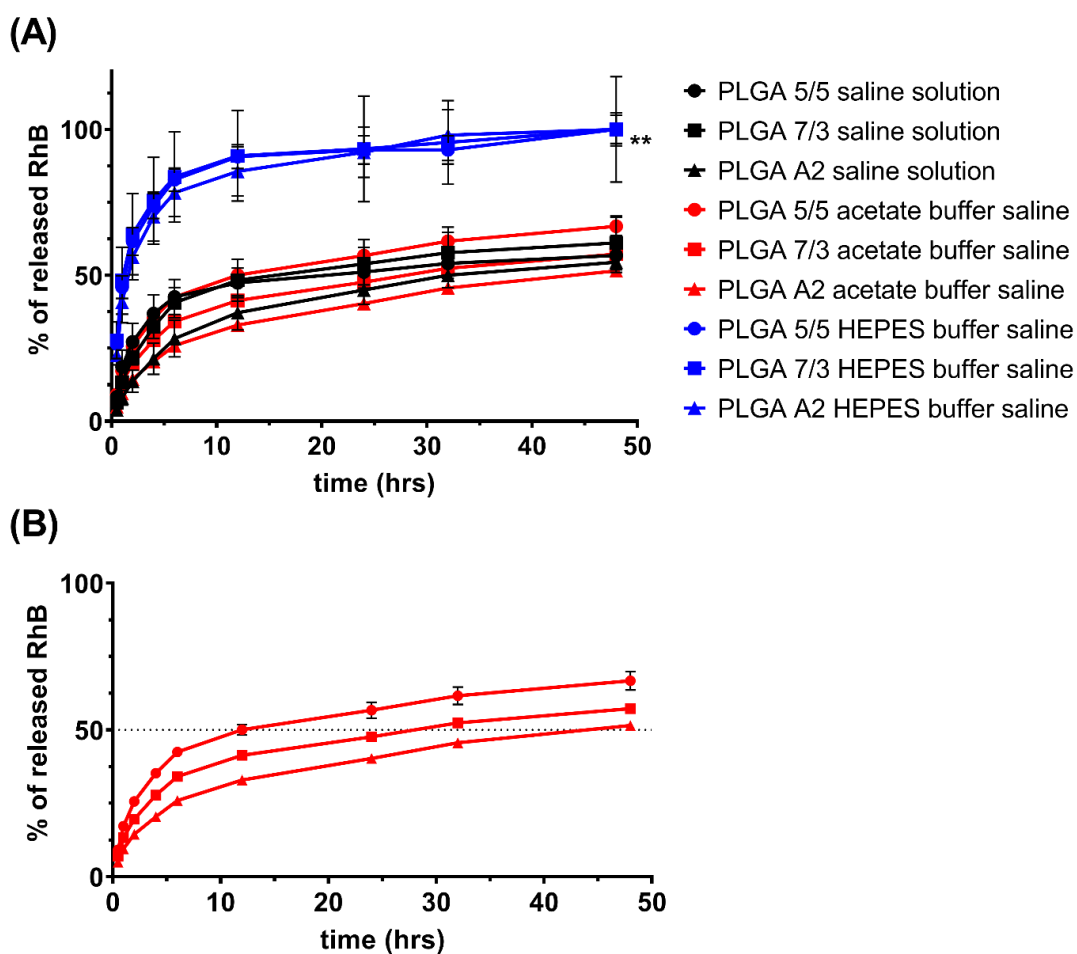
Figure 26:*In vitro* release profile of RhB. (A) The release profiles of RhB from three different polymers in three release media. Release profile in HEPES buffer saline significantly differed from the saline solution and acetate saline solution (**p<0.01) (n=3). (B) The release profiles of RhB in acetate buffer saline. Intercepts of the dotted line and the release curves show considerably different time points at which 50% of RhB releases.

Interestingly, release was significantly slower in the acidic acetate buffer saline and the non-buffered saline solution, with no significant difference between these two media. In both cases, the initial burst release was present for the first 12 hrs, again likely due to good water-solubility of RhB. Less than 50% of RhB was released in both saline solution and acetate buffer saline compared to 90% released in the HEPES buffer saline. Zero-order release followed the initial 12 hours of the release curves and could be described by linear regression. Over this time period, diffusion was the rate controlling mechanism [85].

It is noteworthy, that PLGA A2 showed a significantly slower release at all time points relatively to PLGA 5/5 and PLGA 7/3 in the acetate buffer saline (**Figure 26B**). The cumulative amount of RhB released from PLGA 5/5 and PLGA 7/3 significantly differed in all time points except from the ones at 0.5, 1, 36 and 48 hours. The differences in the release profile considerably changed the time at which 50% of RhB was released: 12, 29.8 and 43.3 hours for PLGA 5/5, PLGA 7/3 and PLGA A2, respectively. Apparently, the kind of polymer can influence the release profile of RhB at the acidic pH unlike at the neutral pH. Out of the tested experimental polymers, PLGA A2 was shown to be the most stable in the acidic environment. Compared to its linear counterparts tested alongside, PLGA A2 is a branched polymer with higher molar weight. More investigation would be required to elucidate the reasoning beyond the different release profile of PLGA A2 in the acidic buffer saline.

So finally, from the course of release curves, we can assume, that pH has higher impact on release of RhB from the tested polymers than osmotic properties of a medium.

The rapid release from prepared NPs in the HEPES buffer could be ascribed to cyclic swelling of the experimental polymers used in this study observed only at pH 7.4 (**Figure 25**). In our release study, the release of RhB could be accelerated by the swelling process as it would allow well-water soluble RhB diffuse out of NPs more easily. As the release profiles were independent of the used polymer, we could assume that the swelling process influenced the release from the branched PLGA A2 and linear PLGA 5/5 and PLGA 7/3 to the same extend.

The phenomenon of cyclic swelling of the experimental polymers is likely to limit the application of these formulations for water soluble molecules such as RhB and lead to rapid release from the NPs upon i.v. administration. However, *in vivo* experiments show that nanoparticles are usually scavenged by macrophages quite rapidly following an i.v. application. Majority of NPs are found in the liver and to a lesser extent in the spleen within a matter of minutes [195]. Having reached acidic lysosomes, the NPs release is likely to be sustained over a longer period of time. Moreover, in order to prevent the rapid burst release in physiological environment (pH 7.4), NPs formulated from these experimental polymers could be coated with a coating stable at the neutral pH. Nevertheless, an effect of the loaded substance needs to be taken into consideration. A more hydrophobic active substance would become hydrated less readily as

hydrophilic RhB. The slower hydration of the active substance could reduce the initial burst release.

Based on the screening through the surfactants and optimised preparation methods, we have chosen the composition and preparation methods for further experiments. The experimental polymers (PLGA 5/5, PLGA7/3 and PLGA A2) were combined with Pluronic F127 (poloxamer 407) and formulated into RhB-loaded NPs using both NPM and ESE. The prepared NPs were shown to be of a spherical shape using atomic force microscopy. Cellular uptake of the NPs was evaluated *in vitro* in mouse bone marrow-derived macrophages, mouse hepatocyte AML-12 cells and human hepatocyte tumour-derived HepG2 cells. Polymeric NPs of size > 100 nm prepared by NPM very selectively taken up by only macrophages. In addition, higher uptake in macrophages was observed upon inflammatory stimulation with lipopolysaccharide compared to non-stimulated ones. The level of uptake into hepatocytes was negligible or non-significant relative to RhB solution. Similarly, negligible uptake of NPs < 100 nm prepared by ESE was observed in macrophages. The formulations were shown to be neither immunogenic nor cytotoxic. The results indicate that these optimised formulations are suitable as macrophage-specific carriers [25].

5 LIPID-BASED NANOCARRIERS FOR DELIVERY OF A POORLY WATER-SOLUBLE DRUG

In this chapter we investigated delivery of poorly water-soluble IND in lipid nanoparticles, more precisely in NLCs. NLCs were prepared by 2 different methods, nanoprecipitation and emulsification solvent evaporation method, and characterized in terms of size, PdI and zeta potential. In addition, thermal analysis to assess their crystalline state was performed. Solubility of IND in lipid excipients was evaluated as well as the encapsulation efficiency of the drug inside the nanocarriers.

This chapter summarizes work conducted as a part of diploma theses co-supervised by the author. For a more detailed description of the formulation process, the reader is referred to the diploma theses by Kateřina Kučerová and Lenka Voldřichová [196,197].

5.1 Materials and methods

5.1.1 Materials

Kolliphor® P188, Span® 20, glyceryl monostearate (GMS), isopropyl myristate (IPM) and indomethacin (IND) were provided from Sigma-Aldrich (Merck Group, Darmstadt, Germany). Stearic acid 50 (SA) was obtained from Dr. Kulich Pharma, Hradec Králové, Czech Republic and lecithin from Rohm und Haas, Germany. Deionised water was purified by Elix Essential Water Purification System (Merck, Darmstadt, Germany). Organic solvents utilised for HPLC were of HPLC-grade quality. All other chemicals were of analytical grade and commercially available.

5.1.2 Preparation of lipid NPs

5.1.2.1 Nanoprecipitation method (NPM)

25 mg of a stearic acid (SA), 10 mg of a liquid lipid (IPM), 50 mg Span 20 were dissolved in 2.5 mL ethanol. This lipophilic solution was added into 10 mL of an aqueous solution of 0.5% (w/v) Kolliphor P188 under stirring at constant speed (300 rpm).

5.1.2.2 Emulsification solvent evaporation method (ESE)

25 mg of glyceryl monostearate (GMS), 10 mg of a liquid lipid (isopropyl myristate) and 15 mg of lecithin were dissolved in 1 mL of chloroform: methanol 1:1. This organic phase of the emulsion was added into 5 mL of 0.1% (w/v) aqueous solution of Kolliphor and sonicated for 1 min at the power output 70 W using a sonication probe Mikrospitze (Bandelin sonoplus, Berlin, Germany), while being cooled with ice bath. After sonication, the resulting emulsion was poured into 5 mL of the 0.1% (w/v) aqueous solution of Kolliphor.

In both preparation methods, NPM and ESE, the required amount of IND (based on section 5.1.3) was added into the lipophilic phase for IND NLCs. In addition, physical mixtures consist of thoroughly mixed lipid excipients used for NLCs preparation without and with IND were prepared and are referred to as blank mixtures and IND mixture, respectively. IND NLCs and IND mixtures were prepared using 80% of determined IND solubility in the lipid excipients, if not otherwise specified. Lower than saturated solubility was utilised in order to avoid undesired IND precipitation.

The utilised amount of excipients described in this section resulted from optimisation of the methods that is further discussed in Results and discussion.

5.1.2.3   Purification of NPs

NPs formed by both methods were allowed to harden by evaporation of the organic solvent for 2 hours under constant stirring (300 rpm) at the room temperature. Subsequently, the dispersion was centrifuged with the centrifuge MPW 260R (MPW Medical Instruments, Warsaw, Poland) using centrifugal concentrators Vivaspin 500 (MWCO 100 kDa) (Sartorius, Göttingen, Germany) for 20 minutes at 12 000 × g [174].

5.1.3   Determination of indomethacin solubility in lipids

An excess of a tested solid lipid excipients (about 1 g) was added in excess to known amount of IND. The mixture was heated to temperature of 10°C above the melting temperature of the lipids. The amount of undissolved IND was observed with the naked eye, and aliquots of lipids were added (100 mg) until the entire amount of the drug dissolved, and visible particles of IND disappeared, in the melted lipid. In the case of liquid lipids, the solubility was tested as for solid lipids, however, without the melting step.

5.1.4   Characterisation of NPs

5.1.4.1   Particle size and zeta potential

100 µL of crude nanosuspension was added to 1900 µL of DI water. The diluted nanosuspension was evaluated in terms of size, PdI and zeta potential using the Zetasizer (Malvern Nano ZS, Malvern, United Kingdom).

5.1.4.2   Differential scanning calorimetry (DSC)

Differences in molecular packing were investigated using differential scanning calorimetry (DSC). The studies were performed using DSC 200 F3 Maia instrument (NETZSCH-Gerätebau GmbH, Selb, Germany) equipped with Proteus Software (NETZSCH-Gerätebau GmbH, Selb, Germany). The measurement was performed in bulk lipids, both blank and IND-loaded NLCs and the respective physical mixtures. NLCs were purified using centrifugal concentrators, as described above, and subsequently dried in a fume hood overnight. Samples were sealed into standard aluminium crucibles, and the lids were pierced. Samples were cooled down to -20°C and kept at this temperature for 10 min. The analysis was performed from -20°C to 180°C at the heating rate 1 K/min. For the bulk lipids, the heating interval was shortened to 100 °C as all the thermal events were reported to be observed in this interval.

5.1.4.3   Analysis of encapsulation efficiency (EE) using HPLC assay

EE was calculated according to Equation (2), respectively. After NP purification, filtrate was diluted 1:1 with the mobile phase and the amount of IND was determined using the HPLC

Infinity 1260 equipped with Agilent Technologies 1200 Series degasser, iso pump, autosampler and ultraviolet-visible detector (Agilent Technologies, Santa Clara, USA).

$$EE = \frac{total\ amount\ of\ IND - \ amount\ of\ IND\ found\ in\ filtrate}{initial\ amount\ of\ IND} \times 100\ \% \qquad (2)$$

The detection method was previously described [198]. Briefly, the reverse phase separation was achieved on the LiChroCART 250-4 column (Lichrosphere 100 RP-18.5 µm, Merck, Darmstadt, Germany). The mobile phase consisted from acetonitrile/water/acetic acid 90/60/5 (v/v/v) at a flow rate 1 mL/min. The temperature of the column was maintained at 40°C and the analyte was detected with UV absorbance at 260 nm. 50 µL of sample were injected into the column. Retention time of IND was found to be 6.5 min. The set of samples of IND used for calibration curve is shown in **Figure 27**.
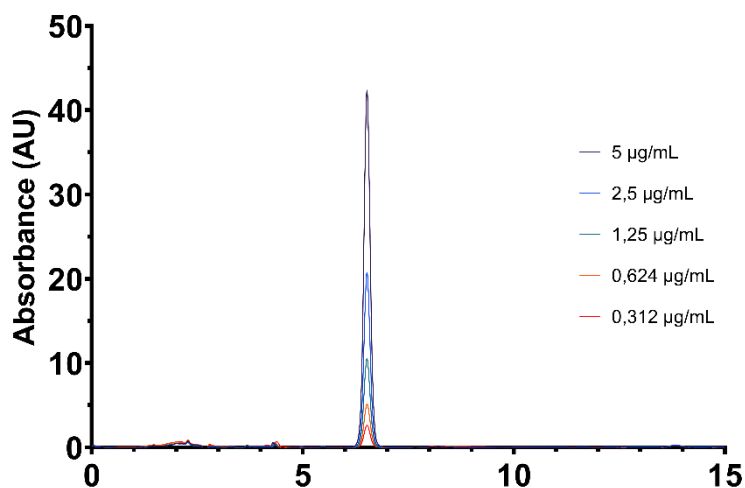
**Figure 27**:Chromatograms of standards used for calibration curve

5.1.5 Statistical analysis

Statistical analysis was performed with the Graph Prism 8 (GraphPad Software, San Diego, California, USA). Size and zeta potential were assessed by unpaired t-test. HPLC data were evaluated by ANOVA followed by Dunnet post hoc test. Data is presented as mean ± standard deviation (SD). Significant difference was considered at $p < 0.05$.

5.2 Results and discussion

5.2.1 Formulation process

For both methods, there was a clear need to use both hydrophilic and lipophilic surfactant. When the NLCs were formulated only with a hydrophilic surfactant (Kolliphor P188, Tween 20 or Pluronic F127) macroscopic lipid aggregates were present (**Figure 28A**). Even when the aggregates were filtered out, the samples were highly polydisperse (PdI >0.4) with particle size over 500 nm. When a lipophilic surfactant (Span 20, lecithin) was added to the lipophilic phase, aggregates disappear (**Figure 28B**). The formed nanosuspension did not require filtration and the NLCs were smaller (< 500 nm). Our observations are in accordance with already published results, as the combination of surfactants in SLNs production was found to work as an efficient prevention from aggregation [175].
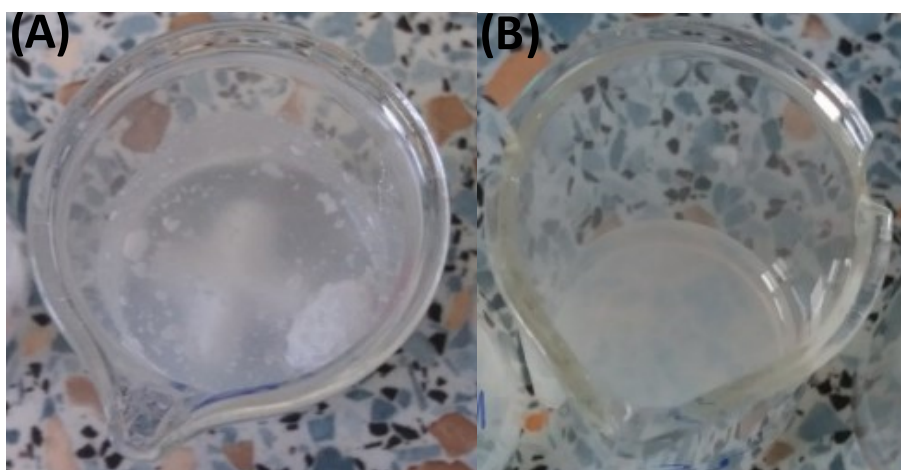

Figure 28: GMS-based NLCs of a similar composition, containing hydrophilic Kolliphor P188 as a surfactant and differing in the presence of a lipophilic co-surfactant (A) NLCs formulated without and (B) with the addition of lecithin by ESE.(adopted from [197])

Moreover, throughout the formulation process we could observe the importance of optimisation of surfactant concentration. High concentration of surfactants decreases surface tension more efficiently so that particle formation is facilitated, and smaller size of NPs is favoured. However, surfactants are often responsible for toxicity of NPs [171]. The optimisation of the surfactant concentrations was necessary for each formulation individually. In the case of SA-based NPs formulated by NPM (**Figure 29A**), the size increased with higher amount of utilised surfactants. As the lipid NPs showed suitable size and PdI with lower surfactant concentrations and in order to avoid possible toxicity, we further utilised 50 mg of Span and 0.5% Kolliphor P188. For GMS-based NPs prepared by ESE (**Figure 29B**), lecithin concentration seemed to have more profound impact on the size of NPs than concentration of Kolliphor P188. There was no difference observed between 0.1% and 1% of Kolliphor P188 and for this reason, the combination of 7 mg of lecithin and 0.1% of Kolliphor was chosen.

Independently of the preparation method, the lipophilic surfactant had a more profound impact on the size of formed NPs than hydrophilic Kolliphor P188. Interestingly, in NPM, higher concentration of the lipophilic surfactant resulted in larger NPs. For NPs prepared using ESE, higher concentration of lipophilic surfactant led to formation of smaller NPs. In order to elucidate the cause of this phenomenon precisely, more investigations are required with less variables (preparation method, uniform lipid excipients) included. However, from the collected data it is apparent that the concentration of lipophilic surfactant is a critical factor when adjusting the particle size.

For our tested composition of SLNs prepared by approaches based on organic solvents, it was necessary to use combination of a hydrophilic and lipophilic surfactant to achieve monodisperse NPs. Testing of optimal surfactant concentration remains crucial for each combination of lipid excipients and preparation method.
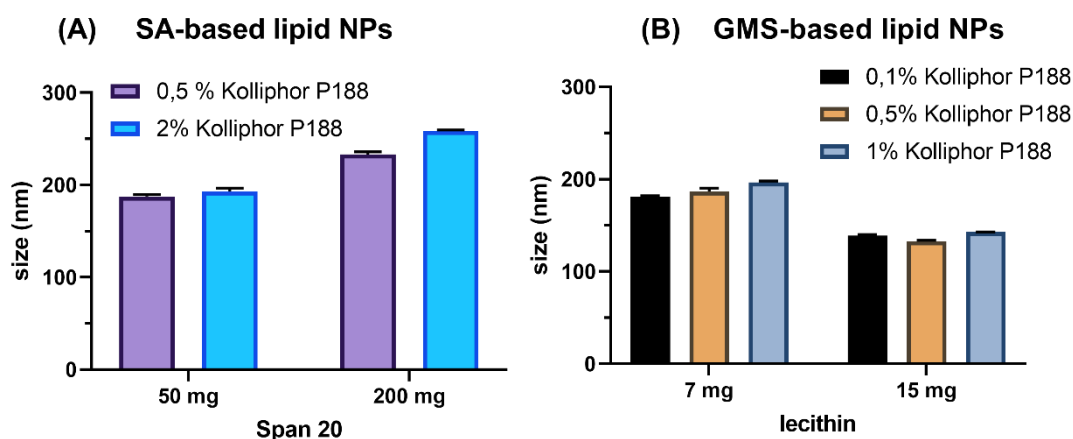
Figure 29: Optimisation of the amount of the used surfactants in blank lipid NPs. (A) SA-based lipid NPs and (B) GMS-based lipid NPs. (A) The composition of lipid NP: 25 mg SA and combination of surfactants. NPs prepared by NPM. PdI varied between 0.24-0.25. (B) The composition of lipid NPs: 25 mg of GMS and combination of surfactants. NPs prepared by ESE. PdI varied between 0.23-0.27.

5.2.2   Particle size and zeta potential

Size, PdI and zeta potential of optimised NCL are summarised in **Table 6**. Neither SA-based NLCs prepared using NPM nor GMS-based NLCs prepared using ESE showed any significant difference in size or zeta potential between blank and loaded NLCs. Lipid-based carriers were considered homogeneous when the PdI is below 0.3 [188]. Both PdI and zeta potential of an absolute value above 30 mV are indicators of stable NPs. The preliminary stability tests over 14 days suggest better stability of GMS-based particles, that is in accordance with their lower PdI and higher absolute value of zeta potential.

Table 6: Properties of prepared NLC (mean ± SD, n=3).

		Size (nm)	PdI	Zeta potential (mV)
SA-based NLCs (NPM)	Blank NLCs	179.1 ± 21.1	0.24	-33.2 ±3.5
	IND NLCs	175.8 ± 7.6	0.23	-37.6 ± 4.4
GMS-based NLCs (ESE)	Blank NLCs	136.6 ± 4.8	0.19	-49.9 ± 6.7
	IND NLCs	141.6 ± 5.2	0.19	-46.1 ± 6.0

5.2.3 Determination of solubility of indomethacin in lipids

Solubility of IND in lipid excipients of NLCs was evaluated (**Table 7**). As expected, lipophilic IND showed better solubility in lipids used for NLCs fabrication. Lipid excipients for NPM, SA and IPM, showed 5-fold solubility enhancement relative to water. In the case of composition used in ESE, GMS, IPM and lecithin, even higher solubility enhancement was observed, more than 10-fold relative to water. In the following experiments we worked with IND loadings that equalled 80% solubility of IND in order to prevent undesired IND precipitation. Moreover, we evaluated EE of also in the case of NLCs supersaturated with IND (200% solubility of IND). The values are depicted in **Table 7**.

Table 7: Solubility of IND

Solvent	Solubility of IND (µg/mg)	80% solubility of IND (µg)	200%solubility of IND (µg)
water	0.94	-	-
25 mg SA + 10 mg IPM	4.75	133	333
25 mg GMS + 10 mg IPM+ 15 mg lecithin	10.35	414	1035

5.2.4 Differential scanning calorimetry

The data from thermoanalysis by DSC are summarized in **Figure 30**, **Table 8** and **Table 9**.

In both formulations, melting temperature decreased in a following order: bulk lipid > mixture> NLCs blank> NLCs loaded with IND. Differences in crystallisation and melting behaviour characterised by melting point depression are associated with the addition of the liquid lipid, which reduces the crystallinity. Decreasing melting temperature indicates increasing lattice defects. The less structured matrix of NLCs contributes to increased drug load and decreases drug repulsion over time [106]. The changes in peak position were apparent also between thermograms of NLCs relative to the respective lipid mixtures confirming different excipients ordering after NLCs formulation.

Generally, the endotherm of NPs is broadened and shifted to lower temperatures in comparison to respective bulk lipids. This phenomenon caused by polydispersity of NPs and molecules of emulsifier present in the NPs. This is called, particle size effect, as NPs tend to melt individually, causing peak fronting and broadening [199].

A more pronounced peak can be observed in IND mixtures relative to blank mixtures. The presence of IND could enhance formation of lipid phase aggregates, presence of which suggests the melting peak in IND mixture. A similar peak formation caused by a presence a drug was also observed by Catelli et al. [173]. This phenomenon cannot be seen in NLCs suggesting negligible effect of IND on the structure of NLCs.

IND peak was not observed either in thermogram of mix IND or NLCs IND. The peak disappearance could be considered a proof of successful IND incorporation into lipid matrix. Some authors suggest existence of the active substance in amorphous form [200] and/or molecularly dispersed [201,202]. As a thermoanalytical technique, DSC is not designed to detect minor amounts of crystal substances. The samples should be assessed with X-ray powder diffraction in order to fully describe the form on IND in NLCs [199].

In this study, the thermogram of SA showed 2 melting peaks (**Figure 30A, Table 9**). The larger one with the peak at 56.7 °C is in accordance with the freezing point of SA 50, as described in European Pharmacopoeia[203]. Moreover, only a single peak of SA at 59.7 °C (onset 55.5 °C) was observed when the thermoanalysis was performed at higher heating rate of 10 K/min (data not shown). Hu et al. observed a progressive decrease of melting point of stearic acid with the increasing addition of palmitic acid. 45% of palmitic acid shifted the melting peak from 67.8 °C (0% palmitic acid) to 59.8 °C, which agrees with our measurements [204].
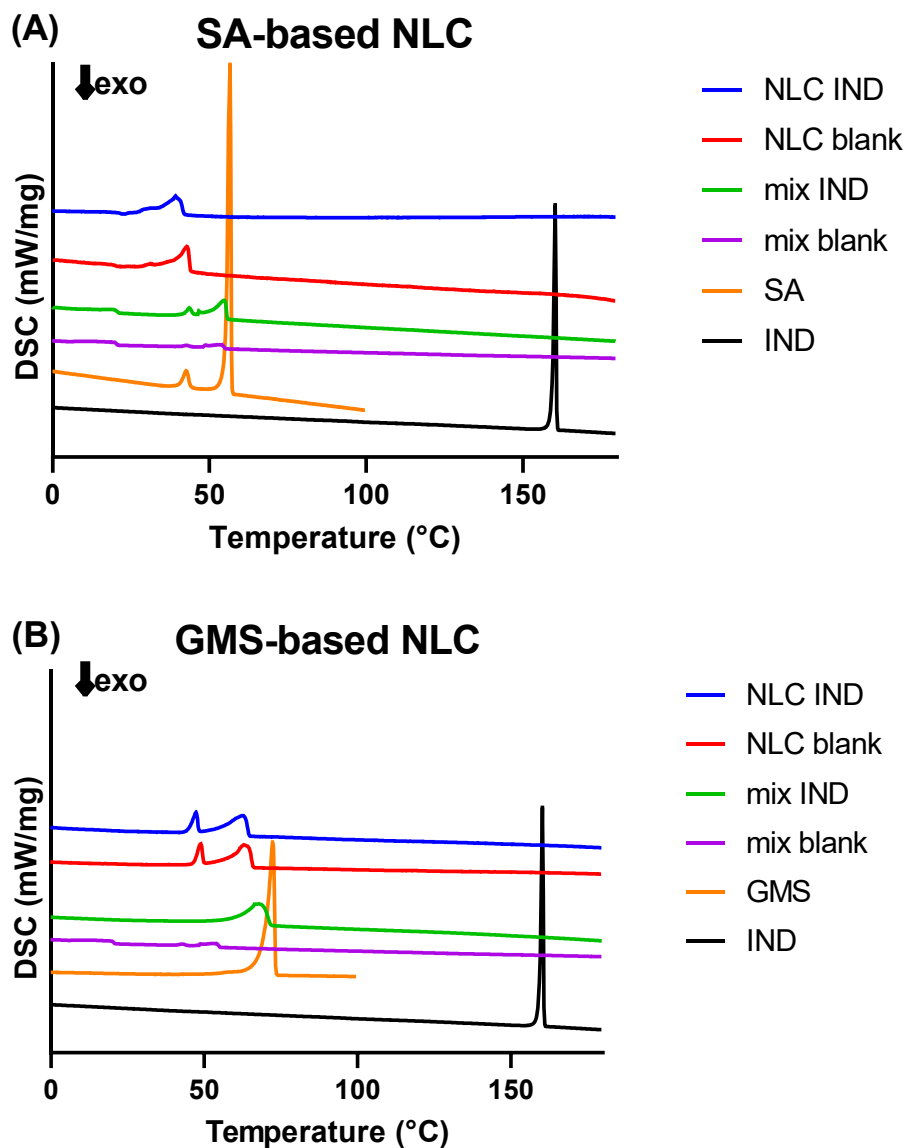
Figure 30: Differential scanning calorimetric heating curves. (A) NLCs formulated by NPM from SA as the solid lipid (B) NLCs formulated by ESE from GMS as the solid lipid.

Table 8: Characterisation of peaks observed in the set of heating curves depicted in Figure 30A.

| SA-based NLCs (NPM)	Peak (°C)	Onset (°C)	Area (J/g)
IND	160.3	159.4	102.5
SA	42.6	40.9	14.6
	56.7	55.5	200.1
mix blank	42.9	41.4	1.40
	53.9	53.9	3.64
mix IND	43.6	42.2	5.58
	54.6	51.7	26.9
NLCs blank	42.8	39.8	67.68
NLCs IND	39.3	37.5	59.73

Table 9:Characterisation of peaks observed in the set of heating curves depicted in Figure 30B.

GMS-based NLCs (ESE)	Peak (°C)	Onset (°C)	Area (J/g)
IND	160.3	159.4	102.5
GMS	72.3	69.8	192.7
mix blank	66.9	59.4	69.4
mix IND	67.8	64.8	85.45
NLCs blank	48.8	46.8	17.44
	63.0	60.2	63.28
NLCs IND	47.3	45.1	18.8
	62.3	56.9	63.94

5.2.5 Evaluation of EE using HPLC assay

Upon purification of prepared NLCs using centrifugation concentrators, filtrate was withdrawn to evaluate the non-encapsulated amount of IND. We tested both 80% and 200% IND solubility in lipid matrices. As can be seen in **Figure 31**, the chromatograms lacked the peak at 6.5 min. Moreover, AUCs of the peak at 6.13 min did not differ significantly, indicating no interference or peak merging with the peak of IND. Nonetheless, a limitation of this analysis is that the spike of IND into filtrate of blank NLCs was not performed to exclude the interference completely.

These results indicate that the amount of non-encapsulated IND was below the detection limit of the system and thus close to 100% of IND was encapsulated into NLCs. It is possible that unstructured lipid matrix consisting of both solid and liquid lipid allows for loading of higher amount of IND. On the contrary, that precipitation of IND in the supersaturated NLCs (200% IND solubility) might occur, however, further investigation would be needed to elucidate this process.
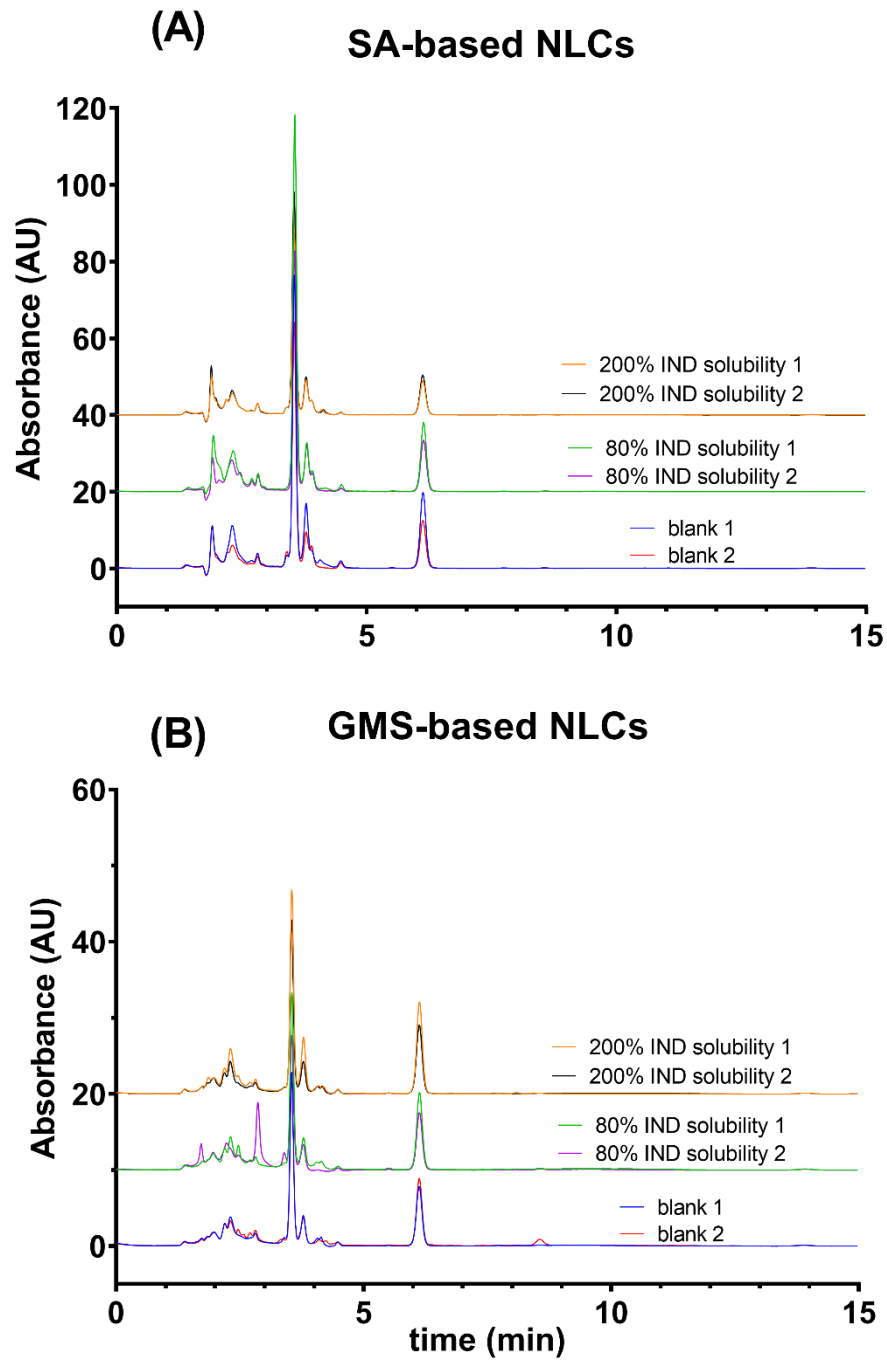
Figure 31: Chromatograms. Duplicate samples prepared from filtrate taken after NLCs purification, blank NLCs, loaded NLCs with 80% and 200% IND solubility of (A) SA-based NLCs and (B) GMS-based NLCs.

6 LIPID-BASED SELF-EMULSIFYING DRUG DELIVERY SYSTEM FOR ORAL ADMINISTRATION OF AN OLIGONUCLEOTIDE

Firstly, OND was ion-paired with a cationic lipid, either dimethyldioctadecylammonium bromide (DDAB) or 1,2-dioleoyl-3-trimethylammonium-propane (DOTAP), and the resulting complexes were thoroughly characterised. Secondly, due to reduction in hydrophilicity, the complexes could be dissolved easily in SEDDS preconcentrates. We worked with both negatively charged and neutral SEDDS based on permeation enhancing MCFA. Dispersed SEDDS loaded with the OND complexes were analysed in terms of size, zeta potential, lipolysis, their protective ability upon contact with nucleases, and imaged with cryogenic transmission electron microscopy (cryo-TEM). Finally, the Caco-2 permeation study was performed.

This chapter summarizes results of a study conducted in cooperation with a research group Physiological Pharmaceutics supervised by Prof. Anette Müllertz at University of Copenhagen, Denmark.

The study was published by Kubackova et al. as Oligonucleotide Delivery across the Caco-2 Monolayer: The Design and Evaluation of Self-Emulsifying Drug Delivery Systems (SEDDS) [205]. The article can be found as *Appendix III*.

6.1 Materials and methods

Methods provided in this chapter are described only shortly. For more details of this section, the reader is referred to *Appendix III*.

6.1.1 Preparation of hydrophobic ion-pairs

Hydrophobic ion-paired complexes between a cationic lipid, DDAB or DOTAP, and OND were prepared using Bligh-Dyer extraction method, as previously described [206]. The required amount of cationic lipid and OND was dissolved in chloroform: methanol: water 1:2.2:1 forming Bligh-Dyer monophase. The monophase was partitioned in a two-phase system by the addition of an aliquot of both chloroform and water, followed by vortexing and centrifugation. The bottom chloroform phase containing the ion-paired complex was collected and the solvent was evaporated. The amount of complexed OND was evaluated indirectly from the aqueous phase measuring fluorescence of non-io n-paired OND.

Physical mixtures of cationic lipids and OND were prepared by mixing a bulk lipid with a bulk OND at the charge ratio 3:1.

6.1.2 Characterization of ion-paired complexes

Morphological features and size of OND and its complexes with cationic lipids were evaluated using atomic force microscopy (AFM). Samples were deposited on mica substrate.

Differential scanning calorimetry (DSC) was performed with bulk cationic lipids, cationic lipid-OND complexes and physical mixture of OND and a cationic lipid. The samples were subjected to the analysis at a heating rate of 10 K/min from -50 to 150°C.

Attenuated total reflectance-Fourier Transform Infrared spectroscopy (ATR-FTIR) was recorded from solid samples applied over ATR crystal. Samples included OND, bulk lipids, OND-cationic lipid complexes in three charge ratios and physical mixtures.

6.1.3 Loading of the ion-paired complexes into SEDDS

SEDDS were prepared by stirring of all excipients (**Table 10**) with a magnetic bar overnight at 37°C. The composition was previously described by Ramakrishnan Venkatasubramanian et al. (data not published, manuscript in preparation). The SEDDS were loaded by dissolving the payload under stirring at 37 °C overnight, as summarized in **Table 11**.

Table 10: Composition of utilised SEDDS (self-emulsifying drug delivery system)

SEDDS	Captex 300 (%w/w)	Labrasol (%w/w)	Lipoid S LPC 80 (%w/w)	Citrem (%w/w)	Maisine CC (%w/w)	Peceol (%w/w)
Citrem (negatively charged)	20	40	20	20	-	-
Standard (neutral)	20	40	20	-	10	10

Table 11: Loading SEDDS

Name of formulation	Payload	Loaded amount
DDAB-OND in SEDDS	Complex of DDAB and OND at the charge ratio 3:1	100 nmol of OND/g SEDDS
DOTAP-OND in SEDDS	Complex of DOTAP and OND at the charge ratio 3:1	100 nmol of OND/g SEDDS
DDAB in SEDDS	DDAB	3.8 mg/g SEDDS
DOTAP in SEDDS	DOTAP	4.2 mg/g SEDDS
SEDDS + Orlistat	Orlistat (lipase inhibitor)	0.25%(w/w)

Size and zeta potential were evaluated upon dilution 1:100 (w/w) in DI water and MES-HBSS buffer using dynamic light scattering and laser Doppler electrophoresis, respectively.

Dispersed SEDDS were imaged using cryogenic transmission electron microscopy (cryo-TEM) in fasted-state simulated intestinal fluid at dilution 1:100 (w/w). Non-loaded and complex-loaded SEDDS, both Citrem and Standard SEDDS, were imaged.

The protective ability of both SEDDS against nuclease degradation was assessed. Experiments were performed with a nuclease specific for single strand nucleotides, S1 nuclease. The S1 nuclease assay was performed according to the manufacturer's instructions for 30 min and subsequently intact OND was precipitated using ethanol precipitation and centrifuged. The pelleted intact OND was dissolved in the mobile phase and analyzed with a previously described HPLC method [207].

Lipolysis of the SEDDS was conducted in fasted-state simulated fluid under dynamic conditions over 60 min [134,208]. In addition to the non-loaded Citrem and Standard SEDDS, these formulations were subjected to lipolysis when loaded with 0.25% (w/w) orlistat, a lipase inhibitor.

6.1.4 Caco-2 cell monolayer permeability and cytotoxicity study

The permeability study was performed using Caco-2 cell monolayer grown on permeable filters for 120 min with following samples: OND solution, DDAB-OND in the SEDDS, DOTAP-OND in the SEDDS, DDAB in the SEDDS dispersed in OND solution, DOTAP in the SEDDS

65

in dispersed OND solution, and non-loaded blank SEDDS dispersed in OND solution for both the Citrem and Standard SEDDS.

Before the initiation of the experiment and after its termination, trans-epithelial electrical resistance (TEER) was measured with Endohm chamber. In the course of the experiment, TEER value was monitored ever 30 min with chopstick electrodes. The experiment was initiated by application of the samples into the basolateral compartment. At 15, 30, 45, 60, 90 and 120 min samples from the basolateral compartment were withdrawn and replaced with the same amount of preheated fresh medium. The amount of permeated OND was evaluated with fluorescence spectroscopy.

Cytotoxicity was assessed subsequent to the permeability experiment using lactate dehydrogenase (LDH) assay to evaluate level of membrane perturbation [209]. The cytotoxicity study was conducted according to manufacturer's instructions.

6.2 Results and Discussion

6.2.1 Preparation of hydrophobic ion-pairs

In order to reduce hydrophilicity of OND, we used hydrophobic ion pairing between the negatively charged OND backbone and a cationic lipid, either DDAB or DOTAP. Utilising Bligh-Dyer extraction method, complexation efficiency over 95% for both cationic lipids was reached at molar ration cationic lipid: OND 60:1, which equals charge ratio 3:1 (**Table 12**). Higher CE achieved with DOTAP compared to DDAB at all ratios is likely to be attributed to higher flexibility of unsaturated C18 chains of DOTAP [210].

Table 12: Complexation efficiency (%) of OND with a cationic lipid (DDAB or DOTAP) using the Bligh-Dyer extraction.

| molar ratio cationic lipid: OND	charge ratio $N^+: PO_2^-$	complexation efficiency (%)	
		DDAB	DOTAP
20:1	1:1	58.3 ± 0.7	84.6 ± 1.4
40:1	2:1	84.0 ± 2.8	100.1 ± 0.1
60:1	3:1	96.5 ± 2.0	100.4 ± 0.1

Results are presented as mean $\pm$ SD (n=3).

6.2.2 Characterization of ion-paired complexes

Size of complexes was evaluated using AFM. Solid state of formed complexes and prepared physical mixture was characterized with DSC and ATR-FTIR.

The size to DDAB-OND and DOTAP-OND complexes was estimated by atomic force microscopy to be 31.6 – 63.4 nm and 75.4 – 128.2 nm, respectively (**Figure 32BC**). In addition, the size of OND was measured to be around 1 nm in height (**Figure 32A**). The shape of images

structures reminded of a disc of lipids flatten around the core consisting of OND. This shape indicated formation of inverted micelles, as reported previously [183].
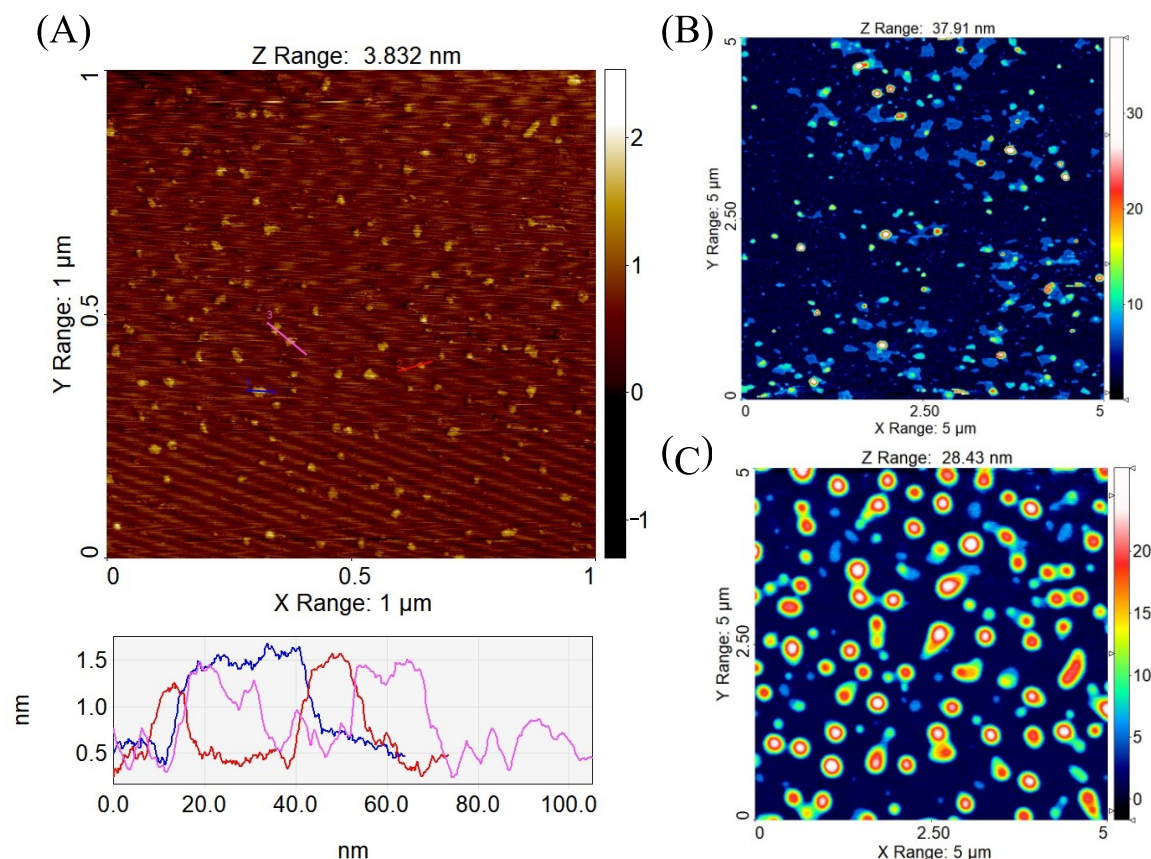
Figure 32: Atomic force microscopy (AFM) images. (A) OND, the height profile corresponds to three coloured sections in the graph below the image; (B) DDAB-OND complex; (C) DOTAP-OND complex

Formation of ion-paired complexes was further confirmed with DSC and ATR-FTIR spectroscopy, and major differences between complexes and the physical mixture were observed using both methods. As show in **Figure 33**, DSC analysis showed that the position and shape of the endothermal events differed in the bulk lipids, physical mixtures and complexes.
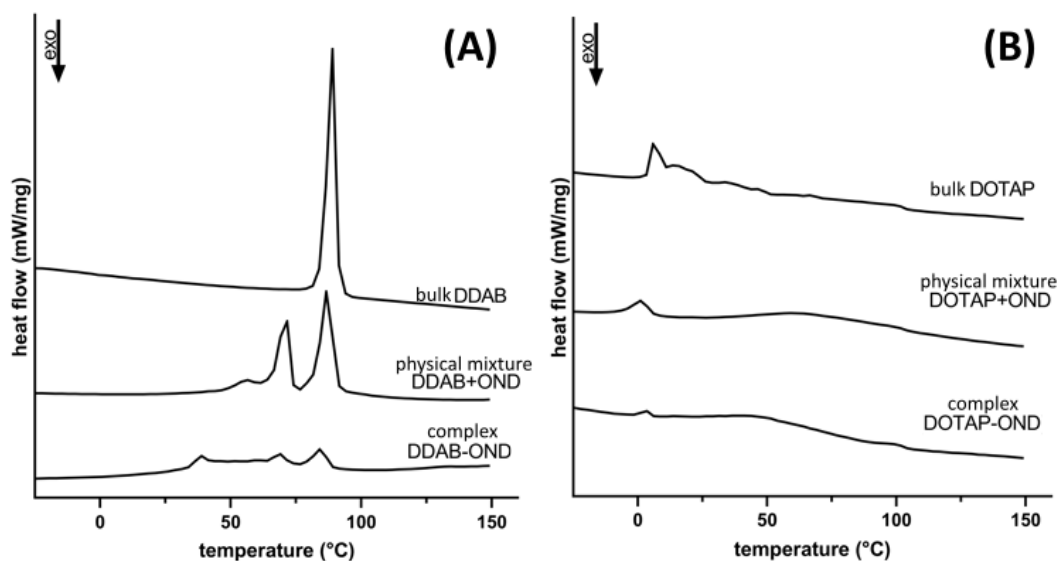

Figure 33: Differential scanning calorimetry thermograms of the bulk lipids, physical mixtures and complexes of (A) DDAB and (B) DOTAP

ATR-FTIR revealed complex-specific bands that could not be observed in respective physical mixtures. The complex-specific bands (as summarized in **Table 13** and marked in **Figure 34** in bold) could be found mainly in the phosphate-deoxyribose region indicating direct involvement of this part of the OND molecule in complex formation process. This is in agreement with suggested shape of inverted micelles as mentioned above.

Table 13: A list of complex-specific bands assigned to specific functional groups of OND.

Complex-specific bands (cm^{-1})	Marker bands characteristic for	Assignment	Reference
1257	Phosphate-deoxyribose backbone	Organic phosphate P=O, vibrational asymmetric band	[211–214]
1095 DDAB-OND 1088-1080 DOTAP-OND	Phosphate-deoxyribose backbone	Organic phosphate P=O, vibrational symmetric band	[211,213,214]
1018	Phosphate-deoxyribose backbone	P-O-C aliphatic phosphate	[212]
802	Deoxyribose conformation	N-type (C3′-endo) puckering mode	[213]
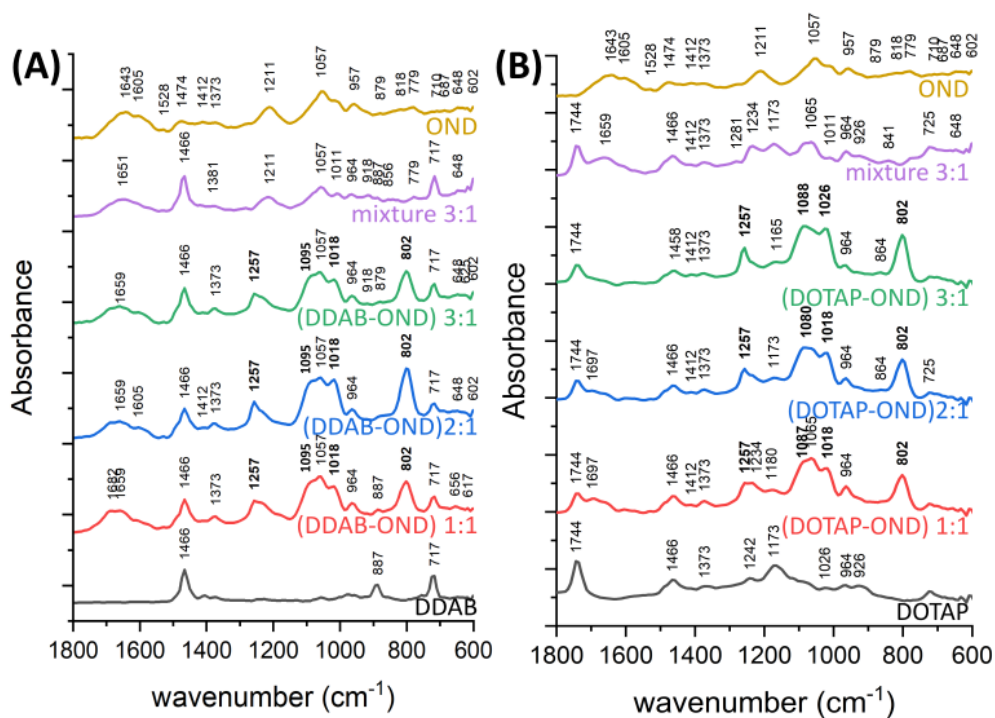
Figure 34:ATR-FTIR absorbance spectra of OND, physical mixture, complexes at tested charge ratios and a cationic lipid for (A) DDAB (B) DOTAP. The depicted region 1800-600 cm-1 is of interest when analysing OND spectra [213]. Complex-specific peaks are in bold.

6.2.3 Loading of the ion-paired complexes into SEDDS

SEDDS are lipid-based drug delivery system well-established in systemic oral delivery of poorly-water soluble drugs. In this study we intended to employ this delivery system for local delivery into lamina propria of the intestine for treatment of intestinal inflammation.

We worked with two SEDDS of a similar composition developed by Ramakrishnan Venkatasubramanian et al. (data not published, manuscript in preparation). Both SEDDS were based on medium chain fatty acids that are known as permeation enhancers. The SEDDS formed nanostructures of about 200 nm upon dispersion, differing in surface charge- being negatively charged (Citrem SEDDS) and neutral (Standard SEDDS).

The size of and PdI were evaluated both in DI water and in MES-HBSS buffer of pH 6.5, which mimics the pH of the small intestine (**Table 14**). No significant difference in size of Citrem SEDDS was observed, independent of loading and the medium. In Standard SEDDS, DDAB-OND in MES-HBSS and DOTAP-OND in DI water were larger than their respective non-loaded controls. PdI varied between 0.125 and 0.360. Lipid-based carriers are considered as homogeneous when the PdI is below 0.3 [188]. Even though PdI, an indicator of long-term stability, is not of major concern as SNEDDS disperse upon administration, PdI of the tested formulations was found close to this value.

Table 14: Size and PdI of tested SEDDS in DI water and MES-HBSS medium.

SEDDS	payload	Size (nm)		PdI	
		DI water	MES-HBSS	DI water	MES-HBSS
Citrem (negatively charged)	non-loaded	201 ± 11	207 ± 16	0.36	0.27
	DDAB-OND	209 ± 14	237 ± 11	0.30	0.23
	DOTAP-OND	195 ± 19	213 ± 5	0.30	0.22
Standard (neutral)	non-loaded	223 ± 10	213 ± 44	0.17	0.22
	DDAB-OND	256 ± 22	267 ± 10***	0.28	0.12
	DOTAP-OND	240 ± 9*	183 ± 27	0.23	0.25

*p<0.05 statistical difference relative to non-loaded Standard SEDDS in DI water, ***p<0.001 statistical difference relative to non-loaded Standard SEDDS in MES-HBSS buffer. Results are presented as mean ± SD (n=3).

SEDDS composition influenced zeta potential of the formulations measured in DI water (**Table 15**). Zeta potential of SEDDS loaded with ion-paired OND complexes significantly increased compared to the respective non-loaded SEDDS. This is likely due to the excess of the cationic lipid used for the complexation with OND. In contrast, this increase was not observed in MES-HBSS buffer of pH 6.5 as the ions present in the buffer seem to mitigate the differences in surface charge upon SEDDS loading.

Table 15: Zeta potential of tested SEDDS.

SEDDS	payload	Zeta potential (mV)	
		DI water	MES-HBSS
Citrem (negatively charged)	non-loaded	-35.5 ± 0.6	-10.9 ± 0.7
	DDAB-OND	-24.1 ± 0.8[###]	-9.9 ± 0.7
	DOTAP-OND	-26.5 ± 1.2[###]	-9.4 ± 0.5
Standard (neutral)	non-loaded	-5.2 ± 2.1	-1.2 ± 0.5
	DDAB-OND	13.0 ± 1.3[###]	0.2 ± 0.5
	DOTAP-OND	14.0 ± 0.9[###]	0.3 ± 0.3

[###]$p < 0.001$ statistical difference relative to respective non-loaded SEDDS. Results are presented as mean $\pm$ SD (n=3).

Under cryoTEM (**Figure 35**) we observed formation of oil droplets as well as vesicular structures, mainly in the size range 100 -300 nm. Moreover, complex multilamellar spherical and elongated structures over 300 nm were also present. The dispersed nanostructures of Citrem and Standard SEDDS were similar, no difference was apparent between non-loaded and loaded formulation. Previous studies that observed SEDDS under cryo-TEM, showed prevalence of oil droplets [158,215]. Citrem and Standard SEDDS contain higher fraction of lipophilic surfactants that might cause formation of larger number of vesicular structures.
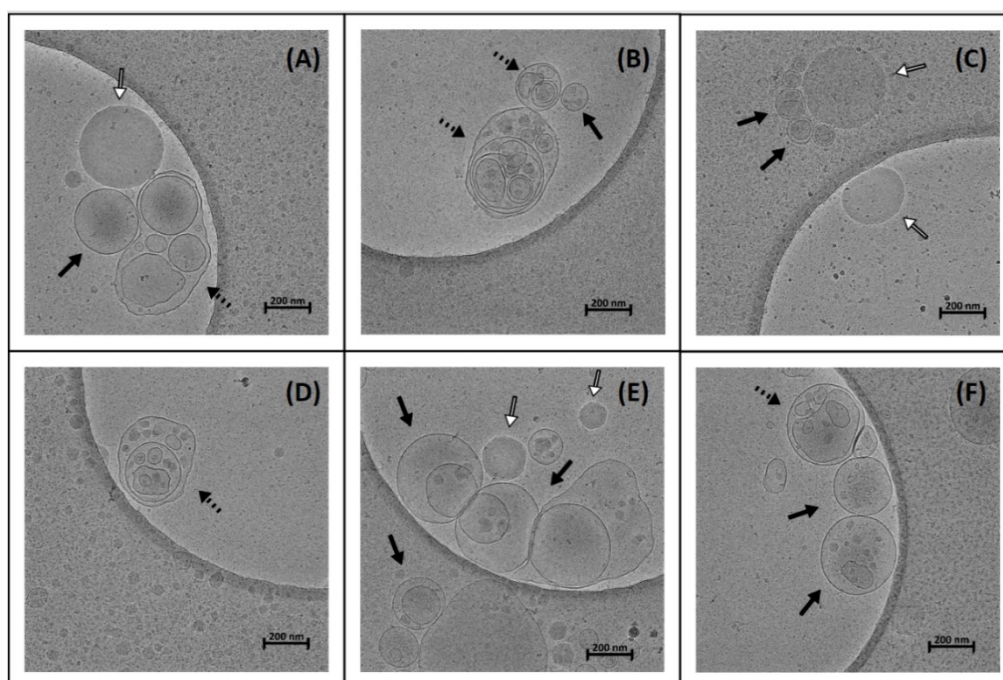
Figure 35: Cryo-TEM images of SEDDS, dilution 1:100 (v/v) in FaSSIF. (A) non-loaded Citrem SEDDS (B) DDAB-OND loaded Citrem SEDDS (C) DOTAP-OND loaded Citrem SEDDS (D) non-loaded Standard SEDDS (E) DDAB-OND loaded Standard SEDDS (F) DOTAP-OND loaded Citrem SEDDS. Full arrows indicate uni-and multilamellar vesicles, dashed arrows indicate more complex vesicular structures and open arrows indicate oil droplets.

In the study with the enzyme specifically cleaving single strand oligonucleotides, S1 nuclease, we showed that SEDDS enabled protection of OND against nuclease degradation after loading of the OND complexes into SEDDS. Subjecting OND solution to S1 nuclease for 30 min resulted into degradation of the entire amount of OND. The SEDDS had no impact on the activity of the enzyme. The neutral Standard SEDDS fulfilled their protective role better, protecting more

than 3-times more OND, as depicted in **Table 16**. This fact could be ascribed to negative surface charge as it might lead to destabilization of ion pairing between the OND and cationic lipids.

Table 16:The amount of OND (%) protected from degradation in the presence of specific nuclease for 30 min

SEDDS	Intact OND (%)	
	DDAB-OND in SEDDS	**DOTAP-OND in SEDDS**
Citrem (negatively charged)	16.0 ± 1.5	15.7 ± 1.0
Standard (neutral)	59.9 ± 3.4 ***	57.1 ± 3.0***

*** p<0.001 statistically significant difference between Citrem and Standard SEDDS. Data are presented as mean $\pm$ SD (n=3).

In addition, in order to prolong protection of OND over passage through the GI tract, orlistat, a lipase inhibitor, was added to the formulations. As little as 0.25 % orlistat in SEDDS was sufficient to inhibit lipolysis of both dispersed SEDDS to about 10% (**Figure 36**). Previously published data excluded interference of orlistat with permeation enhancement effect of MCFA-based excipients [153,216].
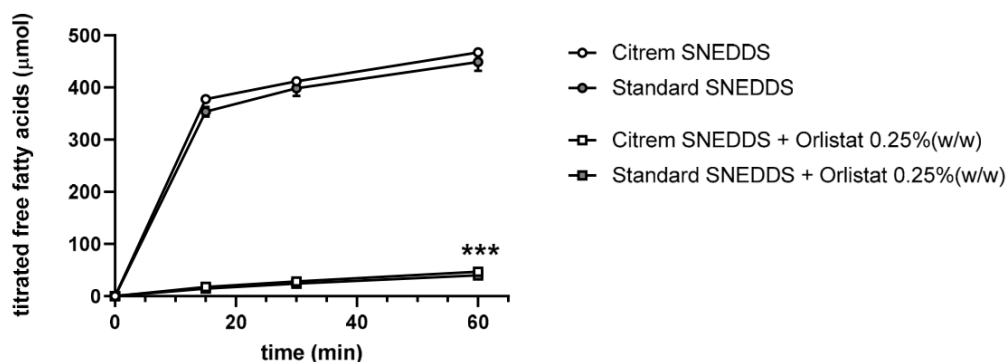
Figure 36: Dynamic in vitro lipolysis of SEDDS without and with the addition of orlistat for 60 min. Data are presented as mean $\pm$ SD, (n=3). *** p<0.001- significant effect of orlistat on SEDDS lipolysis

6.2.4 Caco-2 cell monolayer permeability and cytotoxicity study

Finally, DDAB-OND and DOTAP-OND loaded in both neutral and negatively charged SEDDS were tested *in vitro* in Caco-2 cell intestinal monolayer. Caco-2 cells grown on filters as a monolayer are a common static model and are considered the golden standard in *in vitro* prediction of intestinal permeability [217,218]. Under standard culture conditions they polarize into apical and basolateral side with TJs and brush border with microvilli on the apical side [219]. TJs are protein complexes between enterocytes in the small intestine that regulate the paracellular route of permeation into the basolateral compartment [220]. The integrity of TJs can be reliably measured by TEER as a function of electrical resistance across the monolayer. This parameter depends on the temperature and measurement technique, so the results can be compared only if it is monitored under the same experimental conditions [221].

OND as hydrophilic macromolecules use predominantly paracellular transport, therefore its permeability under physiological conditions is very limited [222]. Permeation enhancers based

on MCFA were found to open TJs in a reversible manner by interaction with cytoskeleton [146,152]. Even though at higher concentrations their action might be supported by transcellular permeation as a result of cell membrane alteration [209]. Permeation is limited by molecular weight of the macromolecule, not allowing 70 kDa dextran to pass across, neither much larger bacteria [153].

Firstly, TEER was evaluated as an indicator of permeation enhancement. TEER inversely correlates with permeation enhancing effect, so the lower TEER value, the higher permeation can be expected. In our study, TEER was evaluated at the beginning and at the end of the experiment by the more precise Endohm chamber. We observed that the more pronounced drop in TEER was caused by neutral Standard SEDDS. Namely TEER decreased to about 70% and 35 % of the initial TEER values of Citrem and Standard SEDDS, respectively (**Figure 37A**). In addition, we monitored TEER throughout the experiment by chopstick electrodes and related the changes to the first time point measured at 30 min. The neutral Standard SEDDS reached a plateau after 60 min unlike the negative Citrem SEDDS, in which the final TEER was reached already at 30 min (**Figure 37CD**). This phenomenon had translated into the permeated amount of OND.
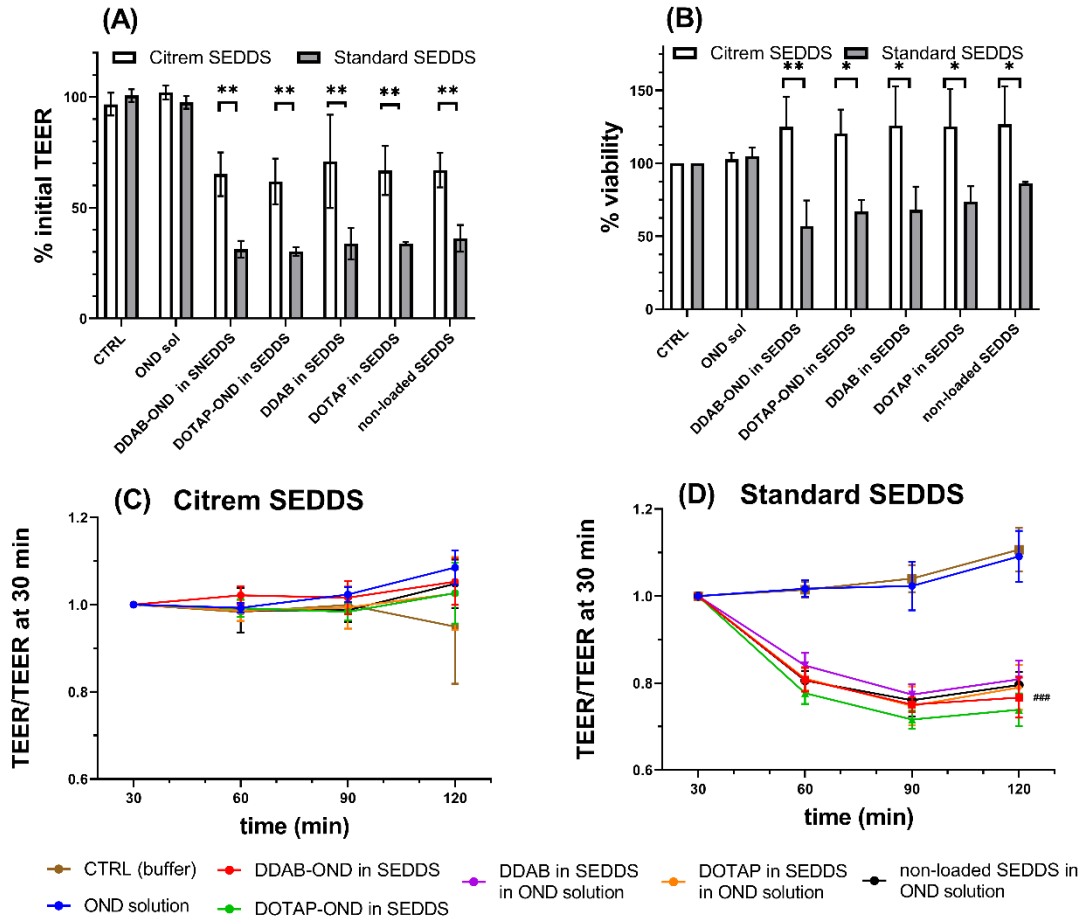
Figure 37: (A) % of initial TEER measured by Endohm chamber after 120 min of incubation at 25°C in both Citrem and Standard SEDDS. ** denotes a significant difference of TEER decline (p <0.01) between Citrem and Standard SEDDS. All SEDDS-incubated cells showed significantly lower TEER relative to respective CTRL (buffer) and OND solution. (B) % viability by LDH assay after 120 min of incubation with Citrem and Standard SEDDS. * and ** denotes a significant difference in viability between different SEDDS (*p <0.05 and **p<0.01). In (C) and (D), relative TEER values measured by chopstick electrodes at 37°C for Citrem SEDDS (C) and Standard SEDDS (D). In (D), ### represents a significant difference of relative TEER values of SEDDS-treated cells relative to CTRL and OND solution (p <0.001). Results are presented as mean ± SD (n=5-6).

The slope of the flux curves of the neutral Standard SEDDS became steeper after 60 minutes. In contrast, in the negatively charged Citrem SEDDS, the profile of the flux curves was more stable over the entire time of the experiment (**Figure 38AB**). In the presence of any SEDDS, permeation of OND was significantly enhanced (**Figure 38CD**). Moreover, in neutral SEDDS, permeation of OND in solution in the presence of non-loaded SEDDS showed better permeation in comparison to OND complexes in this SEDDS. Due to complexation with a cationic lipid, OND is associated within the dispersed SEDDS and not readily available for permeation. However, co-delivery of permeation enhancers and permeating OND is crucial and cannot be ensured under dynamic *in vivo* conditions without the formulation process [209].
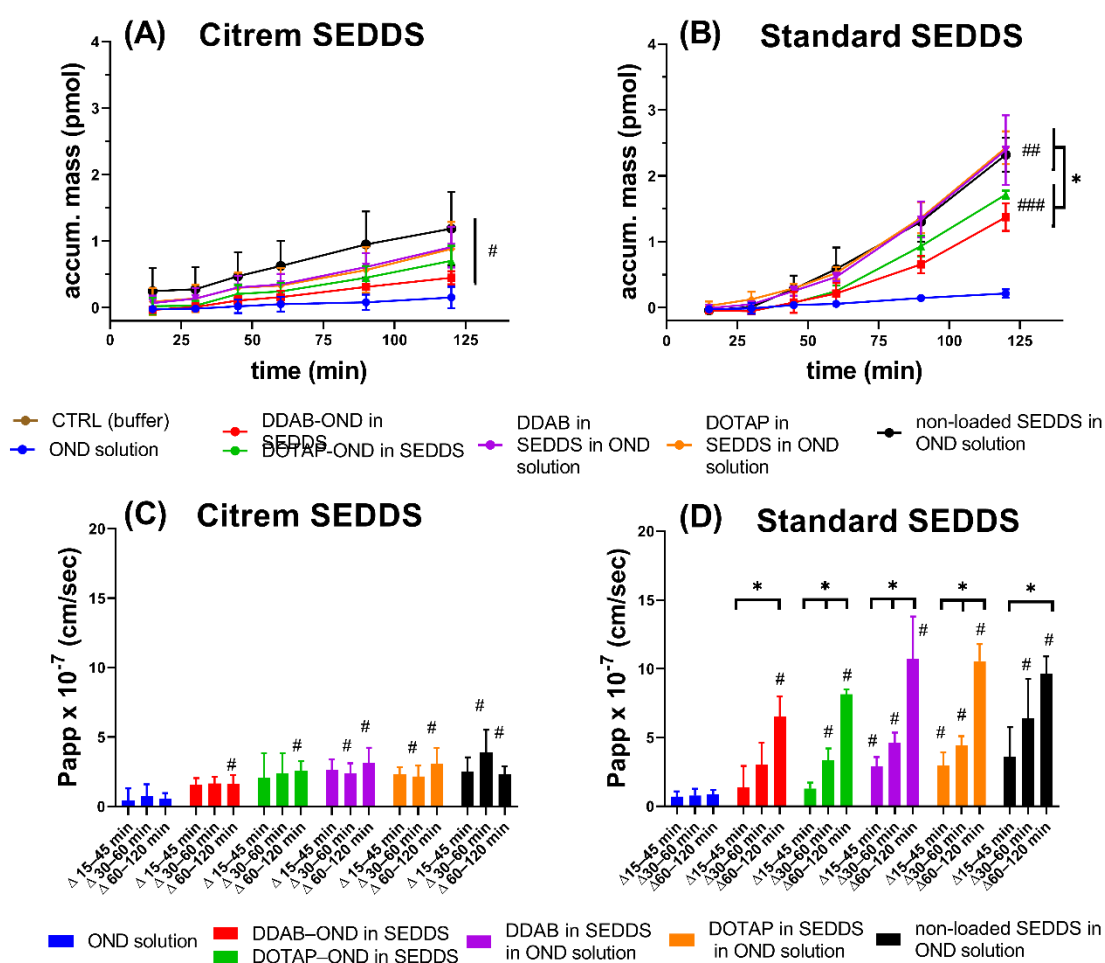
Figure 38: The transported OND accumulated in the basolateral compartment for Citrem SEDDS (A) and Standard SEDDS (B). P_{app} values for specified time intervals in Citrem SEDDS (C) and Standard SEDDS (D). In (A) and (B), [#], [##], [###] represents a significant difference of the flux curves of SEDDS-treated cells relative to OND solution ([#]$p <0.05$, [##]$p<0.01$ and [###]$p<0.001$)). In (B), * represents a significant difference between complex loaded Standard SEDDS and a group of other Standard SEDDS formulations (*$p<0.05$). In (C) and (D), bars marked by [#] showed a significant difference in P_{app} relative to respective bars of OND solution ($p<0.05$). In (D), significant difference between the time intervals in Standard SEDDS is denoted as * ($p<0.05$). Results are presented as mean $\pm$ SD (n=5-6).

Viability of Caco-2 was evaluated after the 2-hour long permeability study using LDH assay (**Figure 37B**). All lipid excipients used for formulation of the SEDDS are GRAS and/or approved by European and US Pharmacopeia [149,155,159]. Lower viability in presence of the neutral Standard SEDDS might be explained by more frequent interactions with the SEDDS resulting in membrane disturbance. As cell surface is negatively charged, negative surface charge of a formulation seems to act as a protective factor resulting in negligible impact of the negatively charged SEDDS on Caco-2 cells. Changes in viability caused by MCFA-based excipients were described to be reversible and less pronounced in *in vivo* models with higher repair capacity [153].

7 CONCLUSION

The application of nanotechnology to drug delivery is a promising approach to make drug therapy more effective and targeted. From a wide range of nanomaterials, this work utilised biodegradable and biocompatible polymeric and lipid carriers to address three challenges: sustained release, poor water solubility and oligonucleotide delivery.

- Formulation of polymeric nanocarriers with sustained release

Two different preparation methods, NPM and ESE, were employed and optimized for preparation of monodisperse NPs of size up to 300 nm and negative surface charge in order to achieve sustained intracellular delivery of a model fluorescent trace RhB. Polymeric NPs were prepared from experimental polymers, linear PLGA 5/5 and PLGA 7/3, and branched PLGA A2. The polymers were combined with low concentrations of surfactants (0.1-1%), namely Pluronic F127, Kolliphor P188, Tween 20 and PVA.

NPM yielded NPs of narrow size distribution of around 200 nm independently of the polymer and kind and concentration of surfactant used. The prepared NPs had negative surface charge and zeta potential was sufficiently low to assume colloidal stability. Out of the tested surfactants, only PVA increased zeta potential with its increasing concentration. The amount of loaded Rhodamine B was about 20% and was independent of both the utilised polymer and surfactant. In ESE, the amount and type of surfactant played a crucial role in size control. Increasing concentration of a surfactant resulted in size decrease of formed NPs, increasing surfactants from 0.1 to 1% resulted into size decrease from 200 to less than 100 nm. In Pluronic F127 and PVA, the concentration of surfactant also influenced zeta potential in the same manner as PVA in NPM, the higher concentration of surfactant, the higher zeta potential.

Finally, NPs formulated from the three experimental polymers and 0.1% solution of Pluronic F127 using NPM were loaded with RhB and subsequently subjected to release study. In 48 hours, the entire amount of RhB was released in the isosmotic HEPES buffer saline at pH 7.4, mainly as the initial burst. In the isosmotic saline solution and acetate buffer saline, pH 4.0, up to 50% of RhB were released during the same time period. The rapid release in the HEPES buffer saline is likely to be ascribed to spontaneous cyclic swelling that was observed only at neutral pH. Swelling could enhance diffusion of RhB as a water-soluble compound resulting in its faster release at pH 7.4 than at acidic conditions of the acetate buffer saline, pH 4.0. There was no difference in release profiles between polymers in the saline solution and HEPES buffer saline. In the acetate buffer saline, the release of RhB from PLGA A2 was significantly slower relative to PLGA 5/5 and PLGA 7/3.

- Formulation of lipid-based nanocarriers for delivery of a poorly water-soluble drug

This study addressed an important limitation of poor water solubility of a commonly administrated anti-inflammatory drug, IND. We utilised approaches based on organic solvents with no need of any specific instrumentation. NLCs were formulated from SA and GMS as solid lipids employing NPM and ESE, respectively. Using these non-complicated procedures, we prepared SA-based NLCs (NPM) of about 175 nm as well as GMS-based NLCs (ESE) of about 140 nm. Both formulations are considered homogeneous (PdI~0.2) and of sufficient negative zeta potential of about -35 mV and -45 mV, for SA-based NLCs and GMS-based NLCs, respectively. In both preparation methods, a combination of a hydrophilic and hydrophobic surfactant was necessary to form acceptable NLCs. The concentration of the hydrophobic surfactant had a more pronounced effect on the particle size and the concentration of both surfactants had to be optimised.

DSC showed irregularities in crystalline lattice of solid lipids likely caused by the presence of the liquid lipid IPM. These irregularities created unstructured lipid matrix, which is known to positively impact drug load capacity.

The composition of prepared SA- and GMS-based NLCs showed potential to enhance solubility of IND 5 and 10-fold relative to water, respectively. This enhancement was subsequently confirmed by evaluation of EE as the amount equal not only to 80% solubility of IND in lipid excipients, but also to 200% solubility of IND were successfully loaded into both NLCs. In order to better understand processes beyond IND encapsulation into NLCs, further research should focus on detailed evaluation of EE in a wider range of IND concentrations as well as evaluation of these formulations using X-ray powder diffraction.

- Formulation of lipid-based self-emulsifying drug delivery system for oral administration of an oligonucleotide

In order to deliver OND locally across the intestinal monolayer into lamina propria, we studied a well-established drug delivery system for oral delivery, SEDDS. To enable loading of a hydrophilic OND into hydrophobic lipid-based drug delivery system, ion-paired complexes of OND and DDAB/DOTAP were prepared by Blight-Dyer extraction method. The complexes were formed at the charge ratio 3:1 (N^+: PO_2^-) as >95% of OND was complexed at this charge ratio. Subsequently, the ion-paired complexes formed inverted micelles and were characterized in terms of size: DDAB-OND being 31.6-63.4 nm in diameter and DOTAP-OND of about the double size.

Hydrophobized OND complexes were loaded into two permeation enhancing SEDDS, both of them forming oil nanodroplets and vesicular structures. The SEDDS varied in their surface charge- neutral and negatively charged SEDDS, however, both of size around 200 nm.

The protective effect against nucleases was 3.5-times higher in the neutral SEDDS than in the negatively charged one, namely 58% and 16%, respectively. In order to prolong the protective effect of the formulations, orlistat was added in order to inhibit lipolysis of this lipid-based carrier in the GI tract. Only 0.25% of orlistat was necessary to inhibit lipolysis to 10% of its initial level.

Permeability of OND formulated into the SEDDS was tested in Caco-2 cell monolayer. Out of the two evaluated formulations, the neutral SEDDS enhanced OND permeability more. In terms of viability, negatively charged SEDDS seemed to stress cells less. In addition, positively charged proteins are known to be overexpressed in the inflamed tissue. Therefore, negative charge could be suitable for passive targeting into inflamed areas of the GI tract. Finally, no difference between cationic lipids used for hydrophobic ion pairing was observed, neither in permeability enhancement nor OND protection against nucleases.

8 REFERENCES

1. Whitesides, G.M. The "right" size in nanobiotechnology. *Nat. Biotechnol.* 2003, *21*, 1161–1165.

2. Commissioner, O. of the Nanotechnology - Nanotechnology Fact Sheet Available online: https://www.fda.gov/scienceresearch/specialtopics/nanotechnology/ucm402230.htm#overview (accessed on Mar 29, 2019).

3. Commision recommendation Recommendation on the definition of nanomaterial. *Off J Eur Communities* **2011**, *L274*, 1–40.

4. Fanun, M. *Colloids in Drug Delivery*; 2016;

5. Saraf, S. Application of Colloidal Properties in Drug Delivery. In *Colloids in drug delivery*; 2016; pp. 55–70.

6. Sinko, P.J. Colloidal dispersions. In *Martin´s physical pharmacy and pharmaceutical sciences*; Lippincott Williams & Wilkins: Philadelphia, 2011; pp. 386–409 ISBN 978-1-6091-3402-0.

7. Pelaz, B.; Alexiou, C.; Alvarez-Puebla, R.A.; Alves, F.; Andrews, A.M.; Ashraf, S.; Balogh, L.P.; Ballerini, L.; Bestetti, A.; Brendel, C.; et al. Diverse Applications of Nanomedicine. *ACS Nano* **2017**, *11*, 2313–2381, doi:10.1021/acsnano.6b06040.

8. Parekh, G.; Shi, Y.; Zheng, J.; Zhang, X.; Leporatti, S. Nano-carriers for targeted delivery and biomedical imaging enhancement. *Ther. Deliv.* **2018**, *9*, 451–468, doi:10.4155/tde-2018-0013.

9. Shi, J.; Kantoff, P.W.; Wooster, R.; Farokhzad, O.C. Cancer nanomedicine: progress, challenges and opportunities. *Nat. Rev. Cancer* **2017**, *17*, 20–37, doi:10.1038/nrc.2016.108.

10. Li, Z.; Tan, S.; Li, S.; Shen, Q.; Wang, K. Cancer drug delivery in the nano era: An overview and perspectives (Review). *Oncol. Rep.* **2017**, *38*, 611–624, doi:10.3892/or.2017.5718.

11. Walvekar, P.; Gannimani, R.; Govender, T. Combination drug therapy via nanocarriers against infectious diseases. *Eur. J. Pharm. Sci.* **2019**, *127*, 121–141, doi:10.1016/j.ejps.2018.10.017.

12. Kheirollahpour, M.; Mehrabi, M.; Dounighi, N.M.; Mohammadi, M.; Masoudi, A. Nanoparticles and Vaccine Development. *Pharm. Nanotechnol.* **2020**, *8*, 6–21, doi:10.2174/2211738507666191024162042.

13. Zhao, L.; Seth, A.; Wibowo, N.; Zhao, C.X.; Mitter, N.; Yu, C.; Middelberg, A.P.J. Nanoparticle vaccines. *Vaccine* 2014, *32*, 327–337.

14. Stevenson, R.; Hueber, A.J.; Hutton, A.; McInnes, I.B.; Graham, D. Nanoparticles and Inflammation. *Sci. World J.* **2011**, *11*, 1300–1312, doi:10.1100/tsw.2011.106.

15. Donahue, N.D.; Acar, H.; Wilhelm, S. Concepts of nanoparticle cellular uptake, intracellular trafficking, and kinetics in nanomedicine. *Adv. Drug Deliv. Rev.* 2019, *143*, 68–96.

16. Acharya, S.; Sahoo, S.K. PLGA nanoparticles containing various anticancer agents and tumour delivery by EPR effect. *Adv. Drug Deliv. Rev.* **2011**, *63*, 170–183, doi:10.1016/j.addr.2010.10.008.

17. Laverman, P.; Dams, E.T.M.; Storm, G.; Hafmans, T.G.; Croes, H.J.; Oyen, W.J..; Corstens, F.H..; Boerman, O.C. Microscopic localization of PEG-liposomes in a rat model of focal infection. *J. Control. Release* **2001**, *75*, 347–355, doi:10.1016/S0168-3659(01)00402-3.

18. Duan, X.; Li, Y. Physicochemical characteristics of nanoparticles affect circulation, biodistribution, cellular internalization, and trafficking. *Small* **2013**, *9*, 1521–1532, doi:10.1002/smll.201201390.

19. Tammam, S.N.; Azzazy, H.M.E.; Lamprecht, A. Biodegradable Particulate Carrier Formulation and Tuning for Targeted Drug Delivery. *J. Biomed. Nanotechnol.* **2015**, *11*, 555–577, doi:10.1166/jbn.2015.2017.

20. Alexis, F.; Pridgen, E.; Molnar, L.K.; Farokhzad, O.C. Factors Affecting the Clearance and Biodistribution of Polymeric Nanoparticles. *Mol. Pharm.* **2008**, *5*, 505–515, doi:10.1021/mp800051m.

21.   Fröhlich, E. The role of surface charge in cellular uptake and cytotoxicity of medical nanoparticles. *Int. J. Nanomedicine* **2012**, *7*, 5577–5591, doi:10.2147/IJN.S36111.

22.   Saadat, M.; Zahednezhad, F.; Zakeri-Milani, P.; Reza Heidari, H.; Shahbazi-Mojarrad, J.; Valizadeh, H. Drug Targeting Strategies Based on Charge Dependent Uptake of Nanoparticles into Cancer Cells. *J. Pharm. Pharm. Sci.* **2019**, *22*, 191–220, doi:10.18433/jpps30318.

23.   Chen, L.; Mccrate, J.M.; Lee, J.C.M.; Li, H. The role of surface charge on the uptake and biocompatibility of hydroxyapatite nanoparticles with osteoblast cells. *Nanotechnology* **2011**, *22*, doi:10.1088/0957-4484/22/10/105708.

24.   Lorenz, M.R.; Holzapfel, V.; Musyanovych, A.; Nothelfer, K.; Walther, P.; Frank, H.; Landfester, K.; Schrezenmeier, H.; Mailänder, V. Uptake of functionalized, fluorescent-labeled polymeric particles in different cell lines and stem cells. *Biomaterials* **2006**, *27*, 2820–2828, doi:10.1016/j.biomaterials.2005.12.022.

25.   Boltnarova, B.; Kubackova, J.; Skoda, J.; Stefela, A.; Smekalova, M.; Svacinova, P.; Pavkova, I.; Dittrich, M.; Scherman, D.; Zbytovska, J.; et al. Plga based nanospheres as a potent macrophage-specific drug delivery system. *Nanomaterials* **2021**, *11*, 1–17, doi:10.3390/nano11030749.

26.   Hua, S.; Marks, E.; Schneider, J.J.; Keely, S. Advances in oral nano-delivery systems for colon targeted drug delivery in inflammatory bowel disease: Selective targeting to diseased versus healthy tissue. *Nanomedicine Nanotechnology, Biol. Med.* 2015, *11*, 1117–1132.

27.   Suk, J.S.; Xu, Q.; Kim, N.; Hanes, J.; Ensign, L.M. PEGylation as a strategy for improving nanoparticle-based drug and gene delivery. *Adv. Drug Deliv. Rev.* **2016**, *99*, 28–51, doi:10.1016/j.addr.2015.09.012.

28.   Anselmo, A.C.; Mitragotri, S. Impact of particle elasticity on particle-based drug delivery systems. *Adv. Drug Deliv. Rev.* **2015**, *108*, 51–67, doi:10.1016/j.addr.2016.01.007.

29.   Li, Y.; Zhang, X.; Cao, D. Nanoparticle hardness controls the internalization pathway for drug delivery. *Nanoscale* **2015**, *7*, 2758–2769, doi:10.1039/C4NR05575F.

30.   Champion, J.A.; Mitragotri, S. Role of target geometry in phagocytosis. *Proc. Natl. Acad. Sci.* **2006**, *103*, 4930–4934, doi:10.1073/pnas.0600997103.

31.   Banerjee, A.; Qi, J.; Gogoi, R.; Wong, J.; Mitragotri, S. Role of nanoparticle size, shape and surface chemistry in oral drug delivery. *J. Control. Release* **2016**, *238*, 176–185, doi:10.1016/j.jconrel.2016.07.051.

32.   Caldorera-Moore, M.; Guimard, N.; Shi, L.; Roy, K. Designer nanoparticles: Incorporating size, shape and triggered release into nanoscale drug carriers. *Expert Opin. Drug Deliv.* **2010**, *7*, 479–495, doi:10.1517/17425240903579971.

33.   Bahrami, B.; Hojjat-Farsangi, M.; Mohammadi, H.; Anvari, E.; Ghalamfarsa, G.; Yousefi, M.; Jadidi-Niaragh, F. Nanoparticles and targeted drug delivery in cancer therapy. *Immunol. Lett.* **2017**, *190*, 64–83, doi:10.1016/j.imlet.2017.07.015.

34.   Bagalkot, V.; Deiuliis, J.A.; Rajagopalan, S.; Maiseyeu, A. "Eat me" imaging and therapy. *Adv. Drug Deliv. Rev.* 2016, *99*, 2–11.

35.   Weissleder, R.; Kelly, K.; Sun, E.Y.; Shtatland, T.; Josephson, L. Cell-specific targeting of nanoparticles by multivalent attachment of small molecules. *Nat. Biotechnol.* **2005**, *23*, 1418–1423, doi:10.1038/nbt1159.

36.   Nanjwade, B.K.; Bechra, H.M.; Derkar, G.K.; Manvi, F. V.; Nanjwade, V.K. Dendrimers: Emerging polymers for drug-delivery systems. *Eur. J. Pharm. Sci.* **2009**, *38*, 185–196, doi:10.1016/j.ejps.2009.07.008.

37.   Chella, N.; Shastri, N.R. Lipid carriers: Role and applications in nano drug delivery. In *Particulate Technology for Delivery of Therapeutics*; Springer Singapore, 2017; pp. 253–289 ISBN 9789811036477.

38.   Allen, T.M.; Cullis, P.R. Liposomal drug delivery systems: From concept to clinical applications. *Adv. Drug Deliv. Rev.* **2013**, *65*, 36–48, doi:10.1016/j.addr.2012.09.037.

39. Weissig, V.; Pettinger, T.K.; Murdock, N. Nanopharmaceuticals (part 1): products on the market. *Int. J. Nanomedicine* 2014, *9*, 4357–4373.

40. Ventola, C.L. Progress in nanomedicine: Approved and investigational nanodrugs. *P T* **2017**, *42*, 742–755.

41. Siepmann, J.; Faham, A.; Clas, S.D.; Boyd, B.J.; Jannin, V.; Bernkop-Schnürch, A.; Zhao, H.; Lecommandoux, S.; Evans, J.C.; Allen, C.; et al. Lipids and polymers in pharmaceutical technology: Lifelong companions. *Int. J. Pharm.* 2019, *558*, 128–142.

42. Chung, Y.H.; Beiss, V.; Fiering, S.N.; Steinmetz, N.F. COVID-19 Vaccine Frontrunners and Their Nanotechnology Design. *ACS Nano* **2020**, *14*, 12522–12537, doi:10.1021/acsnano.0c07197.

43. Milane, L.; Amiji, M. Clinical approval of nanotechnology-based SARS-CoV-2 mRNA vaccines: impact on translational nanomedicine. *Drug Deliv. Transl. Res.* **2021**, 1–7, doi:10.1007/s13346-021-00911-y.

44. Weiss, C.; Carriere, M.; Fusco, L.; Capua, I.; Regla-Nava, J.A.; Pasquali, M.; Scott, J.A.; Vitale, F.; Unal, M.A.; Mattevi, C.; et al. Toward Nanotechnology-Enabled Approaches against the COVID-19 Pandemic. *ACS Nano* **2020**, *14*, 6383–6406, doi:10.1021/acsnano.0c03697.

45. Chen, S.; Hao, X.; Liang, X.; Zhang, Q.; Zhang, C.; Zhou, G.; Shen, S.; Jia, G.; Zhang, J. Inorganic nanomaterials as carriers for drug delivery. *J. Biomed. Nanotechnol.* **2016**, *12*, 1–27, doi:10.1166/jbn.2016.2122.

46. Roy, S.; Liu, Z.; Sun, X.; Gharib, M.; Yan, H.; Huang, Y.; Megahed, S.; Schnabel, M.; Zhu, D.; Feliu, N.; et al. Assembly and Degradation of Inorganic Nanoparticles in Biological Environments. **2019**, doi:10.1021/acs.bioconjchem.9b00645.

47. Singh, P.; Pandit, S.; Mokkapati, V.R.S.S.; Garg, A.; Ravikumar, V.; Mijakovic, I. Gold nanoparticles in diagnostics and therapeutics for human cancer. *Int. J. Mol. Sci.* 2018, *19*, 1979.

48. Kong, F.Y.; Zhang, J.W.; Li, R.F.; Wang, Z.X.; Wang, W.J.; Wang, W. Unique roles of gold nanoparticles in drug delivery, targeting and imaging applications. *Molecules* 2017, *22*, 1445.

49. Dadfar, S.M.; Roemhild, K.; Drude, N.I.; von Stillfried, S.; Knüchel, R.; Kiessling, F.; Lammers, T. Iron oxide nanoparticles: Diagnostic, therapeutic and theranostic applications. *Adv. Drug Deliv. Rev.* **2019**, *138*, 302–325, doi:10.1016/j.addr.2019.01.005.

50. El-Boubbou, K. Magnetic iron oxide nanoparticles as drug carriers: Clinical relevance. *Nanomedicine* **2018**, *13*, 953–971, doi:10.2217/nnm-2017-0336.

51. Vangijzegem, T.; Stanicki, D.; Laurent, S. Magnetic iron oxide nanoparticles for drug delivery: applications and characteristics. *Expert Opin. Drug Deliv.* **2019**, *16*, 69–78, doi:10.1080/17425247.2019.1554647.

52. Zhou, Y.; Quan, G.; Wu, Q.; Zhang, X.; Niu, B.; Wu, B.; Huang, Y.; Pan, X.; Wu, C. Mesoporous silica nanoparticles for drug and gene delivery. *Acta Pharm. Sin. B* 2018, *8*, 165–177.

53. Tang, F.; Li, L.; Chen, D. Mesoporous silica nanoparticles: Synthesis, biocompatibility and drug delivery. *Adv. Mater.* **2012**, *24*, 1504–1534, doi:10.1002/adma.201104763.

54. Wang, Y.; Zhao, Q.; Han, N.; Bai, L.; Li, J.; Liu, J.; Che, E.; Hu, L.; Zhang, Q.; Jiang, T.; et al. Mesoporous silica nanoparticles in drug delivery and biomedical applications. *Nanomedicine Nanotechnology, Biol. Med.* **2015**, *11*, 313–327, doi:10.1016/j.nano.2014.09.014.

55. Bakry, R.; Vallant, R.M.; Najam-ul-Haq, M.; Rainer, M.; Szabo, Z.; Huck, C.W.; Bonn, G.K. Medicinal applications of fullerenes. *Int. J. Nanomedicine* 2007, *2*, 639–49.

56. Kazemzadeh, H.; Mozafari, M. Fullerene-based delivery systems. *Drug Discov. Today* 2019, *24*, 898–905.

57. Sinko, P.J. Pharmaceutical Polymers - Chapter 20. In *Martin's physical pharmacy and pharmaceutical sciences*; 2006; pp. 492–515 ISBN 978-0-7817-9766-5.

58. Sandoval-Yañez, C.; Rodriguez, C.C. Dendrimers: Amazing platforms for bioactive molecule delivery systems. *Materials (Basel).* **2020**, *13*, 1–20, doi:10.3390/ma13030570.

59. Chauhan, A.S. Dendrimers for Drug Delivery. *Molecules* **2018**, *23*, 938, doi:10.3390/molecules23040938.

60. Kubackova, J.; Zbytovska, J.; Holas, O. Nanomaterials for direct and indirect immunomodulation: A review of applications. *Eur. J. Pharm. Sci.* **2020**, *142*, 105139, doi:10.1016/j.ejps.2019.105139.

61. Croy, S.; Kwon, G. Polymeric Micelles for Drug Delivery. *Curr. Pharm. Des.* **2006**, *12*, 4669–4684, doi:10.2174/138161206779026245.

62. Movassaghian, S.; Merkel, O.M.; Torchilin, V.P. Applications of polymer micelles for imaging and drug delivery. *Wiley Interdiscip. Rev. Nanomedicine Nanobiotechnology* **2015**, *7*, 691–707, doi:10.1002/wnan.1332.

63. Ahmad, Z.; Shah, A.; Siddiq, M.; Kraatz, H.B. Polymeric micelles as drug delivery vehicles. *RSC Adv.* **2014**, *4*, 17028–17038, doi:10.1039/c3ra47370h.

64. Tyler, B.; Gullotti, D.; Mangraviti, A.; Utsuki, T.; Brem, H. Polylactic acid (PLA) controlled delivery carriers for biomedical applications. *Adv. Drug Deliv. Rev.* 2016, *107*, 163–175.

65. Mkhabela, V.J.; Ray, S.S. Poly(ε-caprolactone) Nanocomposite Scaffolds for Tissue Engineering: A Brief Overview. *J. Nanosci. Nanotechnol.* **2014**, *14*, 535–545, doi:10.1166/jnn.2014.9055.

66. Grossen, P.; Witzigmann, D.; Sieber, S.; Huwyler, J. PEG-PCL-based nanomedicines: A biodegradable drug delivery system and its application. *J. Control. Release* 2017, *260*, 46–60.

67. Dash, T.K.; Konkimalla, V.B. Polymeric modification and its implication in drug delivery: Poly-ε-caprolactone (PCL) as a model polymer. *Mol. Pharm.* **2012**, *9*, 2365–2379, doi:10.1021/mp3001952.

68. Vauthier, C.; Dubernet, C.; Fattal, E.; Pinto-Alphandary, H.; Couvreur, P. Poly(alkylcyanoacrylates) as biodegradable materials for biomedical applications. *Adv. Drug Deliv. Rev.* **2003**, *55*, 519–548, doi:10.1016/S0169-409X(03)00041-3.

69. Vauthier, C. A journey through the emergence of nanomedicines with poly(alkylcyanoacrylate) based nanoparticles. *J. Drug Target.* **2019**, *27*, 502–524, doi:10.1080/1061186X.2019.1588280.

70. Rizeq, B.R.; Younes, N.N.; Rasool, K.; Nasrallah, G.K. Synthesis, bioapplications, and toxicity evaluation of chitosan-based nanoparticles. *Int. J. Mol. Sci.* 2019, *20*, 5776.

71. Kumar, A.; Vimal, A.; Kumar, A. Why Chitosan? From properties to perspective of mucosal drug delivery. *Int. J. Biol. Macromol.* **2016**, *91*, 615–622, doi:10.1016/j.ijbiomac.2016.05.054.

72. Severino, P.; da Silva, C.F.; Andrade, L.N.; de Lima Oliveira, D.; Campos, J.; Souto, E.B. Alginate Nanoparticles for Drug Delivery and Targeting. *Curr. Pharm. Des.* **2019**, *25*, 1312–1334, doi:10.2174/1381612825666190425163424.

73. Jaimes-Aguirre, L.; Gibbens-Bandala, B.V.; Morales-Avila, E.; Ocampo-García, B.E.; Seyedeh-Fatemeh, M.; Amirhosein, A. Polymer-Based Drug Delivery Systems, Development and Pre-Clinical Status. *Curr. Pharm. Des.* 2016, 2886–2903.

74. Liu, X.; Yang, Y.; Urban, M.W. Stimuli-Responsive Polymeric Nanoparticles. *Macromol. Rapid Commun.* **2017**, *38*, 1–20, doi:10.1002/marc.201700030.

75. Molavi, F.; Barzegar-Jalali, M.; Hamishehkar, H. Polyester based polymeric nano and microparticles for pharmaceutical purposes: A review on formulation approaches. *J. Control. Release* **2020**, *320*, 265–282, doi:10.1016/j.jconrel.2020.01.028.

76. Martins, C.; Sousa, F.; Araújo, F.; Sarmento, B. Functionalizing PLGA and PLGA Derivatives for Drug Delivery and Tissue Regeneration Applications. *Adv. Healthc. Mater.* **2018**, *7*, 1–24, doi:10.1002/adhm.201701035.

77. Mir, M.; Ahmed, N.; Rehman, A. ur Recent applications of PLGA based nanostructures in drug delivery. *Colloids Surfaces B Biointerfaces* 2017, *159*, 217–231.

78. Wang, Y.; Li, P.; Tran, T.T.D.; Zhang, J.; Kong, L. Manufacturing techniques and surface engineering of polymer based nanoparticles for targeted drug delivery to cancer. *Nanomaterials* **2016**, *6*, 1–18, doi:10.3390/nano6020026.

79. Soppimath, K.S.; Aminabhavi, T.M.; Kulkarni, A.R.; Rudzinski, W.E. Biodegradable polymeric nanoparticles as drug delivery devices. *J. Control. Release* 2001, *70*, 1–20.

80. Panyam, J.; Zhou, W.; Prabha, S.; Sahoo, S.K.; Labhasetwar, V. Rapid endo-lysosomal escape of poly(DL-lactide- co glycolide) nanoparticles: implications for drug and gene delivery . *FASEB J.* **2002**, *16*, 1217–1226, doi:10.1096/fj.02-0088com.

81. Galliani, M.; Tremolanti, C.; Signore, G. Nanocarriers for Protein Delivery to the Cytosol: Assessing the Endosomal Escape of Poly(Lactide-co-Glycolide)-Poly(Ethylene Imine) Nanoparticles. *Nanomaterials* **2019**, *9*, doi:10.3390/nano9040652.

82. Faraji, A.H.; Wipf, P. Nanoparticles in cellular drug delivery. *Bioorganic Med. Chem.* 2009, *17*, 2950–2962.

83. Siepmann, J.; Siepmann, F. The Modified-Release Drug Delivery Landscape: Academic Viewpoint. In *Modified-release drug delivery Technology*; Rathbone, M.J., Ed.; New York, 2008; pp. 17–34 ISBN 978-1-4200-5355-5 q.

84. Zolnik, B.S.; Burgess, D.J. Effect of acidic pH on PLGA microsphere degradation and release. *J. Control. Release* **2007**, *122*, 338–344, doi:10.1016/j.jconrel.2007.05.034.

85. Xu, Y.; Kim, C.S.; Saylor, D.M.; Koo, D. Polymer degradation and drug delivery in PLGA-based drug–polymer applications: A review of experiments and theories. *J. Biomed. Mater. Res. - Part B Appl. Biomater.* **2017**, *105*, 1692–1716, doi:10.1002/jbm.b.33648.

86. Tomic, I.; Vidis-Millward, A.; Mueller-Zsigmondy, M.; Cardot, J.M. Setting accelerated dissolution test for PLGA microspheres containing peptide, investigation of critical parameters affecting drug release rate and mechanism. *Int. J. Pharm.* **2016**, *505*, 42–51, doi:10.1016/j.ijpharm.2016.03.048.

87. Rao, J.P.; Geckeler, K.E. Polymer nanoparticles: Preparation techniques and size-control parameters. *Prog. Polym. Sci.* **2011**, *36*, 887–913, doi:10.1016/j.progpolymsci.2011.01.001.

88. Anton, N.; Benoit, J.P.; Saulnier, P. Design and production of nanoparticles formulated from nano-emulsion templates-A review. *J. Control. Release* **2008**, *128*, 185–199, doi:10.1016/j.jconrel.2008.02.007.

89. Rao, J.P.; Geckeler, K.E. Polymer nanoparticles: Preparation techniques and size-control parameters. *Prog. Polym. Sci.* **2011**, *36*, 887–913, doi:10.1016/j.progpolymsci.2011.01.001.

90. Nicolas, J.; Mura, S.; Brambilla, D.; Mackiewicz, N.; Couvreur, P. Design, functionalization strategies and biomedical applications of targeted biodegradable/biocompatible polymer-based nanocarriers for drug delivery. *Chem. Soc. Rev.* **2013**, *42*, 1147–1235, doi:10.1039/C2CS35265F.

91. Crucho, C.I.C.; Barros, M.T. Polymeric nanoparticles: A study on the preparation variables and characterization methods. *Mater. Sci. Eng. C* 2017, *80*, 771–784.

92. Donno, R.; Gennari, A.; Lallana, E.; De La Rosa, J.M.R.; D'Arcy, R.; Treacher, K.; Hill, K.; Ashford, M.; Tirelli, N. Nanomanufacturing through microfluidic-assisted nanoprecipitation: Advanced analytics and structure-activity relationships. *Int. J. Pharm.* **2017**, *534*, 97–107, doi:10.1016/j.ijpharm.2017.10.006.

93. Dubey, S.; Mody, N.; Sharma, R.; Agrawal, U.; Vyas, S.P. Nanobiomaterials. In *Nanobiomaterials in Drug Delivery*; Elsevier, 2016; pp. 111–146.

94. Snejdrova, E.; Podzimek, S.; Martiska, J.; Holas, O.; Dittrich, M. Branched PLGA derivatives with tailored drug delivery properties. *Acta Pharm.* **2020**, *70*, 63–75, doi:10.2478/acph-2020-0011.

95. Davaran, S.; Omidi, Y.; Mohammad Reza Rashidi; Anzabi, M.; Shayanfar, A.; Ghyasvand, S.; Vesal, N.; Davaran, F. Preparation and in vitro evaluation of linear and star-branched PLGA nanoparticles for insulin delivery. *J. Bioact. Compat. Polym.* **2008**, *23*, 115–131, doi:10.1177/0883911507088276.

96. Frauke Pistel, K.; Breitenbach, A.; Zange-Volland, R.; Kissel, T. Brush-like branched biodegradable polyesters, part III: Protein release from microspheres of poly(vinyl alcohol)-graft-poly(D,L-lactic-co-glycolic acid). *J. Control. Release* **2001**, *73*, 7–20, doi:10.1016/S0168-3659(01)00231-0.

97. Li, Y.; Zhang, X.; Zhang, J.; Ma, J.; Chi, L.; Qiu, N.; Li, Y. Synthesis of a biodegradable branched copolymer mPEG-b-PLGA-g-OCol and its pH-sensitive micelle. *Mater. Sci. Eng. C* **2020**, *108*, 110455, doi:10.1016/j.msec.2019.110455.

98. Fahy, E.; Cotter, D.; Sud, M.; Subramaniam, S. Lipid classification, structures and tools. *Biochim. Biophys. Acta - Mol. Cell Biol. Lipids* **2011**, *1811*, 637–647, doi:10.1016/j.bbalip.2011.06.009.

99. Christie, W.W. *High-performance liquid chromatography and lipids: A practical guide*; Pergamon Books: Oxford, 1987;

100. Fahy, E.; Subramaniam, S.; Brown, H.A.; Glass, C.K.; Merrill, A.H.; Murphy, R.C.; Raetz, C.R.H.; Russell, D.W.; Seyama, Y.; Shaw, W.; et al. A comprehensive classification system for lipids. *J. Lipid Res.* **2005**, *46*, 839–861, doi:10.1194/jlr.E400004-JLR200.

101. Markovic, M.; Ben-Shabat, S.; Aponick, A.; Zimmermann, E.M.; Dahan, A. Lipids and lipid-processing pathways in drug delivery and therapeutics. *Int. J. Mol. Sci.* **2020**, *21*, doi:10.3390/ijms21093248.

102. Müller, R.H.; Mäder, K.; Gohla, S. Solid lipid nanoparticles (SLN) for controlled drug delivery - A review of the state of the art. *Eur. J. Pharm. Biopharm.* **2000**, *50*, 161–177.

103. Wissing, S..; Kayser, O.; Müller, R.. Solid lipid nanoparticles for parenteral drug delivery. *Adv. Drug Deliv. Rev.* **2004**, *56*, 1257–1272, doi:10.1016/j.addr.2003.12.002.

104. Ribeiro, A.P.B.; Masuchi, M.H.; Miyasaki, E.K.; Domingues, M.A.F.; Stroppa, V.L.Z.; de Oliveira, G.M.; Kieckbusch, T.G. Crystallization modifiers in lipid systems. *J. Food Sci. Technol.* **2015**, *52*, 3925–3946, doi:10.1007/s13197-014-1587-0.

105. Souto, E.; Müller, R. Lipid Nanoparticles (Solid Lipid Nanoparticles and Nanostructured Lipid Carriers) for Cosmetic, Dermal, and Transdermal Applications. In *Nanoparticluate Drug Delivery Systems*; Thassu, D., Deleers, M., Pathak, Y., Eds.; informa healthcare: New York, 2010; pp. 213–233 ISBN 0-8493-9073-7.

106. Beloqui, A.; Solinís, M.Á.; Rodríguez-Gascón, A.; Almeida, A.J.; Préat, V. Nanostructured lipid carriers: Promising drug delivery systems for future clinics. *Nanomedicine Nanotechnology, Biol. Med.* **2016**, *12*, 143–161, doi:10.1016/j.nano.2015.09.004.

107. Bunjes, H. Lipid nanoparticles for the delivery of poorly water-soluble drugs. *J. Pharm. Pharmacol.* **2010**, *62*, 1637–1645, doi:10.1111/j.2042-7158.2010.01024.x.

108. Khosa, A.; Reddi, S.; Saha, R.N. Nanostructured lipid carriers for site-specific drug delivery. *Biomed. Pharmacother.* **2018**, *103*, 598–613.

109. Ganesan, P.; Narayanasamy, D. Lipid nanoparticles: Different preparation techniques, characterization, hurdles, and strategies for the production of solid lipid nanoparticles and nanostructured lipid carriers for oral drug delivery. *Sustain. Chem. Pharm.* 2017, *6*, 37–56.

110. Schubert, M.A.; Müller-Goymann, C.C. Solvent injection as a new approach for manufacturing lipid nanoparticles - Evaluation of the method and process parameters. *Eur. J. Pharm. Biopharm.* **2003**, *55*, 125–131, doi:10.1016/S0939-6411(02)00130-3.

111. Teixeira, M.C.; Carbone, C.; Souto, E.B. Beyond liposomes: Recent advances on lipid based nanostructures for poorly soluble/poorly permeable drug delivery. *Prog. Lipid Res.* **2017**, *68*, 1–11, doi:10.1016/j.plipres.2017.07.001.

112. Tapeinos, C.; Battaglini, M.; Ciofani, G. Advances in the design of solid lipid nanoparticles and nanostructured lipid carriers for targeting brain diseases. *J. Control. Release* **2017**, *264*, 306–332, doi:10.1016/j.jconrel.2017.08.033.

113. Wissing, S.; Lippacher, A.; Müller, R. Investigations on the occlusive properties of solid lipid nanoparticles (SLN). *J. Cosmet. Sci.* **2011**, *52*, 313–24.

114. López-García, R.; Ganem-Rondero, A. Solid Lipid Nanoparticles (SLN) and Nanostructured Lipid Carriers (NLC): Occlusive Effect and Penetration Enhancement Ability. *J. Cosmet. Dermatological Sci. Appl.* **2015**, *05*, 62–72, doi:10.4236/jcdsa.2015.52008.

115. Zhai, Y.; Zhai, G. Advances in lipid-based colloid systems as drug carrier for topic delivery. *J.*

Control. Release **2014**, *193*, 90–99, doi:10.1016/j.jconrel.2014.05.054.

116. Talegaonkar, S.; Bhattacharyya, A. Potential of Lipid Nanoparticles (SLNs and NLCs) in Enhancing Oral Bioavailability of Drugs with Poor Intestinal Permeability. *AAPS PharmSciTech* **2019**, *20*, doi:10.1208/s12249-019-1337-8.

117. Schneider, H.; Braun, A.; Füllekrug, J.; Stremmel, W.; Ehehalt, R. Lipid based therapy for ulcerative colitis-modulation of intestinal mucus membrane phospholipids as a tool to influence inflammation. *Int. J. Mol. Sci.* **2010**, *11*, 4149–4164, doi:10.3390/ijms11104149.

118. Korzenik, J.R.; Podolsky, D.K. Evolving knowledge and therapy of inflammatory bowel disease. *Nat. Rev. Drug Discov.* 2006, *5*, 197–209.

119. Beloqui, A.; Cococ, R.; Alhouayek, M.; Soliṅis, M.Á.; Rodŕiguez-Gáscon, A.; Muccioli, G.G.; Préat, V. Budesonide-loaded nanostructured lipid carriers reduce inflammation in murine DSS-induced colitis. *Int. J. Pharm.* **2013**, *454*, 775–783, doi:10.1016/j.ijpharm.2013.05.017.

120. Beloqui, A.; Memvanga, P.B.; Coco, R.; Reimondez-Troitiño, S.; Alhouayek, M.; Muccioli, G.G.; Alonso, M.J.; Csaba, N.; de la Fuente, M.; Préat, V. A comparative study of curcumin-loaded lipid-based nanocarriers in the treatment of inflammatory bowel disease. *Colloids Surfaces B Biointerfaces* **2016**, *143*, 327–335, doi:10.1016/j.colsurfb.2016.03.038.

121. Daraee, H.; Etemadi, A.; Kouhi, M.; Alimirzalu, S.; Akbarzadeh, A. Application of liposomes in medicine and drug delivery. *Artif. Cells, Nanomedicine, Biotechnol.* **2014**, *1401*, 1–11, doi:10.3109/21691401.2014.953633.

122. Abu Lila, A.S.; Ishida, T. Liposomal Delivery Systems: Design Optimization and Current Applications. *Biol. Pharm. Bull.* **2017**, *40*, 1–10, doi:10.1248/bpb.b16-00624.

123. Banerjee, R. Liposomes: Applications in medicine. *J. Biomater. Appl.* **2001**, *16*, 3–21, doi:10.1106/RA7U-1V9C-RV7C-8QXL.

124. Carita, A.C.; Eloy, J.O.; Chorilli, M.; Lee, R.J.; Leonardi, G.R. Recent Advances and Perspectives in Liposomes for Cutaneous Drug Delivery. *Curr. Med. Chem.* **2017**, *25*, 606–635, doi:10.2174/0929867324666171009120154.

125. Gupta, A.; Eral, H.B.; Hatton, T.A.; Doyle, P.S. Nanoemulsions: formation, properties and applications. *Soft Matter* **2016**, *12*, 2826–2841, doi:10.1039/C5SM02958A.

126. Sutradhar, K.B.; Amin, L. Nanoemulsions: Increasing possibilities in drug delivery. *Eur. J. Nanomedicine* **2013**, *5*, 97–110, doi:10.1515/ejnm-2013-0001.

127. Tayeb, H.H.; Sainsbury, F. Nanoemulsions in drug delivery: Formulation to medical application. *Nanomedicine* **2018**, *13*, 2507–2525, doi:10.2217/nnm-2018-0088.

128. Singh, Y.; Meher, J.G.; Raval, K.; Khan, F.A.; Chaurasia, M.; Jain, N.K.; Chourasia, M.K. Nanoemulsion: Concepts, development and applications in drug delivery. *J. Control. Release* 2017, *252*, 28–49.

129. Gursoy, R.N.; Benita, S. Self-emulsifying drug delivery systems (SEDDS) for improved oral delivery of lipophilic drugs. *Biomed. Pharmacother.* **2004**, *58*, 173–182, doi:10.1016/j.biopha.2004.02.001.

130. Müllertz, A.; Ogbonna, A.; Ren, S.; Rades, T. New perspectives on lipid and surfactant based drug delivery systems for oral delivery of poorly soluble drugs. *J. Pharm. Pharmacol.* **2010**, *62*, 1622–1636, doi:10.1111/j.2042-7158.2010.01107.x.

131. Mahmood, A.; Bernkop-Schnürch, A. SEDDS: A game changing approach for the oral administration of hydrophilic macromolecular drugs. *Adv. Drug Deliv. Rev.* **2019**, *142*, 91–101, doi:10.1016/j.addr.2018.07.001.

132. Reiss, H. Entropy-induced dispersion of bulk liquids. *J. Colloid Interface Sci.* **1975**, *53*, 61–70, doi:10.1016/0021-9797(75)90035-1.

133. Maurya, D.P.; Sultana, Y.; Kalam, M.A. Self-Emulsifying Drug Delivery Systems. In *Colloids in drug delivery*; 2016; pp. 299–310.

134. Berthelsen, R.; Klitgaard, M.; Rades, T.; Müllertz, A. In vitro digestion models to evaluate lipid based drug delivery systems; present status and current trends. *Adv. Drug Deliv. Rev.* **2019**, *142*, 35–49, doi:10.1016/j.addr.2019.06.010.

135. Kossena, G.A.; Charman, W.N.; Boyd, B.J.; Porter, C.J.H. Influence of the intermediate digestion phases of common formulation lipids on the absorption of a poorly water-soluble drug. *J. Pharm. Sci.* **2005**, *94*, 481–492, doi:10.1002/jps.20260.

136. O'Driscoll, C.M.; Griffin, B.T. Biopharmaceutical challenges associated with drugs with low aqueous solubility-The potential impact of lipid-based formulations. *Adv. Drug Deliv. Rev.* 2008, *60*, 617–624.

137. Jeong, S.H.; Park, J.H.; Park, K. Formulation Issues around Lipid-Based Oral and Parenteral Delivery Systems. In *Role of Lipid Excipients in Modifying Oral and Parenteral Drug Delivery: Basic Principles and Biological Examples*; John Wiley & Sons, Inc.: Hoboken, NJ, USA, 2006; pp. 32–47 ISBN 0471739529.

138. Hunt, J.N.; Knox, M.T. A relation between the chain length of fatty acids and the slowing of gastric emptying. *J. Physiol.* **1968**, *194*, 327–336, doi:10.1113/jphysiol.1968.sp008411.

139. Zhao, G.; Huang, J.; Xue, K.; Si, L.; Li, G. Enhanced intestinal absorption of etoposide by self-microemulsifying drug delivery systems: Roles of P-glycoprotein and cytochrome P450 3A inhibition. *Eur. J. Pharm. Sci.* **2013**, *50*, 429–439, doi:10.1016/j.ejps.2013.08.016.

140. Negi, L.M.; Tariq, M.; Talegaonkar, S. Nano scale self-emulsifying oil based carrier system for improved oral bioavailability of camptothecin derivative by P-Glycoprotein modulation. *Colloids Surfaces B Biointerfaces* **2013**, *111*, 346–353, doi:10.1016/j.colsurfb.2013.06.001.

141. Patel, J.P.; Brocks, D.R. The effect of oral lipids and circulating lipoproteins on the metabolism of drugs. *Expert Opin. Drug Metab. Toxicol.* **2009**, *5*, 1385–1398, doi:10.1517/17425250903176439.

142. Charman, W.N.; Porter, C.J.H.; Mithani, S.; Dressman, J.B. Physicochemical and Physiological Mechanisms for the Effects of Food on Drug Absorption: The Role of Lipids and pH. *J. Pharm. Sci.* **1997**, *86*, 269–282, doi:10.1021/js960085v.

143. Jannin, V.; Musakhanian, J.; Marchaud, D. Approaches for the development of solid and semi-solid lipid-based formulations ☆. *Adv. Drug Deliv. Rev.* **2008**, *60*, 734–746, doi:10.1016/j.addr.2007.09.006.

144. Meyer, J.D.; Manning, M.C. Hydrophobic ion pairing: Altering the solubility properties of biomolecules. *Pharm. Res.* 1998.

145. Maher, S.; Geoghegan, C.; Brayden, D.J. Intestinal permeation enhancers to improve oral bioavailability of macromolecules: Reasons for low efficacy in humans. *Expert Opin. Drug Deliv.* **2020**, doi:10.1080/17425247.2021.1825375.

146. Hayashi, M.; Sakai, T.; Hasegawa, Y.; Nishikawahara, T.; Tomioka, H.; Iida, A.; Shimizu, N.; Tomita, M.; Awazu, S. Physiological mechanism for enhancement of paracellular drug transport. *J. Control. Release* **1999**, *62*, 141–148, doi:10.1016/S0168-3659(99)00031-0.

147. Li, P.; Nielsen, H.M.; Müllertz, A. Impact of Lipid-Based Drug Delivery Systems on the Transport and Uptake of Insulin Across Caco-2 Cell Monolayers. *J. Pharm. Sci.* **2016**, *105*, 2743–2751, doi:10.1016/j.xphs.2016.01.006.

148. Hayashi, M.; Tomita, M. Mechanistic Analysis for Drug Permeation Through Intestinal Membrane. *Drug Metab. Pharmacokinet.* **2007**, *22*, 67–77, doi:10.2133/dmpk.22.67.

149. Swain, S.; Patra, C.N.; Rao, M.E.B. *Pharmaceutical Drug Delivery Systems and Vehicles*; Woodhead Publishing India: New Delhi, 2016; ISBN 987-93-85059-00-1.

150. Small, D.M. A classification of biologic lipids based upon their interaction in aqueous systems. *J. Am. Oil Chem. Soc.* **1968**, *45*, 108–119, doi:10.1007/BF02915334.

151. Yoshitomi, H.; Nishihata, T.; Frederick, G.; Dillsaver, M.; Higuchi, L.T. Effect of triglyceride on small intestinal absorption of cefoxitin in rats. *J. Pharm. Pharmacol.* **1987**, *39*, 887–891, doi:10.1111/j.2042-7158.1987.tb03123.x.

152. Sha, X.; Yan, G.; Wu, Y.; Li, J.; Fang, X. Effect of self-microemulsifying drug delivery systems containing Labrasol on tight junctions in Caco-2 cells. *Eur. J. Pharm. Sci.* **2005**, *24*, 477–486, doi:10.1016/j.ejps.2005.01.001.

153. McCartney, F.; Jannin, V.; Chevrier, S.; Boulghobra, H.; Hristov, D.R.; Ritter, N.; Miolane, C.; Chavant, Y.; Demarne, F.; Brayden, D.J. Labrasol® is an efficacious intestinal permeation enhancer across rat intestine: Ex vivo and in vivo rat studies. *J. Control. Release* **2019**, *310*, 115–126, doi:10.1016/j.jconrel.2019.08.008.

154. Koga, K.; Kusawake, Y.; Ito, Y.; Sugioka, N.; Shibata, N.; Takada, K. Enhancing mechanism of Labrasol on intestinal membrane permeability of the hydrophilic drug gentamicin sulfate. *Eur. J. Pharm. Biopharm.* **2006**, *64*, 82–91, doi:10.1016/j.ejpb.2006.03.011.

155. van Hoogevest, P. Review – An update on the use of oral phospholipid excipients. *Eur. J. Pharm. Sci.* **2017**, *108*, 1–12, doi:10.1016/j.ejps.2017.07.008.

156. Hovgaard, L.; Brøndsted, H.; Nielsen, H.M. Drug delivery studies in Caco-2 monolayers. II. Absorption enhancer effects of lysophosphatidylcholines. *Int. J. Pharm.* **1995**, *114*, 141–149, doi:10.1016/0378-5173(94)00232-T.

157. Tagesson, C.; Franzen, L.; Dahl, G.; Westrom, B. Lysophosphatidylcholine increases rat ileal permeability to macromolecules. *Gut* **1985**, *26*, 369–377, doi:10.1136/gut.26.4.369.

158. Tran, T.; Xi, X.; Rades, T.; Müllertz, A. Formulation and characterization of self-nanoemulsifying drug delivery systems containing monoacyl phosphatidylcholine. *Int. J. Pharm.* **2016**, *502*, 151–160, doi:10.1016/j.ijpharm.2016.02.026.

159. Amara, S.; Patin, A.; Giuffrida, F.; Wooster, T.J.; Thakkar, S.K.; Bénarouche, A.; Poncin, I.; Robert, S.; Point, V.; Molinari, S.; et al. In vitro digestion of citric acid esters of mono- and diglycerides (CITREM) and CITREM-containing infant formula/emulsions. *Food Funct.* **2014**, *5*, 1409–1421, doi:10.1039/c4fo00045e.

160. Azmi, I.D.M.; Wibroe, P.P.; Wu, L.P.; Kazem, A.I.; Amenitsch, H.; Moghimi, S.M.; Yaghmur, A. A structurally diverse library of safe-by-design citrem-phospholipid lamellar and non-lamellar liquid crystalline nano-assemblies. *J. Control. Release* **2016**, *239*, 1–9, doi:10.1016/j.jconrel.2016.08.011.

161. Welling, S.H.; Hubálek, F.; Jacobsen, J.; Brayden, D.J.; Rahbek, U.L.; Buckley, S.T. The role of citric acid in oral peptide and protein formulations: Relationship between calcium chelation and proteolysis inhibition. *Eur. J. Pharm. Biopharm.* **2014**, *86*, 544–551, doi:10.1016/j.ejpb.2013.12.017.

162. Gattefossé Oral Drug Delivery with lipid Excipients Available online: https://www.gattefosse.com/back/files/Gattefosse_brochure_oral drug delivery 2020.pdf.

163. Niu, Z.; Tedesco, E.; Benetti, F.; Mabondzo, A.; Montagner, I.M.; Marigo, I.; Gonzalez-Touceda, D.; Tovar, S.; Diéguez, C.; Santander-Ortega, M.J.; et al. Rational design of polyarginine nanocapsules intended to help peptides overcoming intestinal barriers. *J. Control. Release* **2017**, *263*, 4–17, doi:10.1016/j.jconrel.2017.02.024.

164. Dixon, L.J.; Barnes, M.; Tang, H.; Pritchard, M.T.; Nagy, L.E. Kupffer Cells in the Liver. In *Comprehensive Physiology*; John Wiley & Sons, Inc.: Hoboken, NJ, USA, 2013; Vol. 13, pp. 303–309.

165. Dusek, J.; Carazo, A.; Trejtnar, F.; Hyrsova, L.; Holas, O.; Smutny, T.; Micuda, S.; Pavek, P. Steviol, an aglycone of steviol glycoside sweeteners, interacts with the pregnane X (PXR) and aryl hydrocarbon (AHR) receptors in detoxification regulation. *Food Chem. Toxicol.* **2017**, *109*, 130–142, doi:10.1016/j.fct.2017.09.007.

166. Pavek, P.; Hyrsova, L.; Smutny, T.; Carazo, A.; Moravcik, S.; Mandikova, J.; Trejtnar, F.; Gerbal-Chaloin, S. The pregnane X receptor down-regulates organic cation transporter 1 (SLC22A1) in human hepatocytes by competing for ("squelching") SRC-1 coactivator. *Br. J. Pharmacol.* **2016**, *173*, 1703–1715, doi:10.1111/bph.13472.

167. Zhang, X.-Q.; Even-Or, O.; Xu, X.; van Rosmalen, M.; Lim, L.; Gadde, S.; Farokhzad, O.C.; Fisher, E.A. Nanoparticles containing a liver X receptor agonist inhibit inflammation and

atherosclerosis. *Adv. Healthc. Mater.* **2015**, *4*, 228–36, doi:10.1002/adhm.201400337.

168. Gadde, S.; Even-Or, O.; Kamaly, N.; Hasija, A.; Gagnon, P.G.; Adusumilli, K.H.; Erakovic, A.; Pal, A.K.; Zhang, X.-Q.; Kolishetti, N.; et al. Development of Therapeutic Polymeric Nanoparticles for the Resolution of Inflammation. *Adv. Healthc. Mater.* **2014**, *3*, 1448–1456, doi:10.1002/adhm.201300688.

169. Owens, D.E.; Peppas, N.A. Opsonization, biodistribution, and pharmacokinetics of polymeric nanoparticles. *Int. J. Pharm.* **2006**, *307*, 93–102.

170. Badri, W.; Miladi, K.; Nazari, Q.A.; Greige-Gerges, H.; Fessi, H.; Elaissari, A. Encapsulation of NSAIDs for inflammation management: Overview, progress, challenges and prospects. *Int. J. Pharm.* **2016**, *515*, 757–773, doi:10.1016/j.ijpharm.2016.11.002.

171. Kumar, R.; Singh, A.; Garg, N.; Siril, P.F. Solid lipid nanoparticles for the controlled delivery of poorly water soluble non-steroidal anti-inflammatory drugs. *Ultrason. Sonochem.* **2018**, *40*, 686–696, doi:10.1016/j.ultsonch.2017.08.018.

172. Liu, D.; Jiang, S.; Shen, H.; Qin, S.; Liu, J.; Zhang, Q.; Li, R.; Xu, Q. Diclofenac sodium-loaded solid lipid nanoparticles prepared by emulsion/solvent evaporation method. *J. Nanoparticle Res.* **2011**, *13*, 2375–2386, doi:10.1007/s11051-010-9998-y.

173. Castelli, F.; Puglia, C.; Sarpietro, M.G.; Rizza, L.; Bonina, F. Characterization of indomethacin-loaded lipid nanoparticles by differential scanning calorimetry. *Int. J. Pharm.* **2005**, *304*, 231–238, doi:10.1016/j.ijpharm.2005.08.011.

174. Hippalgaonkar, K.; Adelli, G.R.; Hippalgaonkar, K.; Repka, M.A.; Majumdar, S. Indomethacin-Loaded Solid Lipid Nanoparticles for Ocular Delivery: Development, Characterization, and In Vitro Evaluation. *J. Ocul. Pharmacol. Ther.* **2013**, *29*, 216–228, doi:10.1089/jop.2012.0069.

175. Mehnert, W.; Mäder, K. Solid lipid nanoparticles: Production, characterization and applications. *Adv. Drug Deliv. Rev.* **2012**, *64*, 83–101, doi:10.1016/j.addr.2012.09.021.

176. Kulkarni, V.S.; Shaw, C. Surfactants, Lipids, and Surface Chemistry. In *Essential Chemistry for Formulators of Semisolid and Liquid Dosages*; Elsevier, 2016; pp. 5–19.

177. Rowe, R.C.; Sheskey, P.J.; Quinn, M.E. *Handbook of Pharmaceutical Excipients*; sixth edit.; Pharmaceutical Press: London/Chicago, 2009; ISBN 978 0 85369 792 3.

178. Morshed, M.; Chowdhury, E.H. Gene delivery and clinical applications. In *Encyclopedia of Biomedical Engineering*; Elsevier, 2019; Vol. 1–3, pp. 345–351 ISBN 9780128051443.

179. Andersson, S.; Antonsson, M.; Elebring, M.; Jansson-Löfmark, R.; Weidolf, L. Drug metabolism and pharmacokinetic strategies for oligonucleotide- and mRNA-based drug development. *Drug Discov. Today* **2018**, *23*, 1733–1745, doi:10.1016/j.drudis.2018.05.030.

180. Roth, C.M. Delivery of genes and oligonucleotides. In *Drug Delivery: Principles and Applications*; John Wiley & Sons, Inc.: New Jersey, 2016; pp. 655–673.

181. Tros de Ilarduya, C.; Sun, Y.; Düzgüneş, N. Gene delivery by lipoplexes and polyplexes. *Eur. J. Pharm. Sci.* 2010, *40*, 159–170.

182. Scholz, C.; Wagner, E. Therapeutic plasmid DNA versus siRNA delivery: Common and different tasks for synthetic carriers. *J. Control. Release* 2012, *161*, 554–565.

183. Wong, F.M.P.; Reimer, D.L.; Bally, M.B. Cationic Lipid Binding to DNA: Characterization of Complex Formation †. *Biochemistry* **1996**, *35*, 5756–5763, doi:10.1021/bi952847r.

184. Reimer, D.L.; Zhang, Y.P.; Kong, S.; Wheeler, J.J.; Graham, R.W.; Bally, M.B. Formation of Novel Hydrophobic Complexes between Cationic Lipids and Plasmid DNA. *Biochemistry* **1995**, *34*, 12877–12883, doi:10.1021/bi00039a050.

185. Collnot, E.M.; Ali, H.; Lehr, C.M. Nano- and microparticulate drug carriers for targeting of the inflamed intestinal mucosa. *J. Control. Release* 2012, *161*, 235–246.

186. Shen, J.; Burgess, D.J. In vitro dissolution testing strategies for nanoparticulate drug delivery systems: recent developments and challenges. *Drug Deliv. Transl. Res.* **2013**, *3*, 409–415,

doi:10.1007/s13346-013-0129-z.

187. Grabowski, N.; Hillaireau, H.; Vergnaud, J.; Santiago, L.A.; Kerdine-Romer, S.; Pallardy, M.; Tsapis, N.; Fattal, E. Toxicity of surface-modified PLGA nanoparticles toward lung alveolar epithelial cells. *Int. J. Pharm.* **2013**, *454*, 686–694, doi:10.1016/j.ijpharm.2013.05.025.

188. Danaei, M.; Dehghankhold, M.; Ataei, S.; Hasanzadeh Davarani, F.; Javanmard, R.; Dokhani, A.; Khorasani, S.; Mozafari, M.R. Impact of particle size and polydispersity index on the clinical applications of lipidic nanocarrier systems. *Pharmaceutics* **2018**, *10*, 1–17, doi:10.3390/pharmaceutics10020057.

189. Hernández-Giottonini, K.Y.; Rodríguez-Córdova, R.J.; Gutiérrez-Valenzuela, C.A.; Peñuñuri-Miranda, O.; Zavala-Rivera, P.; Guerrero-Germán, P.; Lucero-Acuña, A. PLGA nanoparticle preparations by emulsification and nanoprecipitation techniques: Effects of formulation parameters. *RSC Adv.* **2020**, *10*, 4218–4231, doi:10.1039/c9ra10857b.

190. Song, X.; Zhao, Y.; Wu, W.; Bi, Y.; Cai, Z.; Chen, Q.; Li, Y.; Hou, S. PLGA nanoparticles simultaneously loaded with vincristine sulfate and verapamil hydrochloride: Systematic study of particle size and drug entrapment efficiency. *Int. J. Pharm.* **2008**, *350*, 320–329, doi:10.1016/j.ijpharm.2007.08.034.

191. Hickey, J.W.; Santos, J.L.; Williford, J.M.; Mao, H.Q. Control of polymeric nanoparticle size to improve therapeutic delivery. *J. Control. Release* **2015**, *219*, 536–547, doi:10.1016/j.jconrel.2015.10.006.

192. Croda Europe Ltd Span and Tween.

193. K. Kolter Technical Information Kolliphor ® P Grades. *Tech. Doc.* **2013**, 1–8.

194. Dittrich, M.; Snejdrova, E. Cyclic swelling as a phenomenon inherent to biodegradable polyesters. *J. Pharm. Sci.* **2014**, *103*, 3560–3566, doi:10.1002/jps.24146.

195. Gustafson, H.H.; Holt-Casper, D.; Grainger, D.W.; Ghandehari, H. Nanoparticle uptake: The phagocyte problem. *Nano Today* 2015, *10*, 487–510.

196. Kučerová, K. Příprava a hodnocení lipidických nanočástic jako nosičů léčiv, Charles University, 2020.

197. Voldřichová, L. Lipidické nanočástice jako platforma pro dodání léčiv, Charles University, 2020.

198. Školová, B.; Janůšová, B.; Vávrová, K. Ceramides with a pentadecasphingosine chain and short acyls have strong permeabilization effects on skin and model lipid membranes. *Biochim. Biophys. Acta - Biomembr.* **2016**, *1858*, 220–232, doi:10.1016/j.bbamem.2015.11.019.

199. Bunjes, H.; Unruh, T. Characterization of lipid nanoparticles by differential scanning calorimetry, X-ray and neutron scattering. *Adv. Drug Deliv. Rev.* 2007, *59*, 379–402.

200. Cavalli, R. Sterilization and freeze-drying of drug-free and drug-loaded solid lipid nanoparticles. *Int. J. Pharm.* **1997**, *148*, 47–54, doi:10.1016/S0378-5173(96)04822-3.

201. Kesharwani, R.; Sachan, A.; Singh, S.; Patel, D. Formulation and Evaluation of Solid Lipid Nanoparticle (SLN) Based Topical Gel of Etoricoxib. *J. Appl. Pharm. Sci.* **2016**, 124–131, doi:10.7324/JAPS.2016.601017.

202. Pandita, D.; Ahuja, A.; Velpandian, T.; Lather, V.; Dutta, T.; Khar, R.K. Characterization and in vitro assessment of paclitaxel loaded lipid nanoparticles formulated using modified solvent injection technique. *Pharmazie* **2009**, *64*, 301–310, doi:10.1691/ph.2009.8338.

203. Council of Europe Acidum stearicum. In *European Pharmacopoeia 10.0*; 2019; p. 3898 ISBN 978-92-871-8923-3.

204. Hu, F.Q.; Jiang, S.P.; Du, Y.Z.; Yuan, H.; Ye, Y.Q.; Zeng, S. Preparation and characterization of stearic acid nanostructured lipid carriers by solvent diffusion method in an aqueous system. *Colloids Surfaces B Biointerfaces* **2005**, *45*, 167–173, doi:10.1016/j.colsurfb.2005.08.005.

205. Kubackova, J.; Holas, O.; Zbytovska, J.; Vranikova, B.; Zeng, G.; Pavek, P.; Mullertz, A. Oligonucleotide Delivery across the Caco-2 Monolayer: The Design and Evaluation of Self-

Emulsifying Drug Delivery Systems (SEDDS). *Pharmaceutics* **2021**, *13*, 459, doi:10.3390/pharmaceutics13040459.

206. Bligh, E.G.; Dyer, W.J. A rapid method of total lipid extraction and purification. *Can. J. Biochem. Physiol.* **1959**, *37*, 911–917.

207. Fountain, K.J.; Gilar, M.; Budman, Y.; Gebler, J.C. Purification of dye-labeled oligonucleotides by ion-pair reversed-phase high-performance liquid chromatography. *J. Chromatogr. B Anal. Technol. Biomed. Life Sci.* **2003**, *783*, 61–72, doi:10.1016/S1570-0232(02)00490-7.

208. Siqueira Jørgensen, S.D.; Al Sawaf, M.; Graeser, K.; Mu, H.; Müllertz, A.; Rades, T. The ability of two in vitro lipolysis models reflecting the human and rat gastro-intestinal conditions to predict the in vivo performance of SNEDDS dosing regimens. *Eur. J. Pharm. Biopharm.* **2018**, *124*, 116–124, doi:10.1016/j.ejpb.2017.12.014.

209. Maher, S.; Brayden, D.J.; Casettari, L.; Illum, L. Application of permeation enhancers in oral delivery of macromolecules: An update. *Pharmaceutics* **2019**, *11*, 1–23, doi:10.3390/pharmaceutics11010041.

210. Lobo, B.A.; Davis, A.; Koe, G.; Smith, J.G.; Middaugh, C.R. Isothermal Titration Calorimetric Analysis of the Interaction between Cationic Lipids and Plasmid DNA. *Arch. Biochem. Biophys.* **2001**, *386*, 95–105, doi:10.1006/abbi.2000.2196.

211. Marty, R.; N'soukpoé-Kossi, C.N.; Charbonneau, D.; Weinert, C.M.; Kreplak, L.; Tajmir-Riahi, H.A. Structural analysis of DNA complexation with cationic lipids. *Nucleic Acids Res.* **2009**, *37*, 849–857, doi:10.1093/nar/gkn1003.

212. Coates, J. Interpretation of Infrared Spectra, A Practical Approach. *Encycl. Anal. Chem.* **2004**, 1–23.

213. Banyay, M.; Sarkar, M.; Gräslund, A. A library of IR bands of nucleic acids in solution. *Biophys. Chem.* **2003**, *104*, 477–488, doi:10.1016/S0301-4622(03)00035-8.

214. Taillandier, E.; Liquier, J. Vibrational Spectroscopy of Nucleic Acids. In *Handbook of Vibrational Spectroscopy*; John Wiley & Sons, Ltd, 2006 ISBN 9780470027325.

215. Fatouros, D.G.; Bergenstahl, B.; Mullertz, A. Morphological observations on a lipid-based drug delivery system during in vitro digestion. *Eur. J. Pharm. Sci.* **2007**, *31*, 85–94, doi:10.1016/j.ejps.2007.02.009.

216. Liu, J.; Werner, U.; Funke, M.; Besenius, M.; Saaby, L.; Fanø, M.; Mu, H.; Müllertz, A. SEDDS for intestinal absorption of insulin: Application of Caco-2 and Caco-2/HT29 co-culture monolayers and intra-jejunal instillation in rats. *Int. J. Pharm.* **2019**, *560*, 377–384, doi:10.1016/j.ijpharm.2019.02.014.

217. Hubatsch, I.; Ragnarsson, E.G.E.; Artursson, P. Determination of drug permeability and prediction of drug absorption in Caco-2 monolayers. *Nat. Protoc.* **2007**, *2*, 2111–2119, doi:10.1038/nprot.2007.303.

218. Sun, H.; Chow, E.C.; Liu, S.; Du, Y.; Pang, K.S. The Caco-2 cell monolayer: usefulness and limitations. *Expert Opin. Drug Metab. Toxicol.* **2008**, *4*, 395–411, doi:10.1517/17425255.4.4.395.

219. Lea, T. Caco-2 Cell Line. In *The Impact of Food Bioactives on Health*; Springer International Publishing: Cham, 2015; pp. 103–111.

220. Suzuki, T. Regulation of intestinal epithelial permeability by tight junctions. *Cell. Mol. Life Sci.* **2013**, *70*, 631–659, doi:10.1007/s00018-012-1070-x.

221. Srinivasan, B.; Kolli, A.R.; Esch, M.B.; Abaci, H.E.; Shuler, M.L.; Hickman, J.J. TEER Measurement Techniques for In Vitro Barrier Model Systems. *J. Lab. Autom.* 2015, *20*, 107–126.

222. Kiptoo, P.; Calcagno, A.M.; Siahann, T.J. Drug delivery: principles and applications. In *Drug Delivery: Principles and Applications*; 2016; pp. 19–34 ISBN 1118833236.

9 LIST OF FIGURES AND TABLES

9.1 List of figures

9.2 List of tables

10 RESEARCH OUTPUTS

10.1 Articles related to the topic of the dissertation

- *Appendix I*

  Kubackova, J., Zbytovska, J., Holas, O.

  Nanomaterials for direct and indirect immunomodulation: A review of applications.

  European Journal of Pharmaceutical Sciences, 2020, 142: 105-139 ($IF_{2019-2020}$=3.616)

  DOI: 10.1016/j.ejps.2019.105139

  Author's contribution:

  - extensive systematic literature search and critical evaluation of collected information
  - writing – original draft
  - graphical visualisation

- *Appendix II*

  Boltnarova, B., Kubackova, J., Skoda, J., Stefala, A., Smekalova, M., Svacinova, P., Pavkova, I., Dittrich, M., Scherman, D., Zbytovska, J., Pavek, P., Holas, O.

  PLGA Based Nanospheres as a Potent Macrophage - Specific Drug Delivery System. *Nanomaterials*, 2021, 3 (11):1-17 (IF=4.324)

  DOI: 10.3390/nano11030749

  Author's contribution:

  - optimisation of preparation methods of polymeric NPs
  - review and editing of the manuscript

- *Appendix III*

  Kubackova, J.; Holas, O.; Zbytovska, J.; Vranikova, B.; Zeng, G.; Pavek, P.; Mullertz, A.

  Oligonucleotide Delivery across the Caco-2 Monolayer: The Design and Evaluation of Self-Emulsifying Drug Delivery Systems (SEDDS).

  Pharmaceutics, 2021, 13 (4): 1-27 (IF=4.421)

  DOI:10.3390/pharmaceutics13040459

  Author's contribution:

  - investigation, data curation and statistical evaluation

    preparation of hydrophobized OND complexes and their characterisation (effect of SEDDS excipients on complex stability, DSC and ATR-FTIR of complexes)

complex loading into SEDDS and characterisation of resulting formulations (dynamic light scattering, dynamic lipolysis, protection against nuclease)

in vitro experiments (permeability, cytotoxicity and uptake study)

- o visualisation of data
- o writing – original draft

10.2 Congress contributions

10.2.1 Oral presentations

- KUBACKOVA, J., HOLAS, O., DITTRICH, M. Polymeric nanoparticles for intracellular delivery. *8th Postgraduate and 6thPostdoc Conference, January 2018, Faculty of Pharmacy in Hradec Kralove, Charles University*, January 2018, Hradec Kralove, Czech Republic

- KUBACKOVA, J., HOLAS, O., ZBYTOVSKA, J., PAVEK, P., MULLETRZ, A. Oral delivery of oligonucleotides for local treatment of inflammatory bowel disease. *9th Postgraduate and 7thPostdoc Conference, January 2019, Faculty of Pharmacy in Hradec Kralove, Charles University*, January 2019, Hradec Kralove, Czech Republic

- KUBACKOVA, J., HOLAS, O., ZBYTOVSKA, J., PAVEK, P., MULLETRZ, A. Oral delivery of oligonucleotides for local treatment of inflammatory bowel disease. *Understanding Gastrointestinal Absorption-related Processes (UNGAP) Spring meeting,* February 2019, Sofia, Bulgaria
flash oral presentation accompanied with poster presentation

- KUBACKOVA, J., HOLAS, O., ZBYTOVSKA, J., PAVEK, P., MULLETRZ, A. SNEDDS for targeted oligonucleotide delivery to inflamed intestinal issue. *10th Postgraduate and 8thPostdoc Conference, Faculty of Pharmacy in Hradec Kralove, Charles University,* January 2020, Hradec Kralove, Czech Republic

- BOLTNAROVA, B. KUBACKOVA J., HOLAS, O., Polymeric particles: A tool for targeted inflammation management. *10th Postgraduate and 8thPostdoc Conference, Faculty of Pharmacy in Hradec Kralove, Charles University,* January 2020, Hradec Kralove, Czech Republic

- KUBACKOVA, J., HOLAS, O., ZBYTOVSKA, J., PAVEK, P., MULLETRZ, A. SNEDDS for targeted oligonucleotide delivery to inflamed intestinal issue. *UNGAP Spring meeting,* February 2020, Ljubljana, Slovenia
flash oral presentation accompanied with poster presentation

- KUBACKOVA, J., HOLAS, O., ZBYTOVSKA, J., PAVEK, P., MULLETRZ, A. Self-emulsifying drug delivery systems enable oral oligonucleotide delivery. *11th Postgraduate and 9thPostdoc Conference, Faculty of Pharmacy in Hradec Kralove, Charles University*, January 2021, Hradec Kralove, Czech Republic

- BOLTNAROVA, B. KUBACKOVA J., HOLAS, O., PAVEK, P. PLGA nanospheres as tool for macrophages targeting. *11th Postgraduate and 9thPostdoc Conference, Faculty of Pharmacy in Hradec Kralove, Charles University*, January 2021, Hradec Kralove, Czech Republic

- IEFREMENKO, D., BOLTNAROVA, B., KUBACKOVA, J., HOLAS, O. Development of nanoformulations for delivery of bile acids. *11th Postgraduate and 9thPostdoc Conference, Faculty of Pharmacy in Hradec Kralove, Charles University*, January 2021, Hradec Kralove, Czech Republic

10.2.2 Conference posters

- KUBACKOVA, J., HOLAS, O. Biodegradable nanoparticles for intracellular delivery. *63rd IPSF World Congress*, August 2017, Taipei, Taiwan.

    poster awarded FIP Industrial Pharmacy Section Scientific Poster Award

    with subsequent presentation at *78th FIP World congress of Pharmacy and Pharmaceutical Sciences*, September 2018, Glasgow, UK

- KUBACKOVA, J., HOLAS, O., ZBYTOVSKA, J. Preparation of polymeric nanoparticles for treatment of inflammatory bowel disease. *UNGAP Spring meeting,* February 2018, Lueven, Belgium

- KUBACKOVA, J., HOLAS, O., ZBYTOVSKA, J., PAVEK, P., MULLETRZ, A. Oral delivery of oligonucleotide for local treatment of inflammatory bowel disease. *NordicPOP annual meeting*, January 2019, Oslo, Norway

- KUBACKOVA, J., HOLAS, O., ZBYTOVSKA, J., PAVEK, P., MULLETRZ, A. SNEDDS for targeted oligonucleotide delivery to inflamed intestinal issue. *NordicPOP annual meeting*, January 2020, Copenhagen, Denmark

- BOLTNAROVA, B. KUBACKOVA J., PAVEK, P., HOLAS, O. Polymeric particles: a tool for targeted inflammation management. *UNGAP Spring meeting*, February 2020, Ljubljana, Slovenia